United States Environmental Protection Agency

EPA/600/R-09/072

STATUS REPORT:

Advances in Inhalation Dosimetry of Gases and Vapors with Portal of Entry Effects in the Upper Respiratory Tract

September 2009

U.S. Environmental Protection Agency
Washington, DC

DISCLAIMER

This report has been reviewed in accordance with U.S. Environmental Protection Agency Policy and approved for publication. Mention of trade names or commercial products does not constitute endorsement or recommendation for use.

AUTHORS, CONTRIBUTORS, AND REVIEWERS

AUTHORS

John J. Stanek—National Center for Environmental Assessment, U.S. Environmental Protection Agency, Research Triangle Park, NC

Gary L. Foureman—National Center for Environmental Assessment, U.S. Environmental Protection Agency, Research Triangle Park, NC

REVIEWERS

This report has been reviewed by scientists internal to the EPA.

RFC WORKGROUP CONTRIBUTORS AND REVIEWERS

Robert Benson—Region 8, U.S. Environmental Protection Agency, U.S. Environmental Protection Agency, Denver, CO

James S. Brown—National Center for Environmental Assessment, U.S. Environmental Protection Agency, Research Triangle Park, NC

Ernest Falke—Office of Pollution Prevention and Toxics, U.S. Environmental Protection Agency, Washington, DC

Anna Lowit—Office of Pesticide Programs, U.S. Environmental Protection Agency, Washington, DC

Eva McLanahan—National Center for Environmental Assessment, U.S. Environmental Protection Agency, Research Triangle Park, NC

Deirdre Murphy—Office of Air Quality Planning and Standards, U.S. Environmental Protection Agency, Research Triangle Park, NC

Babasaheb Sonawane—National Center for Environmental Assessment, U.S. Environmental Protection Agency, Washington, DC

Paul Schlosser—National Center for Environmental Assessment, U.S. Environmental Protection Agency, Washington, DC

Marc Stifelman—Region 10, U.S. Environmental Protection Agency, Seattle, WA

Ravi Subramanian—National Center for Environmental Assessment, U.S. Environmental Protection Agency, Washington, DC

John Whalan—National Center for Environmental Assessment, U.S. Environmental Protection Agency, Washington, DC

Paul White—National Center for Environmental Assessment, U.S. Environmental Protection Agency, Washington, DC

INTERNAL EPA REVIEWERS

Lynn Flowers—National Center for Environmental Assessment, U.S. Environmental Protection Agency, Washington, DC

Connie Meacham—National Center for Environmental Assessment, U.S. Environmental Protection Agency, Research Triangle Park, NC

Molly Rosett—Student Services Contractor, National Center for Environmental Assessment, U.S. Environmental Protection Agency, Research Triangle Park, NC

Reeder Sams—National Center for Environmental Assessment, U.S. Environmental Protection Agency, Research Triangle Park, NC

John Vandenberg—National Center for Environmental Assessment, U.S. Environmental Protection Agency, Research Triangle Park, NC

Deborah Wales—National Center for Environmental Assessment, U.S. Environmental Protection Agency, Research Triangle Park, NC

Debra Walsh - National Center for Environmental Assessment, U.S. Environmental Protection Agency, Research Triangle Park, NC

EXTERNAL REVIEWERS

Harvey Clewell—The Hamner Institute, Research Triangle Park, NC

Jeffry Schroeter—The Hamner Institute, Research Triangle Park, NC

James Ultman—Pennsylvania State University, University Park, PA

TABLE OF CONTENTS

LIST OF TABLES

LIST OF FIGURES

GLOSSARY

Aerosol - A suspension of liquid or solid particles in air.

Critical Effect - The first adverse effect, or its known precursor, that occurs as the dose rate increases. Designation is based on evaluation of overall data base.

Chronic Exposure - Multiple exposures occurring over an extended period of time, or a significant fraction of the animal's or the individual's lifetime.

Computational fluid dynamics (CFD) – A branch of fluid mechanics that uses numerical methods and algorithms to solve and analyze problems of fluid flows. Flows may apply to liquid and gases, including inspired and expired air, and are thus applicable to solving flows within the respiratory tract. The fundamental bases of any CFD problem are the Navier-Stokes equations, which define any single-phase fluid flow. These equations can be simplified by removing terms describing viscosity to yield the Euler equations.

Diffusivity (gas) - The transport of matter from one point to another by random molecular motions to become equalized with respect to concentration. For gases, rates of diffusion increase with the temperature and are inversely proportional to the pressure. The interdiffusion coefficients of gas mixtures are almost independent of the composition. Kinetic theory shows that diffusion of a pure gas is inversely proportional to both the square root of the molecular weight and the square of the molecular diameter.

Dorsal - On or near the upper surface (of the nasal tract).

Dosimetric Adjustment Factor (DAF) - A multiplicative factor used to adjust observed experimental or epidemiological data to human equivalent concentration (HEC) for assumed ambient scenario. See also regional gas dose ratio (RGDR).

Flux - The rate of flow of energy, gas or particles across a given surface.

Gas - Term referring to a compressible fluid phase of a substance. Fixed gases are gases for which no liquid or solid can form at the temperature of the gas, such as air at ambient temperatures.

Inhalation Reference Concentration (RfC) - An estimate (with uncertainty spanning perhaps an order of magnitude) of a continuous inhalation exposure to the human population (including sensitive subgroups) that is likely to be without an appreciable risk of deleterious noncancer health effects during a lifetime. The inhalation reference concentration is for continuous inhalation exposures and is appropriately expressed in units of mg/m^3.

Henry's Law Constant - The law can be expressed in several equivalent forms, a convenient form being: Cg = HC1 where Cg and C1 are the gas-(g) and liquid-(l) phase concentrations. The constant (H) is the ratio at equilibrium of the gas phase concentration to the liquid-phase concentration of the gas (i.e., moles per liter in air/moles per liter in solution).

K_g – The overall mass transfer coefficient describing movement of gas from the air phase into the liquid phase of the respiratory tract (see also MTC).

k_g – The gas phase mass transfer coefficient describing movement of gas from the gas phase to liquid/tissue boundary (see also MTC).

Lowest-Observed-Adverse-Effect Level (LOAEL) - The lowest exposure level at which there are statistically and/or biologically significant increases in frequency or severity of adverse effects between the exposed population and its appropriate control group.

Mass Transfer Coefficient (MTC) - A diffusion rate constant that relates the mass transfer rate, mass transfer area, and concentration gradient as driving force between and through phases. These coefficients may also be viewed in terms of resistance to flow and movement. For purposes of this report (with phases of gas and solid) MTC requires units of mass, time, distance, and concentration: $mol/(s \cdot m^2)$, mol/m^3, or m/s. Examples of MTCs used in this report relate to movement of gases in the respiratory tract. They include the MTC designated for the gas phase only, k_g, and an overall MTC inclusive of both the gas and liquid phases, K_g.

Meatus - A body opening or passage, such as the openings in the nose or ear.

No-Observed-Adverse-Effect Level (NOAEL) - An exposure level at which there are no statistically and/or biologically significant increases in the frequency or severity of adverse effects between the exposed population and its appropriate control. Some effects may be produced at this level, but they are not considered as adverse, nor immediate precursors to specific adverse effects. In an experiment with several NOAELs, the assessment focus is primarily on the highest one for a given critical effect, leading to the common usage of the term NOAEL as the highest exposure without adverse effect.

Physiologically-Based Pharmacokinetic (PBPK) Modeling - A mathematical modeling technique for predicting the absorption, distribution, metabolism and excretion of a compound in humans and other animal species. PBPK models strive to be mechanistic by mathematically transcribing anatomical, physiological, physical, and chemical descriptions of the phenomena involved in complex pharmacokinetic processes. These models have an extended domain of applicability compared to that of classical, empirical function based, compartmental pharmacokinetic models.

Portal-of-Entry Effect - A local effect produced at the tissue or organ of first contact between the biological system and the toxicant.

Regional Gas Dose (RGDr) - The gas dose (mg/cm^2) of respiratory tract surface area (per minute) calculated for the respiratory tract region of interest (r) as related to the observed toxicity (e.g., calculated for the tracheobronchial region for an adverse effect in the conducting airways). Regions of interest may be the extrathoracic (ET), tracheobronchial (TB), or pulmonary (PU).

Regional Gas Dose Ratio (RGDRr) - The ratio of the deposited gas dose in a respiratory tract region (r) for the laboratory animal species of interest to that of humans. This ratio is used to adjust the observed gas exposure level for interspecies dosimetric differences.

Uncertainty Factor (UF) - One of several, generally 3- to 10-fold factors, used in operationally deriving the inhalation reference concentration (RfC) from experimental data. UFs are intended to account for (1) the variation in sensitivity among the members of the human population, (2) the uncertainty in extrapolating laboratory animal data to humans, (3) the uncertainty in extrapolating from data obtained in a study that is of less-than-lifetime exposure, (4) the uncertainty in using LOAEL data rather than NOAEL data, and (5) the inability of any single study to adequately address all possible adverse outcomes in humans. The RfC Methods use 3 for the UF for interspecies extrapolation due to the incorporation of default dosimetric adjustments.

Vapor - a term referring to a gas phase at a temperature below the critical temperature of the substance where the same substance can also exist in the liquid or solid state. If the gas is in contact with the liquid or solid phase, the two phases will be in a state of equilibrium. This report is intended to consider those agents present as gaseous vapors at ambient temperatures.

Ventral - On or near the lower surface (of the nasal tract).

ACRONYMS AND ABBREVIATIONS

AA	Acrylic Acid
Aald	Acetaldehyde
Acr	Acrolein
AEL	Adjusted exposure level
A/H	Animal/Human
BMD	Benchmark dose
BW	Body Weight
C	Gas concentration, variously subscripted (mg/cm^3)
C_{air}	Concentration of toxicant in inspired air
CFD	Computational Fluid Dynamics
C_i	Inhaled concentration (mg/cm^3)
C_{ex}	Exhaled concentration (mg/cm^3)
D	Liquid diffusivity (cm^2/min)
DA	Diacetyl
DAF	Dosimetric Adjustment Factor
DL	Dorsal Lateral
DM	Dorsal Medial
DMS	Dimethyl sulfate
EA	Ethyl acrylate
ET	Extrathoracic respiratory region
f	Breathing frequency
FA	formaldehyde
H_2S	Hydrogen sulfide
$H_{b/g}$	Blood:gas (air) partition coefficient (unitless)
$H_{t/b}$	Tissue:blood partition coefficient (unitless)
$H_{t/g}$	Surface-liquid/tissue:gas (air) partition coefficient (unitless)
HEC	Human equivalent concentration
IRIS	Integrated Risk Information System
K_g	Overall MTC, mass transport coefficient (cm/min)
K_{gc}	Overall mass transport coefficient from gas phase
K_{gm}	Permeability coefficient
k_g	MTC, mass transport coefficient in the gas phase (cm/min)
k_ℓ	Mass transport coefficient in the surface-liquid/tissue phase (cm/min)
k_{mc}	Mass transport coefficient in the mucus phase (cm/min)
ℓ	Thickness of the liquid-tissue layer
ℓ_{muc}	Thickness of the mucus phase diffusion layer
LOAEL	Lowest-Observed-Adverse-Effect Level
MM	Middle Medial
MTC	Mass Transfer Coefficient
N	Overall transport or flux (mg/cm^2-min)
N_g	Flux through the air phase (mg/cm^2-min)
N_l	Flux through the surface liquid-tissue phase (mg/cm^2-min)
NP	Nasophaynx
OE	Olfactory Epithelium
P	Surface liquid/tissue:air partition coefficient (unitless)

PBPK	Physiologically Based Pharmacokinetic (model)
PO	Propylene oxide
POD	Point Of Departure
POE	Point of Entry
PU	Pulmonary respiratory tract region
PV	Posterior nasal vestibule
NOAEL	No-Observed-Adverse-Effect Level
RDDR	Regional deposited dose ratio used in derivation of an HEC for particles
RE	Respiratory Epithelium
RGD	Regional gas dose (mg/cm^2-min)
$RGDR_{ET}$	Regional gas dose ratio (animal to human) for the extrathoracic region
$RGDR_{PU}$	Regional gas dose ratio (animal to human) for the pulmonary region
$RGDR_{TB}$	Regional gas dose ratio (animal to human) for the tracheobronchial region
RfC	Reference concentration
RT	Respiratory tract
SA	Surface area of unspecified respiratory region (cm^2)
SA_{ET}	Surface area of the extrathoracic region (cm^2)
SA_{TB}	Surface area of the tracheobronchial region (cm^2)
SA_{PU}	Surface area of the pulmonary region (cm^2)
TB	Tracheobronchial respiratory tract region
TH	Thoracic respiratory tract region
UF	Uncertainty factor(s)
URT	Upper Respiratory Tract
VA	Vinyl acetate
VL	Ventral Lateral
VM	Ventral Medial
$\dot{V}_E$	Minute ventilation (L/min)

EXECUTIVE SUMMARY

The purpose of this report is to briefly review advances in the state-of-the-science for inhalation gas dosimetry related to the upper respiratory tract (URT) or nasal tract region. The primary results from this review include empirical information related to the assumptions underlying the current methodology used by EPA, as well as how the state of the science and advanced dosimetry modeling techniques inform these assumptions. A principal conclusion from this review that may impact EPA's future inhalation dosimetry methods for the URT is that internal dose equivalency for rats and humans is achieved through similar external exposure concentrations. This evaluation of internal dose equivalency relates to EPA's methods for interspecies extrapolation and not to potential differences in dosimetry among individuals in the human population.

This report reviews advances in science on gas dosimetry in the URT and will serve as a source document to explore revisions to these aspects of Agency's 1994 *RfC Methods (Methods for Derivation of Inhalation Reference Concentrations and Application of Inhalation Dosimetry*; EPA/600/8-90/066F, October 1994). Future reports will review advances on gas dosimetry for other regions of the respiratory tract. This report is intended neither to displace the current procedures for gas dosimetry in *RfC Methods* nor to reflect on use of these procedures in assessments currently in IRIS.

Comparative (animal to human) dosimetry is critical to all inhalation assessment activities that relate effects observed in animals to humans. The basic principle involved in comparative dosimetry is the determination of the internal dose to the target-tissue. This principle, in turn, is founded on the fundamentals of risk, as is stated by the NRC in its 1994 publication "Science and Judgment in Risk Assessment" and discussed further in its 2009 publication "Science and Decisions: Advancing Risk Assessment":

" ... the target-site dose is the ultimate determinant of risk..." .

The goal of comparative inhalation dosimetry is to characterize the steps leading from (1) estimation of the internal target-site dose in an animal resulting from a given external air concentration followed by (2) estimation of the external air concentration to which humans would be exposed to attain that same internal target-site dose. The external concentration of a human exposure scenario producing the equivalent internal target tissue dose is termed a human equivalent concentration (HEC) in the *RfC Methods*.

For gases producing effects in the URT, the approximation of the internal target-site dose from the external exposure concentration presented in the 1994 *RfC Methods* uses species-

specific overall minute ventilation ($\dot{V}_E$) and the overall surface areas (SA) of the URT epithelium or extrathoracic (ET) region. In the default approach to gas dosimetry, the *RfC Methods* uses ratios of these measures as a dosimetric adjustment factor (DAF) that is then applied to the animal external exposure concentration to arrive at an estimate of a HEC. The main assumptions underlying procedures on gas dosimetry currently in use by the Agency follow from the application of overall $\dot{V}_E$/SA relationships assuming uniformity of airflow and uniformity of deposition on surfaces. Chapter 3 of this report is a compendium of theory, observations, simulations, and results that indicate extensive nonuniformity associated with these measures. Information presented and discussed regarding these assumptions includes (1) empirical results of airflow in the URT using casts of animals and humans, (2) observations on the highly divergent geometry and anatomy of the URT between animals and humans, (3) advanced airflow simulation methods employed within and between species, (4) advanced simulations of tissue kinetics in URT tissues, and (5) correlation analysis of lesions and airflow simulations. An extensive section is presented on state of the science estimations of target-tissue dose based on the quantitatively linked airflow and tissue kinetic models. Overall, these advances both inform the original assumptions on airflow and gas deposition of the *RfC Methods* and present solutions to accommodate nonuniformity. A primary outcome is that for gas deposition in the URT the internal target tissue dose equivalency between humans and rats is achieved through equivalency at the level of the externally applied concentration, i.e., for both rats and humans, the same external air concentration leads to the similar internal target-site dose to the URT.

In 2005, EPA consulted with a panel of inhalation toxicology experts external to the Agency to review a range of topics that included the state-of-the-science for gas dosimetry and default procedures advocated in the *RfC Methods* including the gas categorization scheme. The results and recommendations from the 2005 consultation form the basis for the contents of this report. Chapter 1 provides an introduction to this report and a brief history on the practice of inhalation dosimetry. Chapter 2 provides a brief, focused review of the default comparative inhalation dosimetry procedures as they currently exist in the *RfC Methods*. Chapter 3 of this report summarizes the scientific advances in gas dosimetry for the URT region of both laboratory animal species and humans. Chapter 4 provides a listing of source references identified by the panel of experts as part of their consult and review.

Also featured in this report is a possible scheme for characterizing gases that differs fundamentally from the current *RfC Methods*. The *RfC Methods* current gas scheme relates physicochemical properties of gases to a category; this category is then related to the observed toxicity, including that of the target tissue. The scheme featured in this report provides a direct and simplified descriptor approach for characterizing gases that relates the properties of the gas directly to the site of the observed toxicity without an intervening category.

1. INTRODUCTION AND PURPOSE

1.1. PURPOSE OF THIS REPORT

Methods for Derivation of Inhalation Reference Concentrations and Application of Inhalation Dosimetry (U.S. EPA, 1994), referred to in this report as the *RfC Methods*, was made publically available in 1994.

The *RfC Methods* was drafted to advance dosimetry in general and for animal-to-human extrapolation. *RfC Methods* characterized the exposure-dose-response continuum leading to a target-tissue dose and provided a complete spectrum of interspecies dosimetry procedures for gases and particles based on target-tissue dose. Furthermore, it addressed broad areas of dosimetry. In cases where empirical observations had not yet sufficiently characterized theory, the *RfC Methods* provided alternatives based on reasonable scientific theory.

Since 1994, significant advancements have occurred throughout risk assessment sciences; in particular, interspecies comparative dosimetry of gases eliciting effects in the upper respiratory tract (URT). Since many of these advancements impact core components of the *RfC Methods* a need was recognized to assess the state-of-the-science in this area. Based upon that need, an expert panel was assembled in 2005 and tasked with reviewing the state-of-the-science of inhalation dosimetry.

The purpose of this report is to evaluate new science developments in the area of gas dosimetry and evaluate how these advancements may support future revisions to the *RfC Methods* used by EPA in developing RfCs. Specifically, this report summarizes the findings and recommendations of an expert panel (2005) on interspecies gas dosimetry for portal of entry effects in the upper respiratory tract. Future reports will review advances in gas dosimetry for other regions of the respiratory tract. This report relates to methods for interspecies extrapolation and not to differences in dosimetry among individuals in the human population (intraspecies variability).

This report is intended as a source document for potential revisions to gas dosimetry procedures in the *RfC Methods.* However, it is not intended to displace the current procedures for gas dosimetry in *RfC Methods* or to reflect on the use of these procedures in assessments currently in IRIS.

1.2. A PERSPECTIVE ON INHALATION DOSIMETRY

The 1994 *RfC Methods* document considers nearly every aspect of dose-response assessment for inhaled toxicants. This state-of-the-science report is more limited in scope and focuses on procedures and issues surrounding interspecies comparative dosimetry of gases,

particularly those exhibiting portal-of-entry effects in the URT. Also, it expands on the methods for estimating the dose delivered to target tissues; the basis of the interspecies comparative dosimetry established in the *RfC Methods*.

1.2.1. Historical Inhalation Dosimetry

The 1994 *RfC Methods* represented a fundamental shift in the approach for inhalation dosimetry. Therefore, the historical practices to which the *RfC Methods* offered an alternative need to be discussed briefly for the reader to understand the basis for the default procedures that were put forth in the *RfC Methods* for interspecies extrapolation. These default procedures are a primary focus of this report.

1.2.1.1. Total Dose from Concentration Inhaled

Perhaps the most simplistic approach for consideration of delivered dose from inhaling a toxicant is to calculate the mass of the agent in the inspired air and consider that exposure as total dose,

$$\textbf{Dose (mg/day)} = \dot{V}_E\ (\text{m}^3/\text{day}) \times C_{air}\ (\text{mg/m}^3) \qquad \textbf{Equation 1}$$

where $\dot{V}_E$ is minute ventilation expressed here as total volume of air inspired in a day, either for laboratory test animals or for humans, and C_{air} is the concentration of the toxicant in the inspired air. This approach requires multiple assumptions, the most critical being those related to toxicokinetics including amount absorbed, distribution, metabolism, and excretion characteristics. A brief description of these assumptions and limitations follows in this report; however, a complete discussion of the limitations of this approach is not within the scope of this report.

1.2.1.2. Normalization of Dose

Yet another major issue with this simplistic approach relates to how the total dose could be normalized for purposes of dose-response and interspecies extrapolation. Body weight is often used for this purpose, such that the total dose is expressed in units of body weight. This normalization procedure results in units typically encountered in oral dosing studies despite the fact that the exposures occurred via inhalation, i.e.,

$$\textbf{Normalized Dose (mg/kg-day)} = \textbf{Dose (mg/day)/BW (kg)} \qquad \textbf{Equation 2}$$

Nevertheless, this normalization procedure results in units of dose that are the same between species and that are scaled to the ventilatory volumes of the different species, providing a common starting point for interspecies extrapolation.

Normalization of an inhaled dose using body weight has been used for consideration of effects that occurred anywhere in the breathing individual, both systemic and portal-of-entry, i.e. the respiratory tract. For systemic effects from inhaled dose, (i.e., effects that occur elsewhere in the body following systemic transport via the blood) this normalization procedure is based on many toxicokinetic assumptions, and it is conceptually reasonable. Accordingly, inhaled toxicants absorbed into the blood via the respiratory tract and circulated to systemic target tissues of a given volume or weight resulting in a "dose" per mL of blood or mg of tissue, can be conceptualized for any test species and for humans. Part of this conceptualization relies on the consistent interspecies relationship of blood volume, organs and body weights.

On the other hand, exposures involving contact of inhaled materials with portal-of-entry tissues (i.e. those within the respiratory tract) differ fundamentally from contact of materials with tissues remote from the portal-of-entry. Both blood and organs are usually evaluated and functionally described in terms of volume, either directly or indirectly (as weight). Respiratory tract tissues, however, are most often evaluated and functionally described in terms of epithelial surface area or tissue weight. Inhaled materials entrained in breathed air pass over and around thereby exposing these respiratory tract tissue surfaces. Unlike the consistent defined interspecies relationships for weights and volumes, the interspecies relationships for surface areas are known to be divergent and not well defined. Thus, normalizing inhaled doses for effects and exposures based on surface area is not as readily conceptualized for effects and exposures based on weights and volumes. The considerable information that has accumulated on the interspecies differences in breathing physiology and airway anatomy makes normalization procedures for respiratory tract tissues increasingly complex.

It is from this historical perspective of interspecies inhalation dosimetry, where inhalation exposures were first transformed from external air concentrations to units of oral dosing and then normalized to body weight, that the advent of *RfC Methods* is perhaps most appropriately understood and valued.

2. REVIEW OF THE 1994 *RFC METHODS* FOR PORTAL-OF-ENTRY GAS DOSIMETRY

2.1. GAS CATEGORIZATIONS - GENERAL

Numerous model structures have been used for describing aspects of toxicant uptake, including gases and particles, in the respiratory tract.

Common uptake modeling schemes are often founded on the physicochemical characteristics of the gases to which they are applied. For the respiratory tract uptake of ozone, a highly reactive and moderately water soluble gas, Miller et al. (1985) proposed a detailed, distributed parameter model. Key elements incorporated into this convective-diffusion-chemical reaction model include (1) anatomic dimensions of the airspace and tissue thickness, (2) dispersion in the airspace, (3) reactivity in the liquid lining (mucus or surfactant) covering the cells of the lower respiratory tract, and (4) lateral mass transport resistance from the airspace to the blood (Overton et al., 1987). To be inclusive of highly reactive and highly soluble gases (e.g., formaldehyde, hydrogen fluoride), modeling schemes have emphasized the requirement to account for scrubbing of the gas from the airstream by the upper respiratory tract (Casanova et al., 1991; Hanna et al., 1989; Morris and Smith, 1982; Morgan and Frank, 1977; Aharonson et al., 1974). For nonreactive gases, modeling schemes often use the counterpart of these descriptions and characteristics to provide for a category whereby little toxicant is absorbed in the upper respiratory tract. Dahl (1990) categorized gases as stable, reactive, or metabolizable based on their thermodynamic and kinetic properties. Various concepts of "dose" can be related to these properties and the mechanism of action (e.g., macromolecular bound fraction as dose for reactive gases versus inhaled dose for stable asphyxiants).

It should be noted, however, that these uptake schemes are frequently based on the chemical-specific physicochemical characteristics (e.g., solubility and reactivity) of the subject gases, and described in terms of a qualitative continuum (e.g., low, moderate, or high). Therefore, any model scheme comprised of discrete categories has limited application to the broad range of gases that exist and that the RfC methodology must evaluate.

2.1.1. The *RfC Methods* Gas Categorization Scheme

The three category gas scheme currently in *RfC Methods* was constructed based on physicochemical characteristics as determinants of gas uptake as shown in Figure 2-1. A similar scheme has been developed by the International Commission on Radiological Protection (1993). The primary determinants used to construct such a conceptual framework and that direct

development of the default dosimetry scheme, i.e., reactivity and water solubility, are elaborated upon in the following sections. The numerical gas categories are placed on this scheme relative to their character of these determinants; Category 1 in the upper right hand corner corresponding to high reactivity and high water solubility; Category 3 in the lower left hand corner corresponding to low reactivity and low water solubility; and Category 2 occupying the area intermediate to the other two categories. The legend of this figure also indicates the regions of the respiratory tract where uptake is likely to occur for these gas categories. Category 1 gases are indicated to be absorbed in the "extrathoracic" or ET region which corresponds generally to the nasal cavity. Category 3 gases are indicated to be absorbed in the deeper pulmonary region, distal to the "ET" region, whereas Category 2 gases are indicated to be absorbed throughout the entire respiratory tract. Some example gases for each category are provided in Sections 2.1.1.1 – 2.1.1.3. Detail describing the regions of the respiratory tract is included in Section 2.2.1.1.1 of this report.

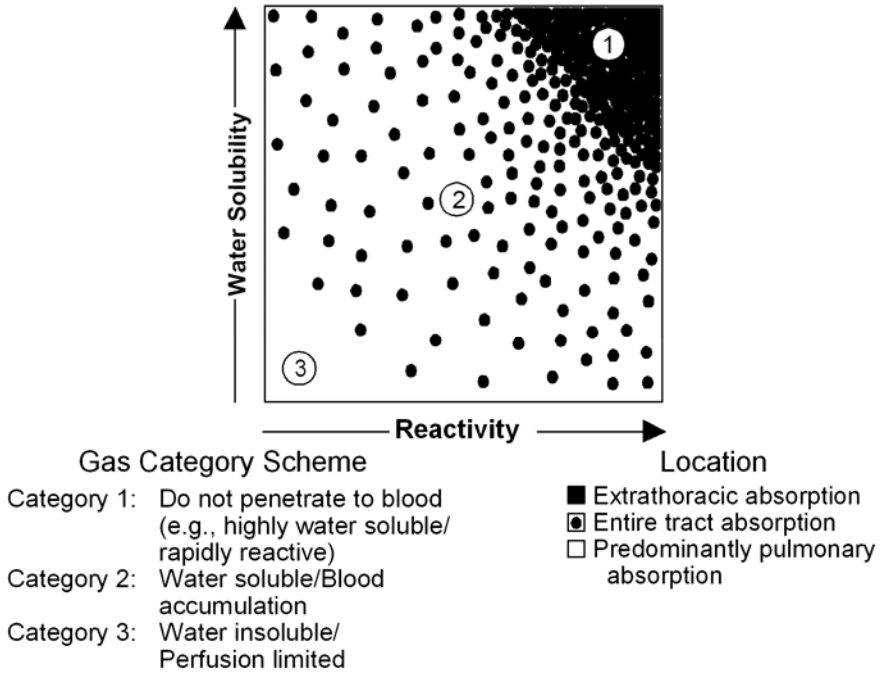

Source: U.S. EPA (1994).

Figure 2-1. Gas categorization scheme based on water solubility and reactivity as major determinants of gas uptake. Reactivity is defined to include both the propensity for dissociation as well as the ability to serve as a substrate for metabolism in the respiratory tract. Definitive characteristics of each category and anticipated location (region) for respiratory tract uptake are shown.

The two categories of gases with the greatest potential for respiratory effects are Category 1 gases that are highly water soluble and/or rapidly irreversibly reactive, and Category 2 water soluble gases that may also be rapidly reversibly reactive or moderately to slowly irreversibly metabolized in respiratory tract tissue. The definition of reactivity includes both the propensity for dissociation as well as the ability to serve as a substrate for metabolism in the respiratory tract. The scheme does not apply to inert gases that exert their effect by reversible "physical" interactions of gas molecules with biomolecules.

The objective of the default RfC modeling approach is to describe the effective dose to the major regions of the respiratory tract by addressing the absorption or "scrubbing" of a relatively water soluble and/or reactive gas from the inspired airstream as it travels down and through the respiratory tract from the nasal cavity to the pulmonary region. That is, the dose to the peripheral regions is influenced by the dose to the region from which the airstream has just exited.

The appropriateness of assessing proximal to distal (i.e., nasal cavity to the pulmonary region) dose representative of the scrubbing (uptake) pattern is supported by the proximal to distal progression pattern of respiratory tract toxicity with increasing concentration that is observed with many chemicals. Exposure to low concentrations of highly water soluble and/or irreversibly reactive gases primarily produces effects in the most anterior region of the nasal tract. At higher concentrations, more severe effects occur in the ET region and toxicity is also observed to progress to the peripheral regions. The severity of toxicity also progresses distally with increasing exposure concentrations. Although the default gas models of the *RfC Methods* do not describe detailed respiratory tract uptake to the level of local airflow distribution that actually exists in the tissues of the respiratory tract (e.g., respiratory versus olfactory epithelium), they do provide a description of the scrubbing of the chemical from the inhaled airstream on a more general regional scale.

2.1.1.1. "Category 1" Gases

A defining characteristic for what the *RfC Methods* describes as Category 1 gases is that they are so highly water soluble and/or rapidly irreversibly reactive in the surface-liquid/tissue of the respiratory tract that they do not develop a significant backpressure (i.e., reversal in the concentration gradient at the gas-liquid interface) from the surface-liquid tissue phase during exhalation. Also, Category 1 gases do not significantly accumulate in the blood which would reduce the concentration differential between tissue and blood and, hence, reduce the absorption rate into the tissue. The default model structure is based on these characteristics. Examples of gases classified as Category 1 are hydrogen fluoride, chlorine, formaldehyde, and volatile organic acids and esters.

2.1.1.2. "Category 2" Gases

Gases in Category 2 are moderately water soluble and rapidly reversibly reactive or moderately to slowly irreversibly metabolized in respiratory tract tissue. Ozone, sulfur dioxide, xylene, propanol, and isoamyl alcohol are examples of Category 2 gases. As has been already stated, these characteristics are continuous in nature such that the boundaries between categories cannot be definitive. Thus, some compounds may appear to be defined by either Category 1 or Category 2. Although sulfur dioxide is reversibly reactive, which would categorize it as a Category 2 gas, it is also highly soluble suggesting it could be a Category 1 gas. Similarly, ozone is highly reactive yet only moderately water soluble. More explicit delineation of categories will be made upon review of the empirical data and the predictability of the model gases that may appear to fit more than one category.

Because Category 2 gases are not as reactive in the respiratory tract tissue as Category 1 gases, they have the potential for significant accumulation in the blood and thus have a higher potential for both respiratory and remote toxicity. Thus, the model structure used to describe uptake of these gases is a hybrid of that for Category 1 and Category 3. The process of estimating the extent and pattern of uptake of such gases through the respiratory tract and into the systemic circulation is highly complex. PBPK models, with their capacity to use flows and partitioning to allow estimation of both absorption on inhalation and the extent of desorption during exhalation, are necessary to evaluate the steady-state blood concentration of such gases. The derivation of such model structures, along with their reduction to forms with a minimal number of parameters, are described in detail in Appendix I of the *RfC Methods* but are not a principal part of this report.

2.1.1.3. "Category 3" Gases

Category 3 gases occupy the opposite pole of Category 1 gases as they are relatively water insoluble and unreactive in surface liquid and tissue. Although exposure would occur throughout the entire respiratory tract with Category 3 gases, uptake is predominantly in the pulmonary region with relatively little uptake (or dose) occurring at the more anterior regions of the respiratory tract. Styrene is an example of a Category 3 gas. The site of toxicity of these gases is generally remote to the respiratory tract and a compartmental approach can be used to describe distribution to various systemic tissues. Thus, the default model for Category 3 gases is similar in structure to the PBPK model used by Ramsey and Andersen (1984) to describe styrene distribution. The model structure and the derivation of the default dosimetric adjustment based on this model are described in detail in the *RfC Methods* but are not a principal part of this report.

2.2. CONCEPTUAL AND HISTORICAL BASIS FOR COMPARATIVE DOSIMETRY OF INSPIRED GASES IN *RfC METHODS* – MINUTE VENTILATION/SURFACE AREA OF RESPIRATORY TRACT ($\dot{V}_E/SA_{RT}$)

The 1994 *RfC Methods* document is broad in its coverage and consideration of nearly every aspect of dose-response assessment for inhaled toxicants. This status report is focused on procedures and issues surrounding interspecies comparative dosimetry of gases, particularly those exhibiting portal-of-entry effects. The basis of the interspecies comparative dosimetry, posited by the *RfC Methods* and expanded upon in this report, is the estimate of delivered dose to target tissues.

The *RfC Methods* presents an in depth consideration of what was known about interspecies dosimetry for inspired gases at the time of publication with expansive commentary on the fundamental underlying determinants of dosimetry. These included species differences in anatomical and physiological characteristics of the respiratory tracts, the wide range of physicochemical properties associated with inhaled chemicals, the diversity of cell types that may be affected throughout the respiratory tract, as well as the many mechanistic and metabolic differences, all combining to make characterization of dosimetry particularly complex.

This section briefly reviews and summarizes knowledge of several of the most critical determinants of inhalation dosimetry that define and control the inhaled gas dose as well as presenting the underlying basis for the *RfC Methods* interspecies normalization of the gas dose. This review provides critical insight into how the *RfC Methods* default approach for dosimetry of gases was developed. It is this insight that will serve the reader as the informational backdrop against which scientific and technical advances described in Chapter 3 have progressed.

It is from this perspective of interspecies inhalation dosimetry established by the *RfC Methods*, in conjunction with the historical perspective given in Chapter 1, that the advent of the *RfC Methods* is most appropriately understood and valued.

2.2.1. Factors Controlling Comparative Inhaled Dose

RfC Methods states clearly that the various species used in inhalation toxicology studies do not receive identical doses in comparable respiratory tract regions when exposed to the same external gas concentration. The health endpoint or response from a gas, therefore, may be more directly related to the quantitative pattern of target tissue dose which is influenced by such factors as volumetric apportionment of air within the respiratory tract than to the external exposure concentration. Such regional deposition and uptake patterns would likely determine not only the initial doses to the respiratory tract tissues but also the specific pathways and rates by which the inhaled agents are cleared and redistributed.

The two major factors controlling the deposition and uptake pattern are: (1) respiratory anatomy and physiology and (2) the physicochemical characteristics of the inhaled toxicant. *Disposition* is the more general term that encompasses the processes of deposition, absorption, distribution, metabolism, and elimination. For gases, initial *deposition* is used in reference to contact with the respiratory tract surface that precedes actual absorption. Mechanisms important for gas deposition include convection, diffusion, chemical reaction (including metabolism), dissolution, and perfusion. Detailed consideration of these mechanisms is beyond the scope of this discussion.

Isolation of individual factors is probably necessary for initial understanding, but further dissection of factors that control inhaled dose into discrete topic discussions may mask the dynamic nature of the intact respiratory system. For example, although deposition in a particular respiratory region will be discussed separately from the clearance mechanisms for that region, retention (the actual amount of inhaled agent found in the respiratory tract at any time) is determined by the relative rates of deposition and clearance. Retention and the toxicological properties of the inhaled agent are related to the magnitude of the pharmacologic, physiologic, or pathologic response. Therefore, although the deposition, clearance mechanisms, and physicochemical properties of the agent are described in distinct sections, assessment of the overall toxicity requires integration of the various factors.

Thus, any description of the continuum defined by exposure, dose, and response requires integration of quantitative knowledge of determinants of chemical disposition, toxicant-target interactions, and tissue responses into an overall model of pathogenesis. Among other things, this process would involve determining the dose delivered to the target organ of various species as well as determining the sensitivity of the target organ to that dose. Once such aspects of dosimetry have been established and species sensitivity has been accounted for, the effective chemical concentration in laboratory animals can be quantitatively related to dose responses in humans. Models employed to perform this interspecies extrapolation would incorporate parameters such as species-specific anatomical and ventilatory differences, metabolic processes, as well as the physicochemical properties of the pollutant and should be based upon the physiological factors that govern transport and removal of the pollutant.

2.2.1.1. Comparative Respiratory Anatomy and Physiology

As introduced earlier, the respiratory systems of humans and various experimental animals, especially rodents which are the most frequently studied experimental species, differ markedly in numerous quantitative and qualitative aspects of anatomy and physiology. These differences affect critical aspects such as air flow patterns in the respiratory tract and thus deposition of an inhaled agent, as well as retention of that agent in the system. These differences

in anatomy and physiology will be discussed according to respiratory regions and branching patterns, clearance mechanisms, and cell types. Clearance mechanisms used here include processes such as the mucociliary escalator, solubilization in various compartments, uptake, and metabolism.

2.2.1.1.1. Regions of the Respiratory Tract Common among Species

The respiratory tract in both humans and experimental animals including the commonly used murine species (i.e., rats and mice) can be divided into three similar regions on the basis of structure and function: the extrathoracic region (ET) that extends from just posterior to the external nares to just anterior to the trachea, the tracheobronchial region (TB) defined as the trachea to the terminal bronchioles where proximal mucociliary transport begins, and the pulmonary region (PU) including the terminal bronchioles and alveolar sacs. The thoracic (TH) region or lower airways is defined as the TB and PU regions combined. The anatomic structures included in each of these respiratory tract regions are listed in Table 2-1 and Figure 2-2 provides a diagrammatic representation of these regions in humans.

Table 2-1. Respiratory tract regions

Region		Anatomic Structures	Other Terminology
Extrathoracic (ET)		Nose Mouth Nasopharynx Oropharynx Laryngopharynx Larynx	Head airways region Nasopharynx (NP) Upper respiratory tract (URT) Upper airways
Thoracic (TH)	Tracheobronchial (TB)	Trachea Bronchi Bronchioles (to terminal bronchioles)	Conducting airways
	Pulmonary (PU)	Respiratory bronchioles (not found in rodents) Alveolar ducts and sacs Alveoli	Gas exchange region Alveolar region Parenchyma

Source: Adapted from Phalen et al. (1988).

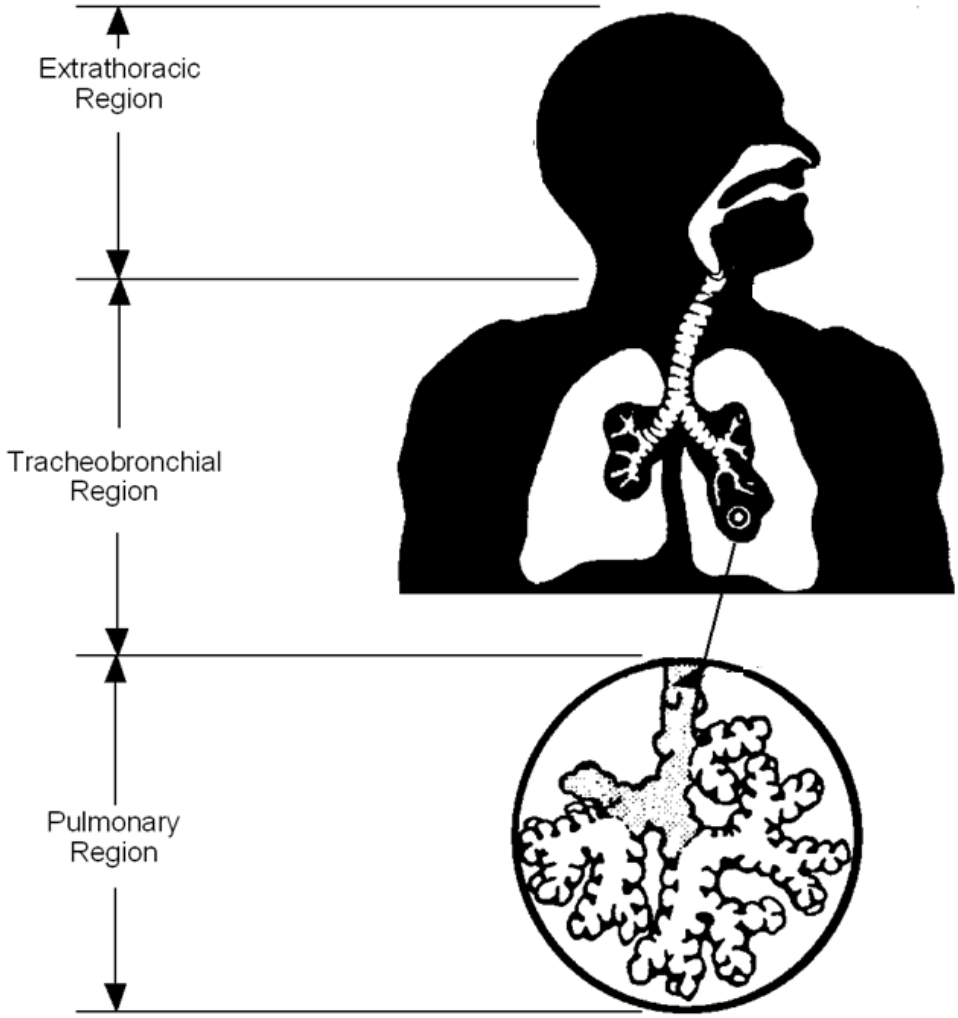

Source: U.S. EPA (1994).

Figure 2-2. Diagrammatic representation of the three respiratory tract regions designated in humans.

These interspecies similarities occur only at this very general level of organization, as analysis at any more refined level begins to reveal marked differences. For example, within the ET region, murine laboratory species have much more extensive and convoluted nasal turbinate systems than do humans. Functionally, murine species are nasal breathers, whereas humans breathe oronasally. Also, leading into the TB region, the length of the nasopharynx in relation to the entire length of the nasal passage also differs between species. In addition, humans have highly symmetric bifurcations whereas murine species have a highly asymmetric pattern featuring secondary subdominant or monopodial branching (Figure 2-3). In the PU regions, the

branching patterns of airway ducts between humans and murine species are also markedly different.

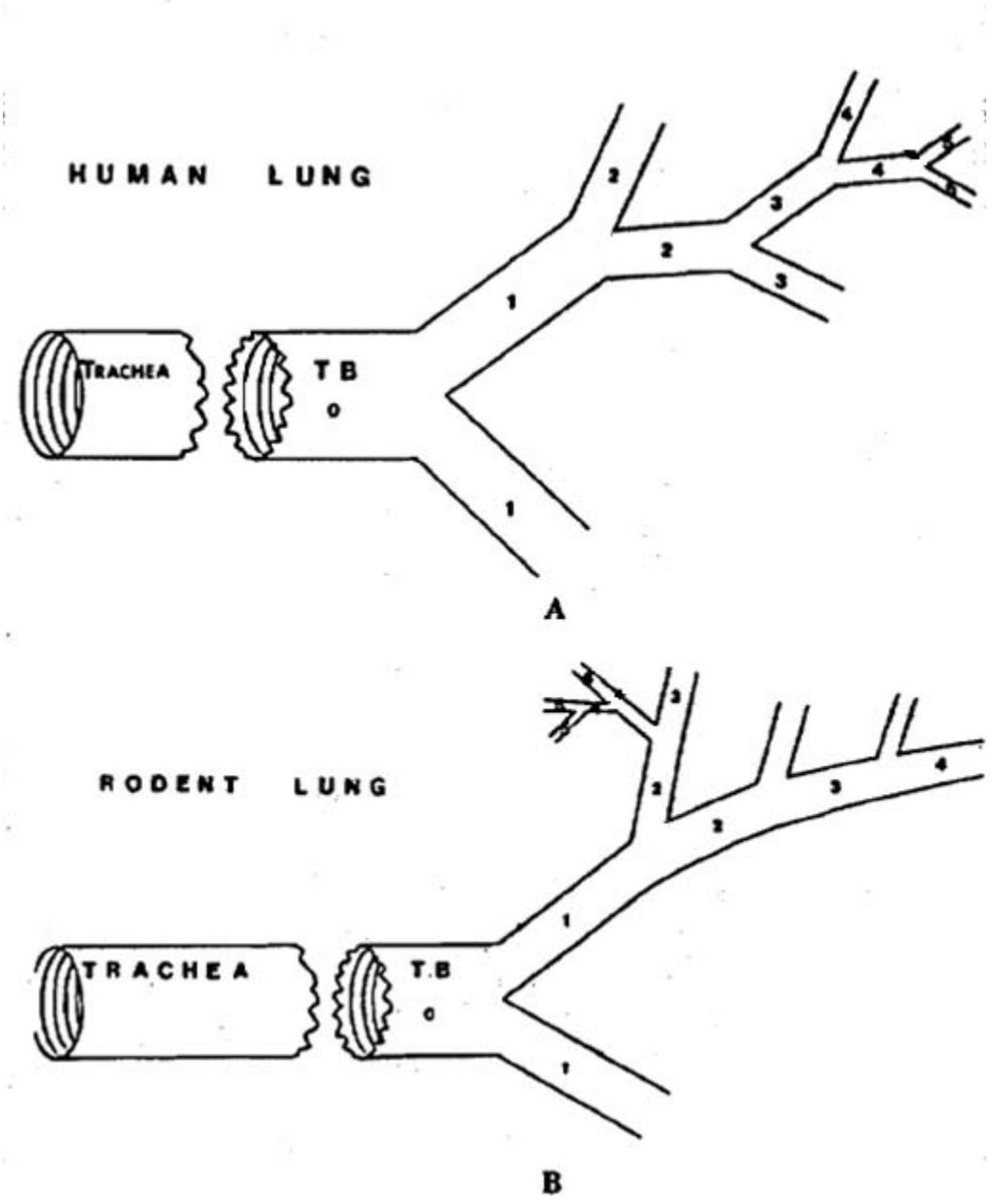

Source: Adapted from Lippman and Schlesinger (1984)

Figure 2-3. A representative model of symmetric (A) and asymmetric (B) airway branching patterns occurring in humans and murine laboratory animals species, respectively. The numbers represent major airway daughters.

These differences, especially the greater degree of nasal passage complexity in rodents and the comparatively high ventilatory rates, are likely to result in greater deposition in the ET region of rodents compared to humans; however, data to support this assertion were limited at the time the *RfC Methods* was developed. It is important to note that the extent of upper respiratory tract removal affects the amount of gas passing to the distal respiratory tract.

Airway size (length and diameter) and branching pattern affect the aerodynamics of the respiratory system in the following ways:

- The airway diameter affects the aerodynamics and the distance from the agent molecule or particle to the airway surface.
- The cross-sectional area of the airway determines the velocity for a given volumetric flow.
- Airway length, airway diameter, and branching pattern variations affect the mixing between tidal and reserve air.

Differences in airway sizes and branching among species therefore may result in significantly different patterns of deposition for gases. For example, differences in airway size and branching pattern are confirmed to be a major source of interspecies differences in inhaled dose for the TB region. As mentioned above, relative to humans, experimental animals tend to have tracheas that are much longer in relation to their diameter. A more complete listing and analysis of comparative airway anatomy differences between humans and murine species is available in the *RfC Methods*.

2.2.1.1.2. Surface Areas (SA) of Common Respiratory Regions

The existence of these general functional regions, the ET, TB and the PU, within the respiratory tracts of humans and murine laboratory species has been thoroughly documented. It is through, within, around and over these regions that inspiratory and expiratory air flows. When recast in terms of an agent that may be entrained or present in the breathed air, the implications become clear and evident that exposure to an agent may occur in this manner to tissues comprising these respiratory tract regions.

Perhaps in partial recognition of this relationship, considerable effort in the scientific community has been expended on estimating the surface areas (SA) for these respiratory tract regions for both humans and a number of the common laboratory test species. Some accepted values for the SA of these various regions are given in the *RfC Methods* and reproduced below, complete with sources listed in the *RfC Methods* in Table 2-2.

Table 2-2. Default surface area values for respiratory effects

	ET[a] (cm^2)	Source	TB[a] (cm^2)	Source	PU[a] (cm^2)	Source
Human	200.0	Guilmette et al. (1989)	3,200.0	Mercer et al. (1994a)	540,000	Mercer et al. (1994b)
Mouse	3.0	Gross et al. (1982)	3.5	Mercer et al. (1994a)	500	Geelhaar and Weibel (1971), Mercer et al. (1994b)
Hamster	14.0[b]		20.0	Yu and Xu (1987)	3,000	Lechner (1978)
Rat	15.0[c]	Gross et al. (1982)	22.5	Mercer et al. (1994a)	3,400	Mercer et al. (1994b)
Guinea Pig	30.0	Schreider and Hutchens (1980)	200.0	Schreider and Hutchens (1980)	9,000	Tenney and Remmers (1963)
Rabbit	30.0	Kliment (1973)	300.0	Kliment (1973)	59,000	Gehr et al. (1981)

Source: U.S. EPA (1994).

[a]ET = Extrathoracic; TB = Tracheobronchial; PU = Pulmonary.
[b]No measurements of hamster ET surface area were found in the literature. This value is estimated based on similarity of the other regional surface areas to the rat.
[c]Additional unpublished measurements of the surface area beyond the ethmoid turbinates are included.

Aspects important to this report should be noted from the values in Table 2-2. The first being that the PU region has the greatest percentage of SA over the respiratory tract, being hundreds of times larger than ET and TB combined. At low concentrations of those gases considered highly soluble and reactive and which would undergo significant clearance in both the ET and TB regions, the residual gas reaching the PU would be dispersed over this large SA of the PU region. A second point is the converse of the first in that for highly soluble and reactive gases, the SA of both the ET and TB regions receives a disproportionate amount of gas relative to the PU region.

Another aspect to be noted from the table is that a single SA figure is given for each region. It is important to note that SA varies with age, and the SA of the PU region is also affected by disease. Although it is established that numerous cell types and tissues exist in these areas, only a single SA is given. For example, perhaps the most problematic region in this respect is the ET region, where no fewer than four different types of epithelial and submucosal tissues exist. Some tissues, such as the olfactory epithelium, possess multiple cell types, some of which are specific targets for certain toxicants. Thus the SAs listed in this table, although appearing as a single uniform number, describe areas that have extreme cellular and functional diversity. The review of Harkema et al. (2006) provides an in-depth discussion of the various

epithelial cell types as well as their toxicological and physiological significance in a variety of species including humans.

2.2.1.1.3. Comparative Respiratory Minute Ventilations ($\dot{V}_E$)

The means by which exposures to any SA would occur from agents in the air is most likely and logically via the agent concentration present within the inspired and expired air, the minute ventilation, $\dot{V}_E$.

The *RfC Methods* provides procedures and parameters for calculating typical minute ventilations, $\dot{V}_E$, expressed as total volume of air inspired in a day, both for laboratory test animals and for humans. The default ventilation values for minute ventilation [$\dot{V}_E$ = tidal volume (V_T) × breathing frequency (f)] are based on accepted body weight allometric scaling equations provided in the literature.

The basis of interspecies allometric scaling is to account for disproportionalities between species. It should be kept in mind that these disproportionalities manifest because smaller species have proportionally greater $\dot{V}_E$ per unit body weight than larger species. $\dot{V}_E$ also varies with age, activity, and disease.

For purposes of interspecies scaling, the RfC Methods specifies a default body weight for the human of 70 kg, and a corresponding $\dot{V}_E$ of 13.8 L/min or 20 m^3/day.

2.3. NORMALIZATION OF INHALED CONCENTRATION TO SURFACE AREA OF RESPIRATORY TRACT REGIONS

2.3.1. Dose-Response in Respiratory Tract Tissues is Based on External Exposure Concentration

A central consistent observation from inhalation exposure has been the capacity of the external exposure concentration to establish and explain the response in the respiratory tract. Pathology in laboratory animals from inhalation exposure to a variety of agents has characterized responses in the ET, TB and PU regions of the respiratory tract. Response characterization based on external exposure concentration has been thorough, extending from the basis of structure and cell biology, from various mechanisms of toxic action, as well as response to injury. Some studies and responses to inhalation exposures have been characterized by inclusion of other variables, e.g. that the response may follow a concentration × duration (C× T) relationship. Even with advanced dose-response modeling approaches for inhalation exposures, the inception of any analysis is the external exposure concentration.

Transformation of the external exposure concentration in air from typical units of ppm or mass/unit air to other units, such as total mg/day, does not provide a metric with a direct

relationship to response, especially when the response being characterized is a portal-of-entry response involving one of the surfaces in the respiratory tract. For extremely reactive gases, deposition may only occur in the first few centimeters of the ET, thus invalidating even those metrics based on the overall surface area of the ET.

2.3.2. Normalization of External Exposure Concentration to Surface Areas

In their investigation designed to resolve marked differences in tumor response to high concentrations of inhaled formaldehyde observed in rats (high response) versus mice (low response), Chang and coworkers (1983) explored several approaches to evaluate whether this difference in response was due to a smaller dose in mice. The authors clearly demonstrated that mice were better able than rats to reduce their $\dot{V}_E$ via decreases in respiratory rate, thus logically resulting in a comparatively smaller dose to mice than rats. When dose was expressed in conventional terms, µg/min/kg body weight, mice were predicted to receive nearly twice the dose of rats. However, when dose was expressed in terms of target tissue (i.e., nasal cavity) surface area, mice were predicted to receive approximately one half the dose of rats. This approach, "normalization" of dose per surface area, offered a satisfactory explanation to account for the observed differences in tumor response. A conclusion of this work was that normalizing the dosimetry to nasal surface area could lead to better understanding of species differences in nasal toxicity. The basis of such an approach was theoretical as the assumptions being made were that formaldehyde was completely absorbed and uniformly distributed over the entire surface area. These same theoretical assumptions will be examined in the following sections.

These conceptual considerations for inhaled dose coupled with observations of Chang and coworkers (1983) that target tissue surface area was explanatory of responses logically led to the construct of the basic dosimetry scheme put forth by the *RfC Methods*. In this scheme, inhaled dose to the respiratory tract is based on species –specific relationships of minute ventilation and surface areas associated with the target regions of the respiratory tract:

$$\dot{V}_E/SA_{ET,TB} \text{ or } _{PU} \qquad \textbf{Equation 3}$$

It is the consideration and exploration of the assumptions underlying this normalization that will provide the impetus for the next steps and advancements for the RfC *Methods*. As will be apparent in Chapter 3 of this report, it is the clarification of these assumptions following from $\dot{V}_E$/SA that will focus and direct advancement of inhalation dosimetry.

2.4. APPLICATION OF $\dot{V}_E$/SA IN CALCULATION OF THE HUMAN EQUIVALENT CONCENTRATION, HEC: THE DEFAULT APPROACH FOR INSPIRED GASES

Overall, this chapter has attempted to present in a concise manner the conceptual basis for choice of the components and procedures used by the *RfC Methods* in performing interspecies inhalation extrapolation for respiratory tract responses. Rather than rely on the historical and problematic procedure involving transformation of inhaled concentration to total dose, the *RfC Methods* relied on empirical evidence to validate the use of the external air concentration. Instead of imposing the typical dose measures for systemic effects (e.g., mg/kg-day) on effects occurring in portal-of-entry respiratory tract tissues, extensive information, not presented here, was synthesized to support a more relevant and explanatory dose measure based on normalization of target surface areas of the respiratory tract.

The overall goal of the RfC procedures is to estimate toxicokinetically equivalent doses to target tissues in laboratory animals to those of humans. *RfC Methods* give application procedures for these various components to produce an estimate of a human equivalent concentration (HEC). *RfC Methods* elaborates upon and outlines practices and data requirements for other procedures that are arranged in a hierarchy of approaches for estimations of human equivalent concentrations for gases (see Table 2-3). The approach being discussed and analyzed in this report is that of the "default" approach only, the most generalized and data limited situation where information is limited to that discussed thus far in this report, principally species $\dot{V}_E$ and SA for the various regions of the respiratory tract As indicated in the hierarchy scheme, the default approach would be bypassed when more sophisticated or chemical-specific models are available, several of which will be explained further in this report (e.g. PBPK, CFD, and CFD-PBPK hybrid).

Table 2-3. Hierarchy of model structures for dosimetry and interspecies extrapolation

Optimal model structure	
	Structure describes all significant mechanistic determinants of chemical disposition, toxicant-target interaction, and tissue response
	Uses chemical-specific and species-specific parameters
	Dose metric described at level of detail commensurate to toxicity data
Default model structure	
	Limited or default description of mechanistic determinants of chemical disposition, toxicant-target interaction, and tissue response
	Uses categorical or default values for chemical and species parameters
	Dose metric at generic level of detail

Source: U.S. EPA (1994)

2.4.1. The Dosimetric Adjustment Factor, DAF

The following equation may be generally applied to estimate an HEC. It demonstrates the application of a correction factor to an external exposure air concentration encountered by the laboratory animal:

$$\mathbf{POD_{(HEC)}\ (mg/m^3) = POD_{(ADJ)}\ (mg/m^3) \times DAF_r} \qquad \textbf{Equation 4}$$

where:

(1) $POD_{(ADJ)}$ is the air concentration used as the "Point Of Departure" corresponding to an effect level obtained from, for example, analysis of a laboratory animal inhalation study. Examples of PODs include the NOAEL (no-observed-adverse-effect-level) or a BMD (benchmark dose). The subscript "ADJ" refers to adjustments made to the POD for considerations other than dosimetry (e.g., duration) and is not a focus of this report.

(2) DAF_r is a dosimetric adjustment factor for respiratory tract region, r (ET, TB, PU, or TOTAL). It represents a multiplicative factor used to adjust an observed exposure concentration in a particular laboratory species to an exposure concentration for humans that would be associated with the same delivered dose also termed the "regional gas dose" or RGD_r. For gases this factor is the "regional gas dose ratio" or $RGDR_r$.

(3) The $POD_{(HEC)}$ is the human equivalent external air concentration of the animal POD that has been dosimetrically adjusted to a human equivalent concentration (HEC) through application of the appropriate DAF_r, in this case for gases, the $RGDR_r$.

2.4.2. The DAF for Gases; the Regional Gas Dose Ratio, $RGDR_r$

The equations to derive the regional gas dose ration ($RGDR_r$) for different gas categories and for the various regions of the respiratory tract (versus remote sites) are provided and described further in *RfC Methods.* The principal focus of this report is the approach and procedures used for gases having effects in the extrathoracic (ET) region of the respiratory tract.

The basic default equation given in *RfC Methods* used to calculate the $RGDR_{ET}$, i.e., the DAF_{ET}, for gases incorporates basic determinants of inhaled dose — species-specific minute ventilation and surface areas:

$$\mathbf{RGDR_{ET}} = \frac{\mathbf{(V_E\ /\ SA_{ET})_A}}{\mathbf{(V_E\ /\ SA_{ET})_H}} \qquad \textbf{Equation 5}$$

where:

$\dot{V}_E$ = minute ventilation (L/min),

SA_{ET} = surface area of the extrathoracic region (cm^2), and

A, H = subscripts denoting laboratory animal and human, respectively.

Basically, the $RGDR_r$ is used as the DAF_{ET} in Equation 5 to dosimetrically adjust the experimental POD (duration adjusted or not) to estimate an HEC POD (POD_{HEC}) as follows:

$$\mathbf{POD_{(HEC)}\ (mg/m^3) = POD_{(ADJ)}\ (mg/m^3) \times RGDR_r} \qquad \textbf{Equation 6}$$

$RGDR_r$ can be seen to be equal to the ratio of the RGD in laboratory animal species to that of humans $(RGD_r)_A/(RGD_r)_H$.

RGDRs have been calculated for several species for all regions of the respiratory tract, including the ET, and are shown in Table 2-4.

Table 2-4. RGDRs and minute ventilation/surface area (V_E/SA) ratios of the ET, TB, and PU regions of respiratory tract for various species and humans

Parameter	Hamster	Guinea Pig	Mouse	Rat	Monkey	Rabbit	Human
$\dot{V}_E(m^3/day)$[a]	0.093	0.41	0.064	0.30	2.55	1.475	20
ET Region							
SA_{ET}[b](cm^2)	14	30	3	15	63[c]	30	200
$\dot{V}_E/SA_{ET}$	0.007	0.014	0.021	0.02	0.04	0.049	0.1
$RGDR_{ET}$[d]	0.07	0.14	0.21	0.20	0.4	0.5	-
TB Region							
SA_{TB}[b](cm^2)	20	200	3.5	22.5	-	300	3200
V_E/SA_{TB}	0.005	0.002	0.018	0.019	-	0.005	0.006
$RGDR_{TB}$[d]	0.8	0.33	3	3.2	-	0.8	-
PU Region							
SA_{PU}[b] (m^2)	0.300	0.900	0.050	0.340	-	5.9	54
Q_{ALV}[e]/SA_{PU}	0.22	0.32	0.9	0.91	-	0.18	0.26
$RGDR_{PU}$[d]	0.8	1.2	3.5	3.5	-	0.67	-

[a](male + female)/2 "mature" values from U.S. EPA (1988a, 1988b).
[b]U.S. Environmental Protection Agency (1994)
[c]Kepler et al. (1995)
[d]RGDR = Regional Gas Dose Ratio for the ET, TB or PU regions = $(\dot{V}_E/SA)$animal/$(\dot{V}_E/SA)$human
[e]Alveolar ventilation rate (Q_{ALV}) calculated as 0.7 × minute ventilation

2.4.3. Some Example HEC Calculations with Commentary

To make application of this dosimetric procedure clearer, a few examples using the entries in Table 2-4 are given, each accompanied by some commentary.

Example 1 - In hamsters, effects in the tracheobronchial (TB) region (cellular degeneration) are noted after exposure to a gas at a POD of 10 mg/m^3 with no duration adjustments to this concentration. Using Table 2-4 and Equation 7, the HEC would be calculated as:

$$\mathbf{POD_{(HEC)}\ (mg/m^3) = POD_{(ADJ)}\ (mg/m^3)\ x\ RGDR_{TB}} \qquad \textbf{Equation 7}$$

$$\mathbf{8\ mg/m^3 = 10\ (mg/m^3)\ x\ 0.8}$$

Commentary: Here the default HEC estimated for this extrapolation from the TB region of the hamster is quite close in value to the animal POD, due to the appropriate $RGDR_{TB}$ being close to unity at 0.8. This indicates that at typical ventilatory parameters, hamster and human lung tissues are predicted to be about equally exposed at a common external concentration.

Example 2 - In mice, effects in the pulmonary region (chronic infiltrate) are noted after a 10 mg/m^3 exposure to a reactive gas, duration adjusted to achieve a final POD concentration of 5 mg/m^3. Using Table 2-4 and Equation 7 the HEC would be calculated as:

$$\mathbf{POD_{(HEC)}\ (mg/m^3) = POD_{(ADJ)}\ (mg/m^3)\ x\ RGDR_{PU}} \qquad \textbf{Equation 8}$$

$$\mathbf{17.5\ mg/m^3 = 5\ (mg/m^3)\ x\ 3.5}$$

Commentary: The default HEC estimated for this extrapolation from the PU region of the mouse is quite divergent from the adjusted animal POD, due to the appropriate $RGDR_{PU}$ being considerably greater than unity at 3.5. This indicates that at typical ventilatory parameters and breathing the same gas concentration, human lung tissues would be receiving considerably less dose (3.5-fold less) than mouse lung tissues. Another view of the extrapolation is that human lung tissues would be exposed to the same internal dose at 17.5 mg/m^3 as mouse lung tissues would be at 5 mg/m^3.

Example 3 – In rats effects are noted in the nasal cavity, the ET region, (necrosis of the respiratory epithelium) at an external gas concentration of 100 mg/m^3. Since no exposure duration or other adjustments are needed, 100 mg/m^3 is the POD. Using Table 2-4 and Equation 7 the HEC would be calculated as:

$$\mathbf{POD_{(HEC)}\ (mg/m^3) = POD_{(ADJ)}\ (mg/m^3)\ x\ RGDR_{ET}} \qquad \textbf{Equation 9}$$

$$\mathbf{20\ mg/m^3 = 100\ (mg/m^3)\ x\ 0.20}$$

Commentary: The default HEC estimated for this extrapolation from the ET region of the rat is also quite divergent from the adjusted animal POD, due to the appropriate $RGDR_{ET}$

being considerably smaller than unity at 0.20, which is opposite of the PU example above. This indicates that at typical ventilatory parameters and breathing the same gas concentration, human ET tissues would be receiving more dose (1/0.20 = 5-fold more) than rat ET tissues. Another view of this extrapolation is that humans ET tissues would be exposed to the same internal dose at 20 mg/m^3 as rat ET tissues would be at 100 mg/m^3.

2.5. ASSUMPTIONS AND LIMITATIONS IN $\dot{V}_E$/SA

Although inhalation dosimetry based on the measure of "dose" estimated through $\dot{V}_E/SA_{ET,TB,\ PU\ or\ Total}$ has been demonstrated to be more explanatory of inhaled dose and responses in the respiratory tract and portal-of-entry effects than alternatives discussed in Sections 1.2.1.1 and 1.2.1.2, such an approach is put forth on assumptions, either explicit or implicit, whose existence, limitations and caveats need to be considered.

Perhaps the most debated aspect of this dosimetric approach concerns the outcome of the example above using the ET region. As demonstrated, the default dosimetric adjustment for gas exposures in this region estimates that human tissues receive a three- to fivefold higher exposure than do rat tissues. One primary reason the $\dot{V}_E/SA_r$ relationship is debated is its marked divergence from the closely related relationship of $\dot{V}_E$/BW. Parallel construction of an RGDR based on body weight instead of SA_{ET} would yield a value of 3 ([(rat $\dot{V}_E$/0.3 kg)/(human $\dot{V}_E$/70 kg)] = 0.6/0.2 = 3) indicating that human tissues would receive threefold less dose than rat tissues.

With $\dot{V}_E$/SA regarded as dose normalized to surface area, this increased ratio in humans indicates that human ET tissues will receive a fivefold higher dose than those of, for example, rats. This circumstance regarding interspecies differences is represented in Figure 2-4 which illustrates the actual values used in application of $\dot{V}_E/SA_{ET}$ to perform interspecies dosimetry through derivation of an RGDR. The right hand side of this figure shows the overall outcome when these differences are applied to interspecies extrapolation; the human ET tissues are projected to always receive more of dose, up to fivefold more, than are rat ET tissues.

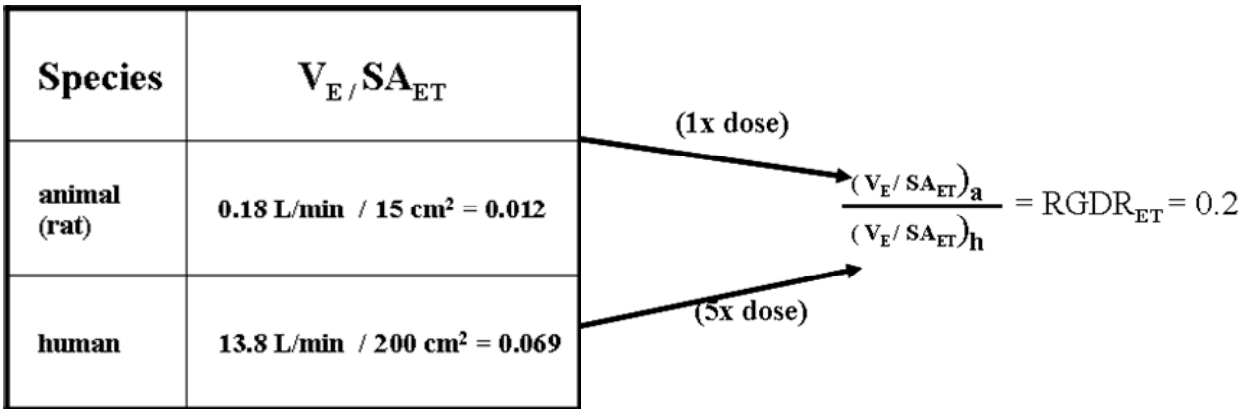

Figure 2-4. Calculation and application of $\dot{V}_E/SA_{ET}$ in the *RfC Methods* default approach for interspecies dosimetric extrapolation through derivation of the regional gas dose ratio for the extrathoracic region, $RGDR_{ET}$. The RGDR value of 0.2 may be seen to relate back to the presumption that humans ET tissues receive the obverse of the RGDR in dose, i.e. fivefold (1/0.2 =5). Also see Equation 5, above.

This divergent interspecies relationship is reflected in the application of $\dot{V}_E/SA$ in actual calculation of an HEC where the DAF (the $RGDR_{ET}$) applied to the animal point of departure approximates the inverse of this ratio, i.e., 0.2-0.3 (i.e., 1/3-5). Thus, human equivalent human exposures based on responses in the ET from rat results are adjusted downward by this fraction. This adjustment lowers the overall estimate for an effect concentration in humans by a factor of 3 to 5 even before consideration of uncertainty factors.

2.5.1. The $\dot{V}_E/SA$ Assumptions

This specific species divergence in dosimetric adjustment has resulted in considerable scientific debate. This debate has led to the identification and clarification of assumptions made, either explicitly or implicitly, underlying the default dosimetric procedures for interspecies extrapolation. It is these assumptions, the most critical and significant of which are listed below, that provide a basis for further revisions and refinement of the dosimetric procedures used by the Agency.

Assumption 1 - The flow of the gas at $\dot{V}_E$ through the respiratory tract region of interest is uniform. As the units of $\dot{V}_E$ are L/min there exists no basis to consider nonuniformity of flow of the gas present or entrained in the breathed air. At the time of the *RfC Methods* development, nonuniformity was suspected although there was no substantial basis to quantitatively evaluate its extent.

Assumption 2 – The SAs of the respiratory tract regions subtending the entrained gas have to be treated as uniform and equivalent, i.e., the cell types, relative amount, and distributions are equivalent in human and animal species. This assumption actually follows from and is a corollary to assumption 1. Although considered valid for the general regions of the respiratory tract, the available SAs incorporate no further refinement regarding tissue- or cell-types within any region. It is essentially an averaged surface area that contains widely divergent nonuniform cell types. Under the *RfC Methods* the most refinement that can be achieved with $\dot{V}_E$/SA is essentially limited to the SA term in the denominator. As discussed elsewhere previously in this report and in the *RfC Methods,* such an assumption may be most problematic for the ET, a region that may be considered the most anatomically complex, divergent, and varied in tissue type of all regions in the respiratory tract.

Assumption 3 - The gas inhaled is uniformly and evenly distributed over the entire surface of the respiratory tract region in question. A further assumption for gases with portal-of-entry effects is that the deposition/uptake is complete or 100% in the region in question and is the same in animals and humans as deposition/uptake information for humans is frequently lacking. These assumptions are somewhat implicit but necessarily follow from the units of $\dot{V}_E$/SA and from the accompanying assumptions of uniform flow and uniform surface area. Also, inspection of the $\dot{V}_E$/SA relationship reveals that modulation of either $\dot{V}_E$ or SA would directly influence the "intensity" or flux of the gas deposited to the SA. For example, increasing $\dot{V}_E$ and decreasing the SA would increase the flux at the SA; decreasing $\dot{V}_E$ and increasing the SA would instead decrease the flux at the SA. Perhaps the most obvious inconsistency of this assumption is the empirically demonstrable proximal to distal, high to low concentration response gradient known to occur for gases that produce respiratory tract lesions. Also, for gases extensively scrubbed from the upper airways (the ET region) such as formaldehyde, the assumption of 100% uptake/absorption may be valid. However, this assumption cannot be valid for a great many other gases. These issues as well as many others critical to the practice of inhalation interspecies dosimetry as given in the historical *RfC Methods* are evaluated in the following chapter.

3. SCIENCE DEVELOPMENTS IN PORTAL-OF-ENTRY GAS DOSIMETRY

3.1. INTRODUCTION

The preceding chapter examined and summarized the origins, underlying principles and concepts, and demonstrated the application of the default procedure in the *RfC Methods* for performing inhalation dosimetry of gases that exhibit portal-of-entry effects. This examination focused on important assumptions made in the application of the basic element of default dosimetry, i.e., $\dot{V}_E/SA$. These three basic assumptions are briefly restated and illustrated in Figure 3-1.

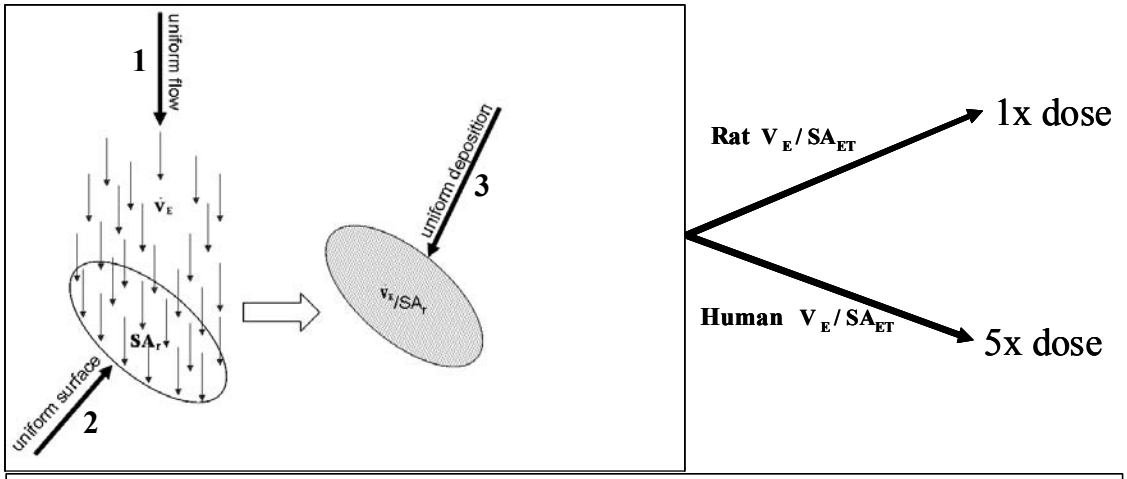

1 – assumption of *uniform even flow* of gas present in V_E through the respiratory tract region
2 – assumption of *uniform even SAs* of tissues in the respiratory tract region subtending V_E
3 – assumption of *uniform even deposition* of gas present in V_E over the entire surface of the respiratory tract

Figure 3-1. Representation of the assumptions of uniformity following from $\dot{V}_E/SA$ as applied to comparative gas dosimetry. Gas is entrained in the $\dot{V}_E$ and impinges upon the subtending epithelial surface area (SA) of the various regions (r) of respiratory tract. The right side of this figure shows the arithmetic outcome of applying $\dot{V}_E/SA$ to the ET regions of rats and humans.

This figure illustrates a major outcome following from the interspecies extrapolation for the ET region with these attendant $\dot{V}_E/SA_{ET}$ assumptions. With the accompanying assumption that all of the gas is absorbed in the region defined by SA, the approximate fivefold higher value for $\dot{V}_E/SA_{ET}$ in humans compared to rats indicates that the surface of the human ET receives a fivefold higher dose than the rat ET.

The intervening period from issuance of the *RfC Methods* from 1994 to date has seen substantive advancements for dosimetry of gases in general and interspecies comparative gas dosimetry in particular. Many of these advancements and investigations directly inform the above three assumptions.

This chapter will present and discuss information that is representative of what has become available concerning these assumptions since the 1994 *RfC Methods* was completed.

3.2. A MODIFIED GAS SCHEME: DESCRIPTORS VERSUS CATEGORIES

On the practical level a gas/vapor dosimetry scheme should be useful as an aid in predicting the site of toxicity. This is especially applicable in describing the fate of inhaled gases. Knowledge of two physicochemical properties, water solubility and reactivity, is useful in predicting the site of uptake of gases/vapors in the respiratory tract tissue and/or absorption into blood and the potential toxic actions in both inhalation portal-of-entry sites and in sites remote from the inhalation portal-of-entry. These properties have been repeatedly used as predictors of the site of gas uptake and effects within the respiratory tract.

Although acknowledged as a continuum, the reactivity-solubility relationship is nevertheless grouped by the *RfC Methods* into a numerical category: Category 1 for a highly water soluble and reactive gas, Category 2 for a gas designated moderately water soluble and moderately reactive, and Category 3 for a relatively insoluble and nonreactive gas. Use of this scheme, conceptually represented and described above, yields a numerical gas category which in turn leads to general principles and statements concerning likely sites and conditions of toxicity.

Medinsky and Bond (2001) put forth a descriptor scheme based on these same two physicochemical properties whose application to gases would be fundamentally different, direct and more useful. In this scheme, water soluble gases are defined as gases that readily dissolve in the mucus lining of the upper respiratory tract followed by diffusion into the underlying epithelial cells and, potentially, into the blood for systemic distribution. Generally, water-insoluble gases penetrate the mucus lining more slowly and are transported to the lower respiratory tract where they may be absorbed into the blood. For gases such as these, deposition and uptake in the URT would be dependent upon other processes controlling uptake (e.g. metabolism). The other principal determinant, reactivity, defined in this scheme as the tendency of a gas to undergo chemical reaction, is simple to understand. However, reactivity at the level of organization relating to tissue dosimetry is complex. In the distance from the airway to the blood, reactive gases may undergo interactions with components in the air, mucus, and tissue. These reactions lead to rapid and substantive decreases in the concentration of the reactive gas across this distance. In fact, some gases have such high reactivity that very little of the gas itself ever reaches the blood. This is in contrast to inert gases that do not react with respiratory tract

tissues or fluids such that the gas can ultimately diffuse through the various respiratory layers with appreciable concentrations eventually reaching the blood for systemic distribution. Thus, chemical reactivity of the gas controls its molecular interactions with respiratory tissues and influences penetration of the vapors to the blood.

Although not explicitly discussed in this scheme, metabolism (i.e., catalyzing actions of enzymes in the respiratory tract) is also considered a component of reactivity in characterizing gas transport in the tissue and predicting site of gas uptake and effect. However, application of the descriptor outlined by this scheme excludes metabolism in designating the parent gas as "reactive". For example, dibasic ester and butadiene are both designated as "non-reactive" gases because their toxicity is dependent upon their metabolite(s) (Medinsky and Bond, 2001). These types of gases often produce site-specific toxicity based on the localization of their metabolic enzymes.

Rather than assigning specific numerical categories to gases, these descriptors are placed on a chart that represents reactivity and water solubility as continuous variables. This scheme, along with the descriptors for the boundary conditions of the variables, is shown in Figure 3-2. It is upon this scheme that information and data can be placed to gain insight regarding sites and conditions of toxicity. Figure 3-2 also illustrates this application with the placement of formaldehyde and its predominant toxicity, effects in the ET portal-of-entry region, in the upper right portion of the chart. This sector of the chart corresponds to high reactivity and high water solubility, characteristics that would predict gas disposition with resultant effects in the anterior most portal-of-entry region, i.e., the nasal cavity or "ET" (for extrathoracic) region, as is noted for formaldehyde. Butadiene, which produces effects in lung tissue, has low water solubility and is non-reactive, and thus, is the obverse entry to formaldehyde in Figure 3-2. It is important to note that this scheme provides examples of gases that fit these discrete descriptors, but that the majority of gases may not fit one particular descriptor. However, examination of these examples at the extremes should facilitate understanding of the behavior of other gases.

Utilization of such a scheme yields direct information about the nature and site of toxicity that is based on the determinative variables of water solubility and reactivity. Direct information on the nature and site of toxicity is crucial to formulating an approach to inhalation dosimetry. This approach and scheme contrasts with the current *RfC Methods* scheme where the outcome is a numerical category whose implications to dosimetry are proscribed, often irrespective of the sites and conditions of the observed toxicity. The current *RfC Methods* scheme has resulted in some confusion in that it is often applied as such and influences dosimetry by placing an unintended emphasis on the numerical gas category as opposed to the site of toxicant effect.

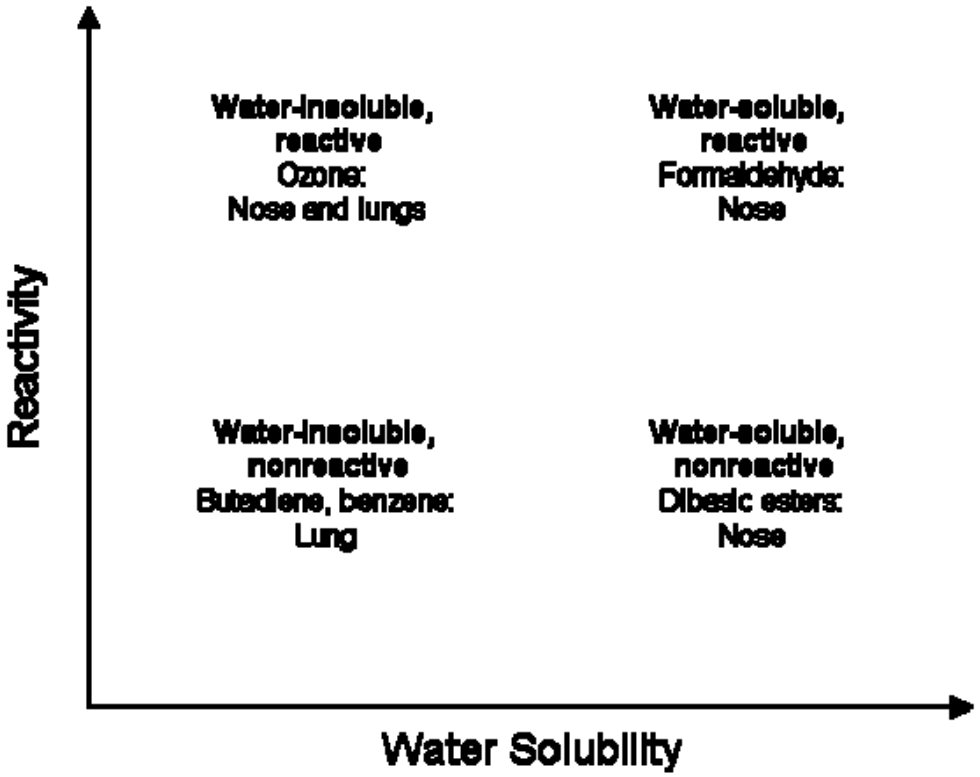

Source: Adapted from Medinsky and Bond (2001).

Figure 3-2. A schematic representation of the physicochemical properties of reactivity and water solubility overlaid with descriptors of their practical limits. Examples of specific chemicals with their primary site of toxicity are also presented.

Such a scheme would have best applicability in situations where gas exposure levels are relatively low and the effects observed are in the most sensitive target tissues. A higher concentration and a broader range of responses would result in less applicability of this scheme.

3.3. FLOW-DYE CAST MODELS

Morgan and co-workers (1991) laid the foundation for studying airflow distribution patterns in the ET region, the nasal tract. In an early work, these investigators prepared clear acrylic casts from molds of the nasal airways (meatuses), including the larynx and proximal trachea, of both F344 rats and Rhesus monkeys. Water flow was introduced through the casts in an anterior to posterior direction using a unidirectional water-dye siphon system. Water-dyes were introduced to visualize and study the dynamics of flow through this system at physiologically relevant rates. Although consistent from cast to cast, the character of the observed flows was not uniform. Rather, the dye-streamlines observed with this technique were consistent in revealing complex flow patterns in both species with major inspiratory streamlines

observed consistently from cast to cast (Figure 3-3). In rats, major inspiratory streams were present medially with a superior and inferior ventral stream, a middle stream and a dorsal stream that bifurcated mid-way through the upper meatuses. Major lateral inspiratory streams were also present and apportioned in this manner into ventral, middle and dorsal streams. The flow patterns in monkeys differed significantly and were far more complex and varied than those in rats. Inspired air flow in monkeys was divided into a number of major streams within the most anterior portion of the nares, the vestibule. These patterns included a relatively disorganized medial fan-shaped jet, ventral and dorsal vortices in addition to major streamlines in both ventral and dorsal regions of the nasal tract. The flow streamlines also allowed for a qualitative assessment of flow velocity within each species. In rats, the flows appeared similar for all major streams except for dorsal streams through regions containing olfactory epithelium (OE), which were slower. In contrast, there were clear velocity differences for monkeys. The fastest velocities occurred in the anterior fan-jet, with slower flows in the principal passageways and a markedly slower flow velocity in the dorsal medial meatus.

Consequences of these (and other similar) observations are significant on several levels. First, the complex but generally consistent and orderly streamlines revealed by the cast method show a sensitive dependence of nasal airflow patterns on nostril geometry throughout the ET region. Second, all observations indicate overwhelmingly that flow into the nasal area, either liquid or air, is in no way uniform but has discernable patterns that could only result in highly nonuniform deposition onto surfaces (i.e., nasal epithelial surfaces). The consistent patterns of both streamlines and estimates of widely varying flow velocity also give support to the proposal that these elements both play a role in the distinct distribution of lesions known to be induced by agents such as formaldehyde (discussed later).

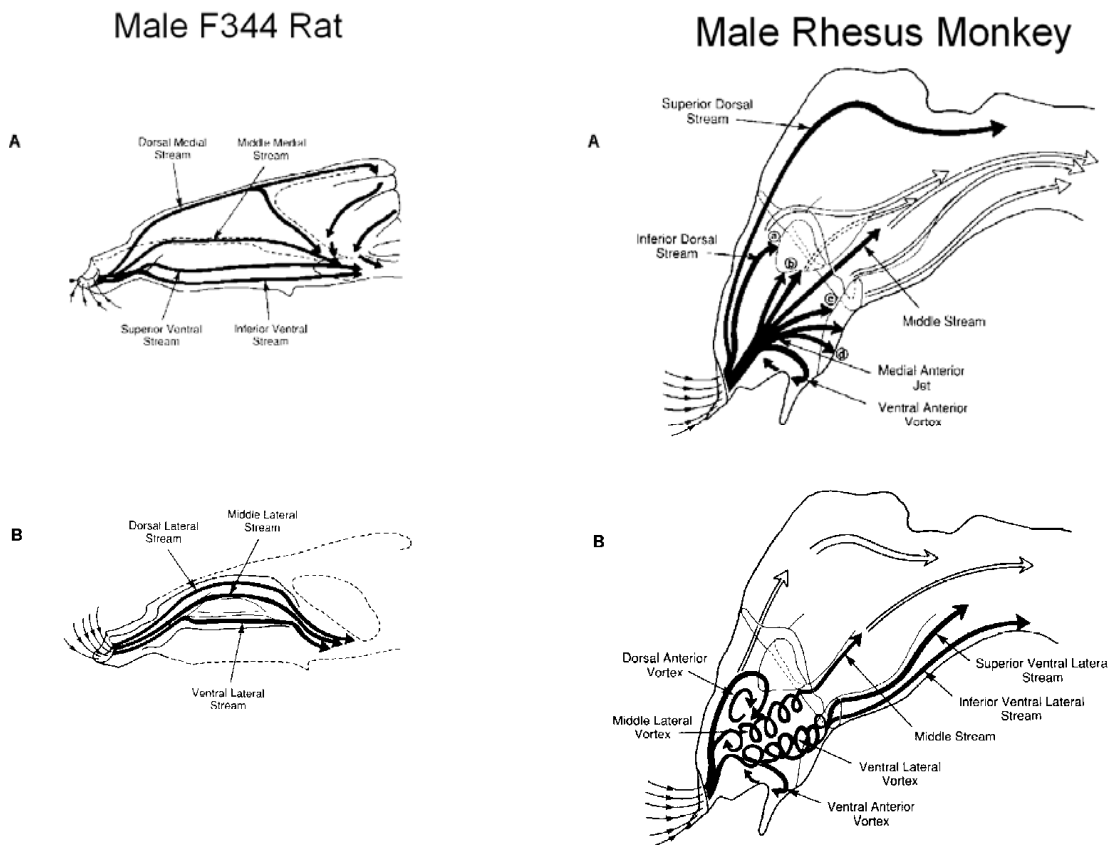

Source: Morgan et al. (1991).

Figure 3-3. Inspiratory airflow patterns in upper respiratory tract of F344 rat and Rhesus monkey. A = major medial streams; B = major lateral streams. Black and white arrows depict high and low velocity airstreams, respectively. The external nostril is to the left.

On the other hand, use of this approach for dosimetric comparisons is limited. These limitations include the accuracy, representativeness and resolution of the casting process itself and the inability to quantitatively evaluate any of the flows and flow rates observed. These limitations remained to be addressed with quantitative mathematical airflow models which are presented and discussed in the following sections.

3.4. COMPUTER MODELING OF FLUID FLOW – INTRODUCTION TO CFD

Computer modeling of fluid flow is an established technology that has been applied extensively in engineering. In general, this modeling approach, known as computational fluid dynamics (CFD), allows for quantitative prediction of all variables of fluid flow (e.g., pressure and velocity) based on the mathematical laws governing fluid behavior and, with proper software, offers a three dimensional visualization of the predicted flow. Fluids are defined to be inclusive of all substances that can flow and thus the process is applicable to both liquids and

gases. CFD and its predictions may therefore be applied to quantitatively evaluate airflow in the airways of the respiratory tract.

Regardless of the fluid flow problem at hand, the same basic procedure to develop a CFD model is followed (see Bailie et al. [2006] for a review). First, the geometry (physical bounds) and volume of the space is defined. For the airways, this step may be accomplished with high resolution CAT (Computer Assisted Tomography) or MRI (Magnetic Resonance Imaging) scans or, for laboratory animals, step-sectioning. This step is followed by dividing the volume occupied by the fluid into a mesh with numerous small but discrete cells, each cell being either uniform or non-uniform in shape. The physical modeling (e.g., motion equations) and boundary conditions are then defined and the model is solved at the level of each individual cell in the mesh. For the airways, the mesh edges (actually cells) represent the external boundaries of flow and will consist of an inlet (nares), an outlet (nasopharynx) and some form of restraining walls (lining tissues/mucus of the ET region). Modeling may be specified such that flow cannot cross these boundaries with specific values given to the inlet and outlet flow. Typically, the boundary condition is of a fixed concentration (e.g., C = 0 implies that the gas is so highly reactive that is disappears at the surface) or of a mixed type (i.e. diffusion flux in the gas is proportional to the surface concentration, implying that there is a linear, steady-state, diffusion-reaction process in the underlying tissue). If the modeling results do not meet the boundary specifications, greater or lesser inlet and outlet flows are chosen and the calculations begin all over again until the boundary specification are met or approached as closely as possible. The resulting solutions are then analyzed and presented, thereby defining the solution for the flow field, i.e., the air in the respiratory tract, with each solution having coordinates of directions and units of velocity (typically m/s).

Once the flow field is defined, a second set of equations is solved to describe the transport of the gas present within the air flow field. These transport solutions consider both convection (i.e., the gas being carried along with the air) and diffusion (i.e., gas transport due to concentration gradients). The predictions for the gas in this fluid flow presented in CFD solutions are in terms of flow or "flux"[1] usually to a surface. Flux is essentially a surface bombardment rate. Depending on the nature of the substance, each type of flow/flux has its own distinct units of measurement along with distinct physical constants. For movement of gas- (or particle-) containing air within spaces such as the regions of the respiratory tract, the units are typically for mass flux with a rate of mass flow across a unit area, e.g., $kg \cdot m^{-2} \cdot s^{-1}$.

The goal of inhalation dosimetry is to estimate dose or concentration in target tissues. Models of air flow, either dye-flow or CFD, visualize or estimate the movement of materials to

[1] *Flux* comes from the Latin *fluxus* meaning "flow".

surfaces. For the regions of the respiratory tract, flow models give estimates of the flux of materials present or entrained in the inhaled air to discrete areas. The rate of transfer across the boundary/surface (i.e. level of flux) may be regarded as an exposure to air with the agent or toxicant of concern having units of mass flow to a unit area. Thus, these model outputs may yield a quantitative estimate of materials flowing to the boundaries of their meshes (i.e., to the tissue surface) but do not afford an estimate of an actual dose to the tissue, whose units are typically mass to a volume or weight.

3.4.1. CFD Air Flow Models of the Rat ET Region- Correlation with Dye-Streamlines

The observations on fluid flow in nasal casts clearly illustrate a basis for nonuniform flow occurring throughout the ET region of the rat. Kimbell and co-workers (1997a) created a three-dimensional mesh grid reconstructed from serial step-sections of the nasal passages of a male F344 rat. The model extended from the external nares posteriorly to the nasopharyngeal meatus, nearly the same range as the acrylic casts discussed above. Computational simulations were then run to solve equations for the direction and speed of the airflow and pressure at each of the more than 143,000 nodes of the mesh. Visualization of these simulations (Figure 3-4) illustrates inspiratory air flow in the anterior nose to consist of five major streams flowing anterior to posterior as was observed in studies using clear casts of rat nasal airways: (1) ventral lateral (VL); (2) ventral medial (VM); (3) middle medial (MM); (4) dorsal lateral (DL); and (5) dorsal medial (DM). Four of these five simulated streams flowed together and then exited via the nasopharynx. These CFD simulations provided further resolution of the DM stream which flows into and out of ethmoid recesses and is itself subdivided into two components. The flow patterns of the DM stream are resolved sufficiently in the simulations to show clear structure with localized areas of high and low flows to the subtending tissues in this area, the olfactory epithelium. Simulations also revealed a portion of flow in and through the recesses in the ethmoid areas flowing in reverse, i.e., posterior to anterior. Furthermore, simulations revealed marked differences in flow rates. Flow in the ethmoid substructure was more than an order of magnitude slower than flow in interior and ventral portions of the nasal airway.

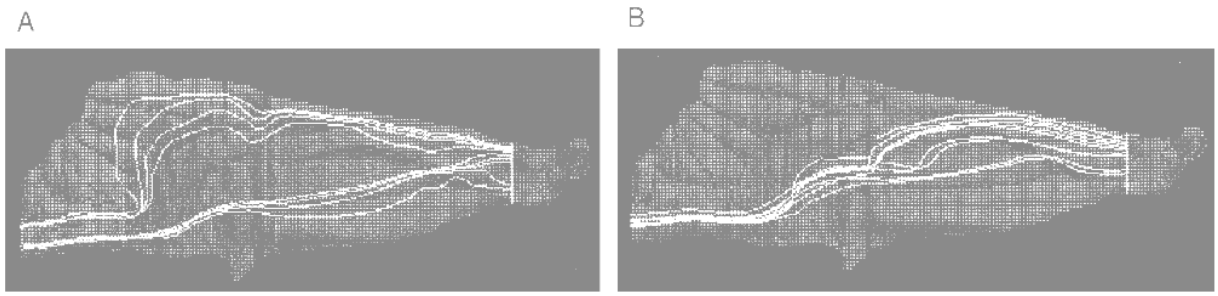

Source: Adapted from Kimbell et al. (1997a)

Figure 3-4. Major inspiratory flow streams simulated in the F344 rat nose. The external nostril is to the right. Simulated streamlines of inspiratory airflow emerging from points near the medial septal wall are shown in (A) and from points near the lateral wall in (B). Dorsal streams are to the top as shown in Figure 3-3. The simulated flow rate was 288 mL/min.

Localized volumetric flows and their apportionment were quantified by integrating the velocity component for designated cross-sections of the model. For the cross-section at a level approximately midway in the airway model, the % apportionments at a flow rate of 100 mL/min are noted in Table 3-1.

Yang et al. (2007) made similar observations using a male Sprague-Dawley rat over a range of tidal volumes.

Table 3-1. Nasal flow stream allocation in the rat and summary of CFD simulated flow apportionment (as a % of total volumetric flow) to various cross-sectional areas (as mm^2) of the ET region.

Flow stream region	Cross-sectional stream area[a](mm^2)	Flow[b] (%)
Dorsal medial	0.65	15.5
Dorsal lateral	1.15	35.6
Middle medial	0.83	29.9
Ventral lateral	0.15	0.9
Ventral medial	0.64	11.5
Total	**3.42**	**93.4**

[a] from Kimbell et al. (1993). SA refers to estimates from a cross-section of the nasal cavity, approximately midway between the anterior nares and the nasopharynx.
[b] from Kimbell et al. (1997a) [%DM = %DMS (dorsal medial stream - septum) + %DMN (dorsal medial stream – nasoturbinate)]

3.4.2. CFD Air Flow Models of the Human ET Region

The observations reported above clearly illustrate the applicability of CFD modeling techniques for resolution of flow occurring in the ET region of the rat. Two independent approaches, dye-visualized and computer-simulated, consistently revealed a high degree of complexity and nonuniformity of airflow patterns in the ET region.

The applicability of this noninvasive approach to investigate nasal airflow characteristics in humans was soon realized. Several investigators proceeded to develop intricate mesh models based on highly refined human MRI and CAT scans and to simulate and characterize flow in, through and around the ET region. Figure 3-5 presents a visual summary of three of these studies. Results analogous to those observed in rat analyses are obvious with medial, ventral, lateral and dorsal airflow streams being observed from the simulations. These simulations of flow in human ET regions also predict low flow apportionments to the dorsal regions with accompanying vortices. Increased airflow resulted in increased complexity, especially in the dorsal regions where larger and multiple vortices were simulated.

Localized volumetric flows and their apportionments were also determined in a number of these studies. The basis of these analyses was by assigned regions of the nasal tract, from dorsal to ventral, typically a total of six. A partial summary of these results is presented in Table 3-2. These results indicate a wide range of flow values to these subregions of the ET. Also, simplistic apportionment of percent flow per mm^2 surface area of these various regions can be seen to result in a range of values; e.g., from 0.12 (1.2%/9.7 mm^2) in region B as reported by Wen (2008) to 1.03 (28.7%/27.9 mm^2) in region E as reported by Keyhani et al. (1995). These composite simulated results clearly indicate a high degree of nonuniformity of flow within the human ET region and variability between models.

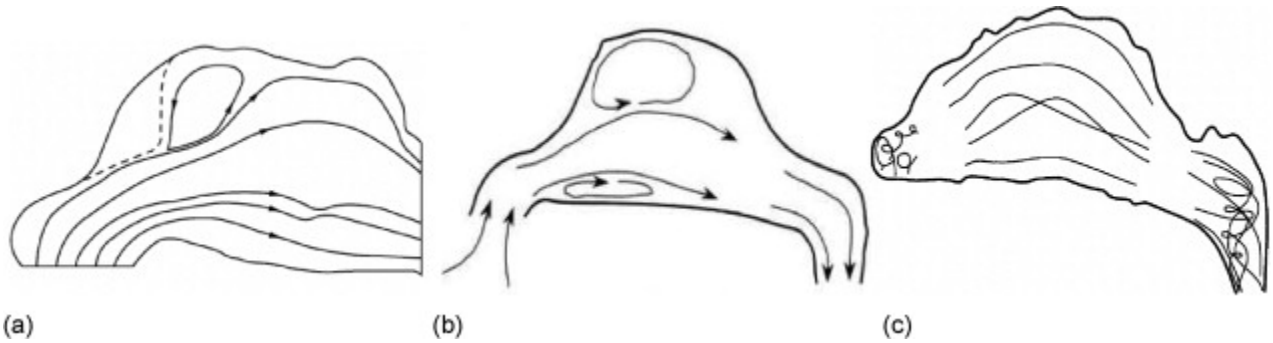

Source: Wen et al. (2008)

Figure 3-5. Representations of CFD-simulations of flow streamlines in human nasal cavitiesfrom (a) Keyhani et al. (1995), (b) Schreck et al. (1993), and Subramaniam et al. (1998). Airflow from left to right.

Table 3-2. Summary of CFD simulated flow apportionment (as a % of total at 15 L/min) on the cross-sectional area in the middle turbinate (as mm^2) of the ET region in selected human models as analyzed by Wen et al. (2008).

Regions: Dorsal (A) to Ventral (E,F)	Wen et al. 2008 (left)		Subramaniam et al 1998		Keyhani et al 1995	
	Cross-sectional area	Flow	Cross-sectional area	Flow	Cross-sectional area	Flow
A	13.7	11.6	7.9	1.9	15.6	11.4
B	9.7	1.2	15.4	1.9	6.0	3.0
C	23.2	21.4	20.8	11.3	35.5	27.3
D	21.6	20.3	54.8	46.7	27.9	18.3
E	50.3	43.7	20.5	24.4	27.9	28.7
F	42.8	1.8	28.9	13.9	26.5	11.3
Total	**161.3**	**100**	**148.3**	**100**	**139.4**	**100**

3.4.3. CFD Air Flow Models - Predictions of Reactive Gas Distribution in the ET Region

The preceding section briefly described basic aspects of CFD methodology applied to inspiratory airflow in both laboratory animals and humans. These results indicate that inspired airflow to the various areas of the ET region is highly nonuniform. Some reasons for the nonuniformity of flow have their basis in the extensive departures from unimpeded flow that airway anatomy and geometry in different species impose on the incoming airstream. This report, however, deals not directly with just flow through and out of the ET region, but more with the flow of gases as they are directed and distributed to the surfaces within the ET, especially in humans. This section is concerned with the application of CFD to address the fate of inspired gases within the upper respiratory tract.

In early efforts, Kimbell and co-workers (1993, 1997b, 2001a, 2001b; Kimbell and Subramaniam, 2001) used CFD modeling of airflow in the ET regions of laboratory animals and humans as a basis to describe disposition of inhaled gases using formaldehyde, a highly water soluble and reactive gas, as an example. These authors, and others following, began this work based on the assumption that low concentrations of a gas present in inspired air do not modify the characteristics of the air (e.g., viscosity, density) and thus do not influence airflow itself.

Although gas present in the airstream would not alter the airflow characteristics of the airstream, the airflow would have an influence on the disposition of the reactive gas through both the airflow apportionment and the molecular diffusivity of the gas. It is the molecular diffusivity of the gas that results in a net transport of mass to the surface. And it is the mass flow rates across a unit area, or mass flux, that are the predictions of CFD solutions. Thus, these authors carried out gas transport simulations by incorporating the molecular diffusivity of formaldehyde with units of cm^2/sec in air. These authors also made assumptions that limited the goal of the study to predicting the transport of the inhaled gas to the surface walls of the ET (or rather the mesh cells at the wall representing the surface wall of the ET).[1] The model simulated mass flux to the walls[1] but not into the tissues at the boundary of the mesh wall.

Results from the gas transport simulations were visualized as a contour plot of simulated formaldehyde mass flux across the nasal septum (Figure 3-6). This visualization is conceptually consistent for a highly soluble and reactive gas entering the nasal cavity along major airstreams and passing to the walls in an anterior to posterior gradient. High mass flux regions or "hot spots", were predicted to include the ventral and lateral margins of the nasoturbinate as well as the lateral wall. Conversely, low flux regions were predicted in regions more posterior to the nares and out of the major flowstreams.

The results of the study by Kimbell et al. (1993) were among the first to demonstrate the application of CFD to regional dosimetry of inhaled gases in predicting quantitative mass flux patterns to surface (mesh) walls, which acted as a sink. Consistent with other advances related to predictive dosimetry for the ET region, these results also give indications that considerable levels of nonuniformity exists across the surfaces of the ET region, in this instance for mass flux. For example, results discussed in this study indicate that maximal mass flux occurred on the lateral aspect of the nasoturbinate and the adjacent lateral wall where flux was predicted to be higher, in a few instances approaching two orders of magnitude higher, than flux on the medial surface of

[1] The walls of the mesh were modeled to act as "sinks" such that the reactive gas concentration at the walls was set to zero effectively allowing maximal uptake consequently eliminating "back pressure" or desorption to limit wall uptake.

the turbinate. These areas of high flux and their relationships to lesions will be discussed in Section 3.4.6 regarding target tissue dosimetry.

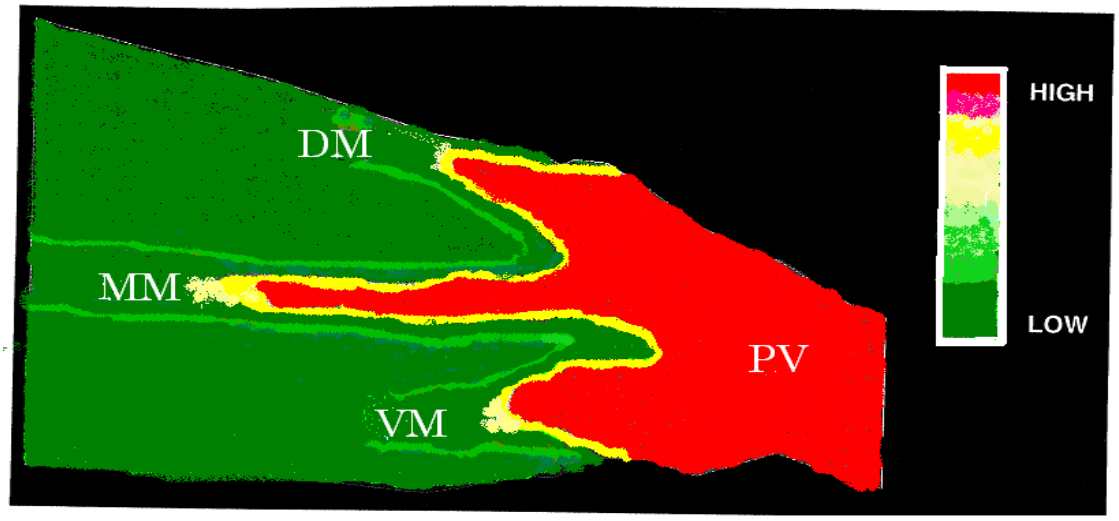

Source: Adapted from Kimbell et al. (1993).

Figure 3-6. Patterns of simulated wall mass flux of formaldehyde across the nasal septum of the rat. Red denotes regions of high flux; PV, posterior nasal vestibule; DM, dorsal medial meatus: MM, middle medial meatus: VM, ventral medial meatus. Airflow from right to left.

3.4.4. Interspecies CFD Air Flow Models Predictions of Gas Distribution in the ET Region

Subsequent to the initial studies of Kimbell et al. (1993), a number of investigators developed and published similar sophisticated models for various species and gases of different solublilites and reactivities. A listing of these studies is provided in Table 3-3.

Inclusion of studies in Table 3-3 was contingent upon a preliminary general evaluative screening of the studies and their models. All studies listed provide sufficient detail of the CFD technique to establish the accuracy of the results. These elements include the source of the geometrical representation used, as well as a description and analysis of the mesh including the basic structure and character of the individual cells of the mesh. Most also include some evaluation as to the dependency of modeling results on mesh size (cell number). Statements regarding the assumptions and simplifications made to the basic Navier-Stokes equations for calculating results were also provided.

Table 3-3. Summary of airway flow studies using CFD techniques.

References	Species	Region	Source for Mesh Construction	Purpose
Elad et al. (1993)	Human	ET	geometric model	Air flow and flux patterns, particularly to olfactory region
Tarabichi and Fanous (1993)	Human	ET	CAT scans	Airflow characteristics
Keyhani et al. (1995)	Human	ET	CAT Scans	Airflow characteristics at resting breathing rates
Bush et al. (1998)	Rat	ET (olfactory)	CAT scans	Airflow data as input to PBPK model simulating uptake in various compartments
Frederick et al. (1998)	Rat/Human	ET (olfactory)	CAT scans	Combine airflow flux with deposition patterns to determine in human olfactory tissues receives more or less than rat
Kepler et al. (1998)	Monkeys	ET (olfactory)	video image	Resting airflow rates used to model uptake of formaldehyde
Shome et al. (1998)	Humans	pharynx	anatomical model	Modeling of laminar and turbulent flow in the pharynx and its effects of morphological changes
Chometon et al. (2000)	Humans	ET	anatomical model	Determination of the separation of airflow between the meatus and olfactory regions
Sarangapani et al. (2000)	Humans	Lung	Weibel 4-lobe model	Modeling the influence of aerosol dispersion on particle deposition in lung
Bush et al. (2001)	Humans	ET	CAT scans	Modeling diffusion and uptake of ozone and chlorine in the respiratory tract using mouth and nasal breathing
Martonen et al. (2001)	Humans	ET and TB	Casting, then sliced, scanned and digitized	Development of upper airway representation for simulations of airflow and particle transport
Kurtz et al. (2004)	Humans	ET,nasopharynx	3-D model of human nose	Comparison of experimental odorant nasal absorption data in humans with simulations
Zhao et al. (2004)	Humans	ET (olfactory)	CT scans to models	Developed a method to convert CT scans of a human nose into a anatomically-correct 3-D model to predict airflow and odorant transport
Zhao et al. (2006)	Humans	ET (olfactory)	CT>3-D models	Used CT scans and CFD to determine improvement in nasal airflow and odorant delivery rates in a patient after surgery
Minard et al. (2006)	Rat	ET	MR imaging	MR imaging used to validate CFD predictions
De Rochefort et al. (2007)	Humans	lung	CT	CFD/CT used to model airflow in upper airways
Wen et al. (2008)	Humans	ET	CT	Comparisons of laminar flow patterns between the left and right nasal cavities
Corley et al. (2009)	Rabbits	ET	MR	Airflow in rabbit respiratory and olfactory epithelium

Furthermore, Kimbell et al. (2001b) constructed anatomically accurate, 3-dimensional computational fluid dynamics models of nasal passages of F344 rat, Rhesus monkey, and humans for the purposes of modeling inhaled formaldehyde. The rat and monkey CFD models were constructed from tracings of airway outlines of the right nasal passages from the nostril to the nasopharynx from serial-step sections of embedded tissue specimens (Kimbell et al. 1993;

Kepler et al.,1995). The human model was constructed from airway tracings of both sides of the nasal passages from the nostril through the nasopharynx from magnetic resonance image scans as described by Subramaniam et al. (1998).

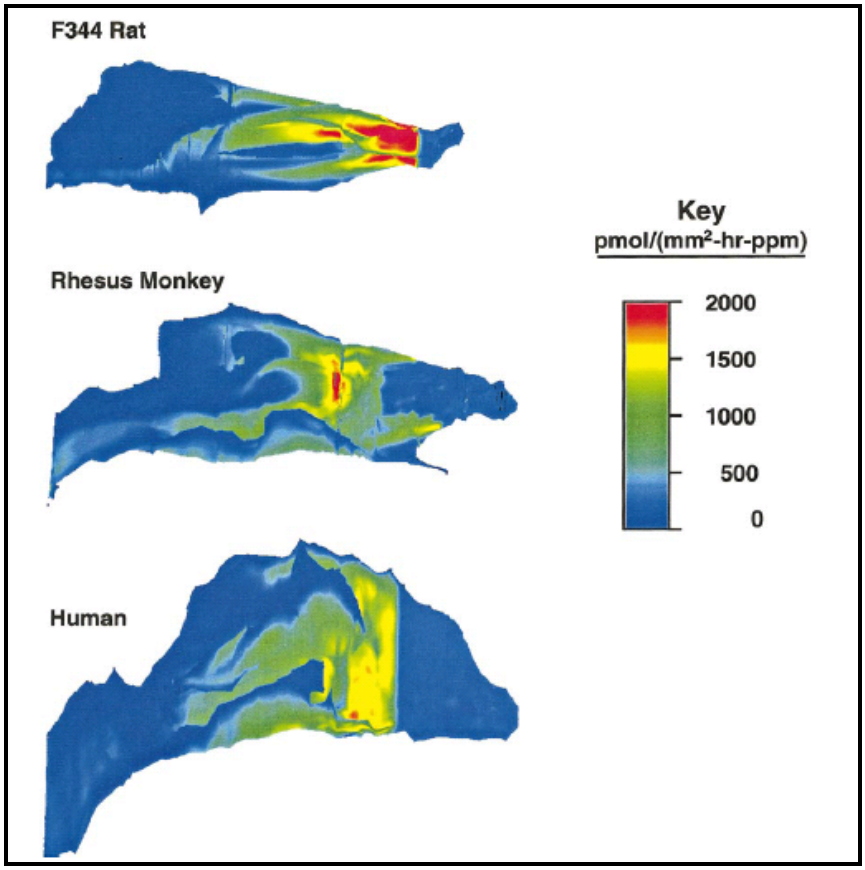

Source: Kimbell et al. (2001b).

Figure 3-7. Nasal wall flux spectra of inhaled formaldehyde simulated in rats, monkey and humans at normal inspiratory flow rates. Nostrils are to the right.

Simulations configured for uptake of formaldehyde were run for all three of the ET models, the results of which are shown in Figure 3-7. Despite the absolute difference in size, with the rat ET being 40-fold smaller than the human ET, comparative aspects regarding flux are apparent. Visual inspection of Figure 3-7 shows clearly, for example, that relative proportions of area for the highest formaldehyde flux in the ET region ("red" in color) is highest in rat, with the rank order following rat > monkey > human. The authors estimated both maximum and average areas of formaldehyde flux over the whole ET in each species in which the maximum:average flux ranged from 3- to 10-fold among these three species (Table 3-4).

Table 3-4. Estimates of formaldehyde flux to ET surface walls for various species.

Formaldehyde flux estimate(pmol/[mm^2-hr-ppm])[A,B]			
Area	**Rat**	**Monkey**	**Human**
Whole nose: maximum	3210	4492	2082
Whole nose: average	336	508	568
Maximum/Average	**10**	**9**	**4**
Nonsquamous: maximum	2620	4492	2082
Nonsquamous: average	284	535	611
Maximum/Average	**9**	**8**	**3**

Source: Adapted from Kimbell et al. (2001b).

[A]Simulations conducted at inhaled concentration of 1 ppm formaldehyde.
[B]Simulations conducted at flow rates of twice the minute ventilation for rat (576 mL/min), monkey (4.8 L/min), and human (15.0 L/min).

3.4.5. Range and Distribution of Flux in ET Regions for Various Species

The general ranges of rat and human flux in the ET region estimated from visual inspection in Figure 3-7 and from the average and maximum ranges in Table 3-4 were further analyzed by Kimbell et al. (2001b). The ET regions for each species were first partitioned into 20 evenly spaced flux levels between zero and the maximum predicted flux value for each species; 2620 pmol/(mm^2 –hr-ppm) at a flow rate of 576 mL/min in the rat and 2082 pmol/(mm^2 –hr-ppm) at a flow rate of 15 L/min in the human. Surface areas of the ET found to be within these flux levels were then assigned or "binned" accordingly. This strategy allowed for estimating the distribution of flux levels over the surface area of the ET, each species being "normalized" to its respective range of flux. The binning revealed that flux values higher than half the maximum flux value (flux median) were predicted for nearly 20% of human ET surfaces whereas only 5% of rat ET surfaces were associated with fluxes higher than flux medians. This relationship was maintained for flux levels higher than 75% of the maximum flux value with approximately 1.8% of human but only approximately 0.6% of rat ET surfaces were exposed to this higher level of flux. Distribution within the ET region of what may be considered "high" flux will be examined in the next section in relation to actual occurrence of lesions in the ET region.

3.4.6. Correlation of High Flux with Lesions in the ET Region

The information discussed and presented thus far in this section on uniform vs. nonuniform airflow in the ET region has been for simulations, either *ex vivo* with water-soluble dyes through clear acrylic casts of ET regions or *in silico* using elaborate CFD models based on

tracings or scans of the ET regions. These modeling approaches have given very similar and internally consistent results concerning patterns and distributions of airflow and gases in the ET region of various species, including humans. Supporting empirical observations would, however, provide a more robust basis for these modeling results.

One logical strategy that could provide support and reinforcement for the modeling results would be to examine the extent of correlation between flux and lesions. More specifically, such an activity would involve localization of areas in the ET region modeled to experience high flux from an inspired gas and then examine the extent of correlation of these areas with actual lesions, both in incidence and severity, observed in response to *in vivo* exposures to the same gas. With flux regarded as a surface bombardment rate, flux of dilute gas in air to ET surfaces could be reasonably anticipated to exhibit some degree of a dose-response relationship. There are currently several examples of such a correlation analysis in the current literature. Results from two of these studies, formaldehyde (Kimbell et al., 1997b) and hydrogen sulfide (Moulin et al., 2002), are summarized here.

Kimbell and colleagues (1997b) investigated the relationship between squamous metaplasia and areas of high formaldehyde flux in the nasal tissues of adult rats. They first performed a pathology analysis on the incidence of squamous metaplasia in specific areas of the nasal tracts of rats that had been exposed via inhalation to formaldehyde at 0, 0.7, 2, 6, 10 or 15 ppm for 6 hr/d, 5 d/wk for 6 months. These specific areas, primarily the lateral meatus and mid-septum of the anterior portion of the nose, known to have extensive distributions of target tissue, were observed for analysis by making a transectional cut at the midline. The perimeter of the airway opening revealed by this cut was then divided into 20 regions based on anatomical landmarks and the location of major airflow streams. The sectioned head of a male rat was then used to generate a computational mesh for CFD analysis with normal squamous epithelium mapped onto the walls of the mesh such that this tissue was a defined area on the airway walls of the CFD model. Transport of formaldehyde through the air and into the nasal epithelium was assumed by the model to occur by convective forces and molecular diffusion. Incidence of squamous metaplasia was then calculated for each region and flux values modeled for each region, both ranked high to low and statistically analyzed for correlation. The results, shown in Figure 3-8, provide clear evidence that, at high flux levels (and high exposures) of formaldehyde, the distribution of squamous metaplasia is related closely to the location of regions of high formaldehyde flux into airway walls.

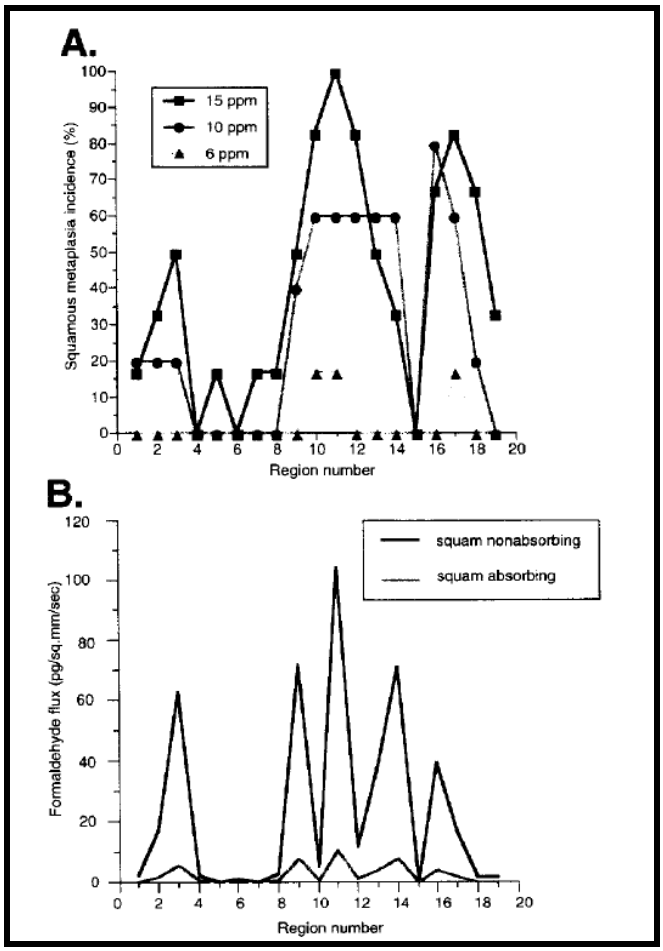

Source: Kimbell et al. (1997b).

Figure 3-8. Graphs showing (A) the incidence of formaldehyde-induced squamous metaplasias and (B) modeled formaldehyde flux values along regions assigned to the perimeter of a transected nasal airway of rats.

Moulin et al. (2002) used a similar approach to investigate the relationship between lesions in olfactory epithelia and areas of high hydrogen sulfide flux in the nasal cavity of adult rats. They also performed a pathology analysis on the incidence of lesions (olfactory neuronal loss and basal cell hyperplasia) in two transverse nasal sections, one directly through the ethmoid turbinates, obtained from adult male rats (n = 12/concentration) that had been exposed to hydrogen sulfide at either 0, 10, 30 or 80 ppm for 6 hr/d for 70 days. The CFD model used consisted of a 3-dimensional nasal airway reconstruction of a mesh from serial cross sections of an adult rat which provided a simulation of flow and mass transport through the entire airway. Flux predictions were made at the same level of the transverse nasal section (through the ethmoid turbinates) that had been demarcated around the perimeter into 39 regions. Transport of hydrogen sulfide through the air and to the nasal epithelium was assumed by the model to occur

by convective forces and molecular diffusion. The incidence of olfactory lesions and flux levels for 80 ppm hydrogen sulfide were then calculated for each of the 39 regions. Rank correlations between lesion incidence and flux were than carried out. Distinct hot spots of regional flux occurred in the ethmoid turbinate section at those regions corresponding to high airstream flow. These results are presented in Figure 3-9. These regions of high flux were closely associated with hydrogen sulfide-induced nasal lesions if that region was lined by olfactory epithelium. An additional observation made regarding high hydrogen sulfide flux was that pathology was not observed in those regions that were lined with respiratory rather than olfactory epithelium. This lack of correlation between high flux and non-olfactory epithelium lesions is apparently due to resistance of this tissue to hydrogen-sulfide toxicity.

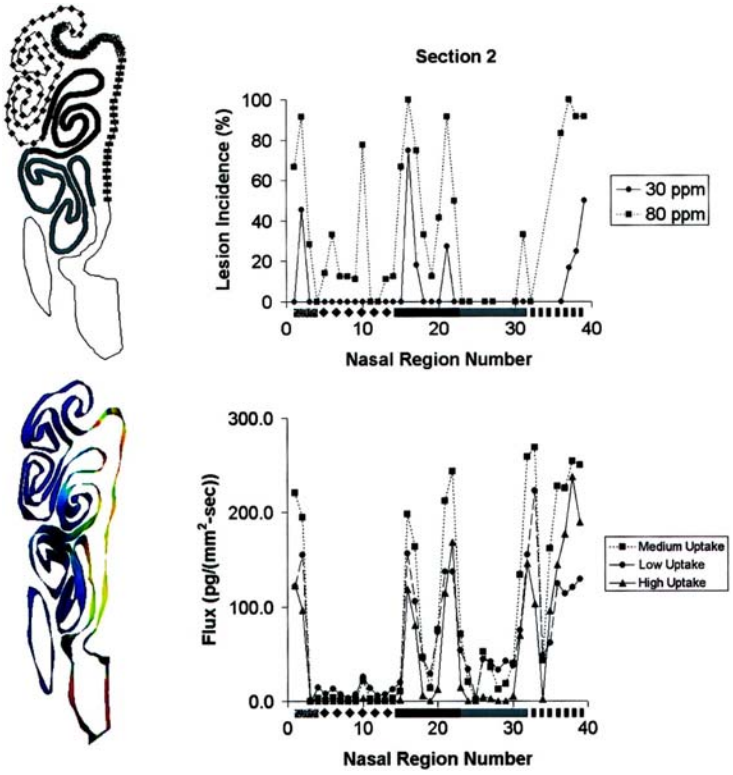

Source: Moulin et al. (2002).

Figure 3-9. Schematic diagram of the transverse nasal section through the ethmoid turbinates (top left, Section 2 of the nasal cavity) with plot of lesion incidence at 30 and 80 ppm (top right). Note coding of surface areas in schematic to the x-axis of plot. Plot of predicted hydrogen sulfide flux under different assumptions of uptake: low – 20%, medium – 40%, and high – 80% (bottom right). Diagram of same section (bottom left) under intermediate uptake conditions at 80 ppm where red corresponds to 320 pg/(mm^2-s) and blue corresponds to 0 pg/(mm^2-s). Plot of predicted flux at 80 ppm (bottom right) on designated regions of Section 2.

Similar correlations between lesion incidence and tissue dose were also observed for acrolein (Schroeter et al., 2008) and diacetyl (Morris and Hubbs, 2009). For acrolein, predicted air:tissue flux from the rat nasal CFD model compared well with the distribution of nasal lesions observed in a subchronic inhalation study. In the case of diacetyl, a strong correlation of injury location and pathology severity scores with CFD-PBPK hybrid model predicted tissue concentrations was observed in nasal tissues.

These examples provide strong support for a direct relationship between flux and responses in tissues in four independent cases. The hydrogen sulfide case offers resolution sufficient to demonstrate expected target tissue specificity as responses were only seen in olfactory epithelium despite equivalent flux levels in more proximal respiratory epithelium. Also, in the case of formaldehyde, the relationship between flux intensity and response appears to be one in which high flux is more predictive of lesions than are low flux levels (i.e., either appreciably above or below the median flux level). A similar relationship between flux intensity and response was observed with acrolein. These additional observations indicate the flux-response relationship to have a high degree of resolution as well as providing predictability of a dose-response relationship. The predicted nasal tissue concentrations of diacetyl corresponded with lesion location and severity. Thus, results from these four examples may be regarded further as providing compelling support for a close correlation between flux and tissue-specific responses.

In summary, the intent of this portion of the report is to bring forth and discuss recent findings that inform short comings with the basic assumptions following from the use of $\dot{V}_E/SA_r$, and in particular $\dot{V}_E/SA_{ET}$, as the basis for default interspecies dosimetry of inspired gases. Chapter 2 presented the reasoning behind the use of $\dot{V}_E$ as a surrogate for gas dose and use of SA_r for normalization of dose along with acknowledgment of the general advancement this concept made to inhalation dosimetry. Figure 3-10 provides an illustrative summary and perspective of what this chapter has presented regarding the default procedure. This figure illustrates the processes and assumptions of uniformity underlying $\dot{V}_E/SA$ originally shown in Figure 3-1 The composite evidence and results from this information indicate nonuniform character of flow, of surface areas, and of deposition for gases in the ET region.

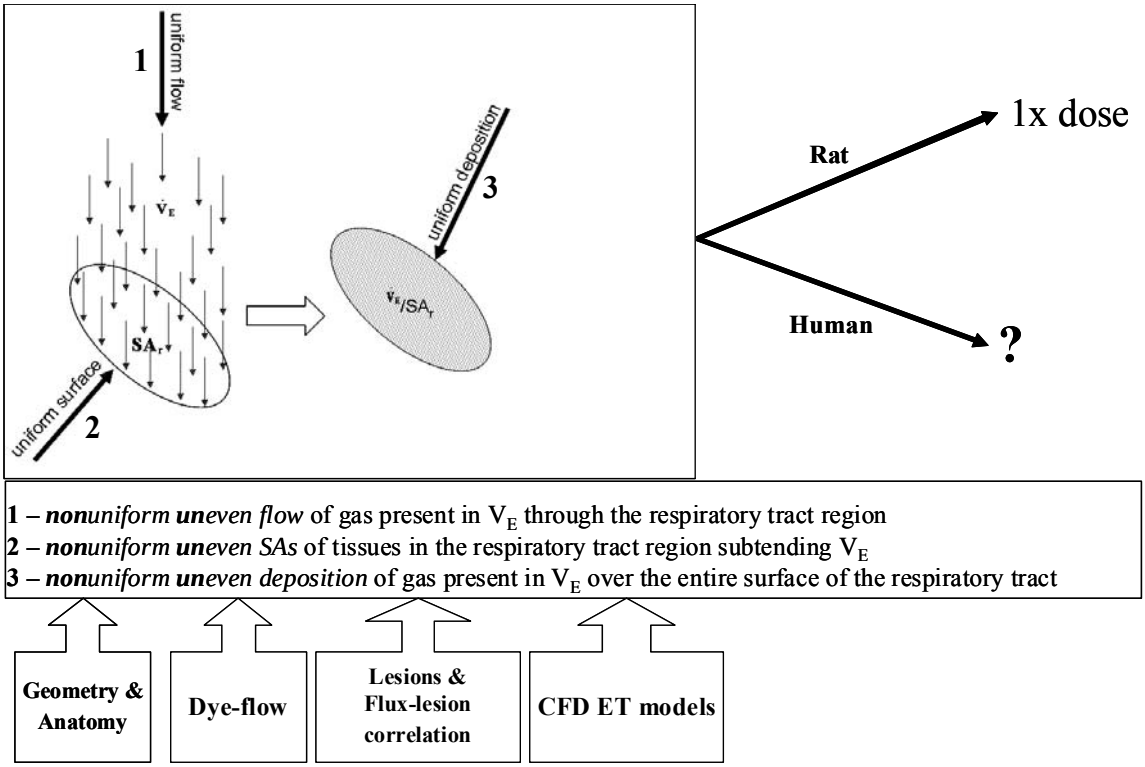

Figure 3-10. Representation of application of current information to the processes, assumptions, influences and outcomes for *RfC Methods* basic default procedures for comparative gas dosimetry. The text-containing arrows below the figure represent the information presented in this chapter that has addressed the assumptions of uniformity. The arrows and labels extending to the right demonstrate the outcome of applying this information to the overall process introduced in Figure 3-1.

Thus, more extensive evaluative tools will need to be used to integrate newer information to the end of making more informed estimates of interspecies dosimetry. These tools and the results from their application are the principal subject of Section 3.5 of this report.

3.5. EVALUATION AND USE OF MODELS IN INTERSPECIES INHALATION DOSIMETRY

As discussed previously, the default RfC method for interspecies dose-extrapolation for the ET region is determined by the ratio $\dot{V}_E/SA_{ET}$ of animals to humans. When applied for an interspecies comparison with rats, for example, the calculation results in a RGDR of approximately 0.2, indicating that the inhalation delivered dose to humans is at least fivefold greater than to the rat.

Evidence indicates that flow and distribution of $\dot{V}_E$ in the respiratory tract is not uniform, and that CFD modeling offers refined and characterized disposition of airflow and of the gases present in $\dot{V}_E$. Also, CFD offers resolution only to the surface of the tissues in contact with the flow. It does not and cannot offer resolution of interspecies tissue dosimetry, that is, the concentration of the gas in the target tissues of the respiratory tract.

The purpose of this section is to present new information that relates these basic issues of dosimetry in the airways, i.e., flux of gas to the tissue surfaces and the concentration of gas in the airway tissues. The focus of this section is on the results and insights gained from the combination of modeling approaches of CFD on airflow and gas disposition in the airways with the state-of-the-science developments from physiologically-based pharmacokinetic or PBPK models describing pharmacokinetics in respiratory tract tissues.

Various models have been developed and utilized to examine and quantitatively estimate dose to target tissues via the inhalation route of exposure in both animals and humans. As discussed above, 3-D, anatomically accurate CFD models were developed to model inspiratory airflow and estimate regional uptake and amount of inhaled gas reaching sites in the nose, with formaldehyde serving as the vanguard example for this application (Kimbell et al., 2001a, 2001b, 1997a, 1997b, 1993; Kimbell and Subramaniam, 2001). One output of these simulations is an estimate of flux which is the rate of mass transport in the direction perpendicular to the nasal wall, typically with units of pmol/(mm^2-h-ppm). In this regard, the CFD model estimates a "dose" of gas delivered to the tissue boundary but not into the tissue itself. CFD modeling simulations can also be utilized to estimate the surface area and volume of specific anatomical features, the allocation of inspired air to specific flow streams, and gas phase mass transfer coefficients (Kimbell and Subramaniam, 2001). While representing a major step forward in describing and refining interspecies inhalation dosimetry compared to the current default RfC methods, the nature of CFD model output (in terms of flux) does not provide a definitive measure of target tissue dose. Developments in tissue physiology and kinetic models, however, have provided this information and allow for more refined and accurate dosimetry in and between species. Combination of these two modeling approaches led to the development of CFD-PBPK hybrid models allowing for the most highly refined and accurate estimates of target tissue dose currently available.

3.5.1. Overview of CFD-PBPK Hybrid Modeling – Combination of Gas Transport in the Air Phase into the Liquid/Tissue Phase

CFD-PBPK hybrid modeling represents the state-of-the-art science for examining inhalation dosimetry. As discussed in Bush et al. (1998), combined CFD and PBPK models were

developed to help address how factors related to airway anatomy might be a reason that other models assuming uniformity, such as the ventilation-perfusion model, failed to fully explain the effects of gas flow on total vapor uptake in different animal species. As discussed above, the CFD models developed by Kimbell and colleagues (1997a, 1997b, 1993) helped to address toxicant transport in the gas phase. The PBPK model developed by Morris et al. (1993) was an attempt to account for toxicant transport in airways and tissue by dividing nasal flow into multiple streams and the nasal epithelial compartments into tissue stacks, but its modeling of the gas phase was less exact than that of CFD. Consequently, Bush and colleagues (1998) developed a hybrid model based on combining these two aspects, the CFD model for consideration of gas disposition in the air phase and the PBPK models for consideration of gas disposition into the liquid and tissue phases within the rat nose.

Bush et al. (1998) proceeded to utilize the CFD model of flux distributions to determine the distribution of air flow and gas phase mass transfer coefficients along the four major flow paths (i.e. the DM, DL, MM, and VM) in the rat nose to predict gas transport to the surface (actually a modeling "boundary"; see below) of the underlying nasal tissues. The VL was combined with the adjacent DM because the CFD simulations revealed that the VL only carried about 1% of the inhaled flow. Using these solutions to guide the PBPK model development, these authors subdivided the four flow paths into four distinct meatuses such that each contained a major air flow stream predicted from CFD simulations. The underlying tissues in these meatuses were then further divided into four serial regions attached to a tissue stack containing mucus, epithelial, and subepithelial compartments. The steady state diffusion equations governing these 16 airway regions and associated tissue stack compartments constituted the PBPK portion of the model. The PBPK and CFD models were coupled at the gas-tissue phase interface by a permeability coefficient – termed K_{gm} – that incorporated the gas phase mass transfer coefficient (k_g) with a mucus phase diffusion parameter. A graphical representation of this approach, including areas of airflow and composition of tissues stacks modeled is presented in Figure 3-11. Similarly structured models to predict interspecies gas dosimetry have been described for both the rat and human nasal regions for other gases including vinyl acetate (see Bogdanffy et al. 1999).

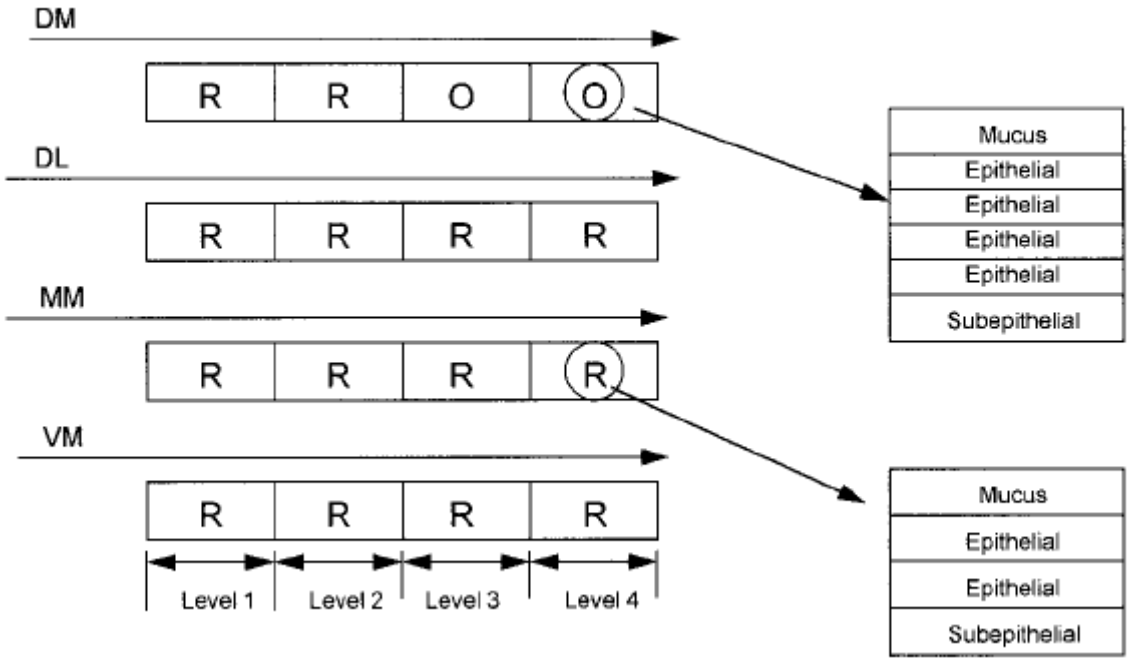

Source: Bush et al. (1998).

Figure 3-11. Schematic of the CFD-PBPK hybrid model of the rat nasal cavity. This model divides the tissue into four serial levels along the DM, DL, MM, and VM flow paths. Each of the resulting 16 tissue stacks is classified as either respiratory (R) or olfactory (O). The exploded views of R and O tissue stacks indicate their internal compartmental structure.

The model and its predictions were then validated by using overall uptake data from rat inhalation studies for three nonreactive vapors that were either completely inert (acetone), reversibly ionized in aqueous media (acrylic acid), or prevented from being metabolized by an enzyme inhibitor (isoamyl alcohol). This CFD-PBPK hybrid model was thus parameterized and validated with empirical observational data to model actual uptake into tissues such that actual tissue concentration of the test case vapors could be predicted.

The results of this modeling work showed variation of surface area, cross-sectional area, and values of k_g along the differing flow paths among the regions, reflecting the convoluted nature and complexity of the rat nasal geometry. The overall uptake predicted by the CFD-PBPK model for the toxicants was not sensitive to the exact value of k_g estimated by the CFD analysis even when reduced by 95% or made essentially infinite. Moreover, as one component of K_{gm} (the coefficient governing the mass flux of gas from the flowstreams into the underlying mucus compartments), increasing k_g had little effect on the concentration or uptake distribution of gas into the first epithelial layer. In fact, when k_g was simulated in the model to be sufficiently large to remove the mass transfer resistance of the gas phase, the uptake of both acetone and acrylic

acid was limited by the rate of diffusion in the mucus and tissue despite a 30-fold difference in their solubilities. These results suggest that, in the rat, diffusion through the gas phase is so rapid relative to diffusion through the mucus and tissue layers that it does not influence the rate of gas absorption. This observation allowed for a simplifying assumption to be made that a compartmental k_g value can be determined by averaging the local values obtained by CFD analysis for those airway sections that constitute the compartment (e.g., respiratory and olfactory). As further discussed in Frederick et al. (1998), a "compartmental mass transport coefficient" (i.e., one k_g value per tissue compartment) used in this context should be derived and defined as an "average mass transfer coefficient" based on a difference in "average compartmental concentrations." This derivation and definition is required when the compartments of the PBPK model are commonly described as "well-mixed", and the results of the CFD simulations need to be appropriately expressed so that the "average air compartment concentration" derived from CFD is defined as the same way as the "average tissue compartment concentration" in the PBPK model.

3.5.2. CFD-PBPK Hybrid Modeling and the Overall Mass Transport Coefficient - K_g

In the hybrid modeling approach described by Bush et al. (1998), the PBPK and CFD models were coupled at the gas-tissue phase interface by K_{gm}. The aim of this approach was to determine the regional dose within the respiratory tract by characterizing the transport of gases between the air phase, the intervening surface liquid and tissue, and the blood. K_{gm} is also referred to as the overall mass transport coefficient or K_g.

As described in Appendix I of the *RfC Methods*, the concept of K_g (the overall mass transport coefficient, MTC) is used to describe transport through several different phases including air and liquid. The most definitive evaluation of transport is to describe absorption by a simultaneous solution of the conservation of momentum and mass in the complex 3-D airway and tissue structure. For purposes here, however, the concept of K_g as a two phase MTC based on the physicochemical properties of the gas may be used to direct development of model structures adequate for estimation of regional gas dose. The structure of the two-phase mass transport model may be further simplified to a minimal number of parameters that may be scaled to gases differing in their physicochemical properties. The basic structure of this approach, which relies on K_g, was used in the CFD-PBPK hybrid models developed by Bush et al. (1998) and subsequently by Frederick et al. (1998), both of which incorporate the output from CFD simulations to describe anatomy, airflow, k_g, and flux of inhaled gas in the portal-of-entry (air phase) linked to a PBPK model describing the systemic compartments (tissue phase).

The basis of the CFD-PBPK hybrid model is very similar to the approach described in Appendix I of *RfC Methods*. There, the respiratory tract is simplified into a two-phase resistance model (because it is applied as an inverse function, K_g may be viewed as a measure of resistance) to illustrate the overall mass transport approach in which it is assumed that the blood concentration is constant. For highly soluble and very reactive gases, such as formaldehyde, the blood concentration has been assumed to be zero. This type of "boundary condition" is used, for example, in the CFD simulations for formaldehyde (Kimbell et al., 2001b) and acrylic acid (Frederick et al., 1998) in which the concentration of gas in the nasal airway lining is zero, so that transport of the gas occurs primarily through the air phase to the surface-liquid/tissue interface but not into the tissue phase. Thus, for this approach, it is assumed that the surface-liquid and tissue phases are a single phase because of the limited data to identify differing transport parameters for these two phases.

Bush et al. (1998) and Frederick et al. (1998) provide an updated and modified version of the approach presented in Appendix I to describe gas phase mass transport in which the estimate of the overall transport or flux, N, across and air:liquid interface is expressed by

$$\mathbf{N = K_g (C_g - C_\ell/P)} \qquad \textbf{Equation 10}$$

where K_g (cm/min) is the overall mass transfer coefficient, C_g (µmol/cm^3) is the air phase gas concentration, and C_ℓ (µmol/cm^3) is the concentration in the liquid/tissue phase, and P (unitless) is the surface liquid/tissue:air partition coefficient.

In general, the overall mass transport coefficient, K_g, from the air phase into the liquid phase may be determined from the transport coefficients of each individual phase, such that

$$\mathbf{1/ K_g = 1/ k_g + 1/(P*k_\ell)} \qquad \textbf{Equation 11}$$

where k_g (cm/min) is the gas phase mass transfer coefficient as defined above, and k_ℓ (cm/min) is the liquid phase mass transfer coefficient. Contextually, K_g may be considered analogous to a tissue clearance term used in compartmental pharmacokinetic studies as similar principles apply (Frederick et al., 1998). In the case where the surface liquid and tissue cannot be assumed to be a single compartment, a separate partition coefficient and transport coefficient would need to be incorporated to account for additional compartments. For example, in cases where gas diffuses through the tissue into the blood and contributes to overall absorption, additional mass transport resistances must be considered to describe this additional compartment. This is important because significant accumulation and recirculation of gas in the bloodstream may reduce the concentration driving force (and thereby reduce the absorption rate) and contribute to the

development of a "back pressure", which may result in desorption during exhalation due to the reversal in the concentration gradient between the air and tissue.

Following in this approach, k_g can be estimated by CFD simulations at several representative inhalation flow rates with CFD models and species-specific meshes for the differing nasal geometries of species using defined boundary conditions for the nasal cavity (Frederick et al., 1998). For example, by conducting CFD simulations assuming that (1) P is very large to establish a "$C_l = 0$" boundary condition such that $k_g \approx K_g$; (2) that the compartment is well-mixed; and (3) that there is negligible change in airflow across the compartment, a compartmental k_g, designated k_{gc}, can be calculated. Thus, k_{gc} describes the compartmental clearance of gas from the gas phase. In addition, data from CFD simulations at various flow rates for each species can be used to calculate k_{gc}, since the regional flow, surface area, and fractional penetration can be evaluated for any defined compartment of the nasal mesh.

A K_{gc}, overall mass transfer coefficient from the gas phase, can now be estimated that combines a compartmental mucus phase transport coefficient k_{mc} (analogous to k_ℓ in the definition of K_g – Equation 11) with the gas phase mass transport coefficient k_{gc} calculated from CFD simulations such that:

$$\mathbf{1/ K_{gc} = 1/ k_{gc} + 1/ (P*k_{mc})} \qquad \textbf{Equation 12}$$

The mucus phase mass transport coefficient, k_{mc}, (and thus, by analogy, k_ℓ) can be calculated as described by Bush et al. (1998) to describe transport to the midpoint of the mucus layer:

$$\mathbf{k_{mc} = D_{muc}/(\ell_{muc}/2)} \qquad \textbf{Equation 13}$$

where D_{muc} (cm^2/min) is diffusivity of the compound in the mucus (liquid) phase, and ℓ_{muc} (cm) is the thickness of the mucus phase diffusion layer.

The definition of the overall mass transport coefficient provided in Equations 11 and 12 may be used to evaluate the conditions in which a single phase, either gas phase or surface-liquid/tissue phase, determines the overall mass transport coefficient. Gas phase controlled absorption (i.e., $k_g << P*k_\ell$ in Equation 11) is typical for a gas considered reactive and/or relatively soluble in both the tissue and blood in which the transport resistance through the gas phase, $1/k_g$, may be greater than the transport resistance in the other phases such that

$$\mathbf{1/K_g \equiv 1/k_g} \qquad \textbf{Equation 14}$$

The gas phase term, k_g, is dependent on flow rate, flow geometry, and the gas phase diffusivity. In interspecies comparisons, the flow geometry differences of the species are likely

to predominately determine k_g as demonstrated in Frederick et al. (1998). Using values of K_g or K_{gc} obtained in a single species, K_g can be scaled within the species for a different gas by decomposing K_g to the individual transport resistances (i.e., the gas phase and surface-liquid/tissue phase mass transport coefficient).

Liquid phase controlled absorption (i.e., $Pk_{\ell} < k_g$) is typically identified by a gas of moderate to low water solubility and low reactivity. In the case of a nonreactive gas, Pk_{ℓ} may be approximated by the surface-liquid/tissue:gas partition coefficient, the liquid diffusivity (D, cm^2/min), and the thickness of the liquid-tissue layer (ℓ, cm) such that

$$P_{k\ell} \equiv P * [D/(\ell/2)] \qquad \textbf{Equation 15}$$

An initial difficulty identified in the *RfC Methods* in using such approaches, i.e., to determine or decompose an empirically founded K_g, was lack of k_g values in airways of laboratory animals (and humans), and the lack of a data base in which Pk_{ℓ} could be determined. However, much of this difficulty has been overcome and resolved by the advancement and validation of CFD models to obtain estimates of k_g as the gas phase term is dependent on flow rate, flow geometry, and the gas phase diffusivity. In cross-species comparisons, the flow geometry differences of the species are likely to predominately determine k_g. For both CFD and PBPK models, the increase in the amount of data available from various sources defining the gas and water diffusivities, and partition coefficients for many compounds, as well as parameters such as tissue surface area, thickness, volume, air flow, etc., used to describe the anatomical and physiological "compartments" in both animals and humans has aided in advancing these approaches. Several of the models represented below use k_g values determined specifically for that study or the compartmental (or regional) k_g values determined by the CFD simulations conducted by Frederick et al. (1998) for both animals and humans for the purpose of describing interspecies inhalation dosimetry.

3.5.3. Results and Analysis of Interspecies Inhalation Dosimetry Modeling

The purpose of this section is to provide an example-based overview of concepts related to the various aspects of inhalation gas dosimetry discussed in the preceding sections. Table 3-5 provides information for various gases including primary toxicological endpoint(s), measured nasal uptake in the rat (if available), as well as water solubilities and partition coefficients. This information was used to provide a physicochemical descriptor for each gas based on the scheme outlined by Medinsky and Bond (2001). Table 3-6 provides some data on the comparative calculated or modeled K_g and k_g ratios between animals and humans for each of these gases. Finally, Table 3-7 compares the various methods for interspecies dose-extrapolation (i.e.,

determination of the HEC) between animals and humans for the ET region based on CFD, CFD-PBPK hybrid, or PBPK modeling for these gases to the default RfC method based on $\dot{V}_E$ /SA. In addition, the most informative results from the CFD-PBPK hybrid model developed for acrylic acid are discussed.

In comparing these physicochemical properties, reactivity, and measured uptake for the representative gases shown in Table 3-5, a general pattern emerges. Those gases with high uptake (>90% - formaldehyde, acrylic acid) in the ET region are reactive, have higher liquid/tissue:air partition coefficients (P), and water solubility. Reactive gases with moderate uptake (acrolein, acetaldehyde, and diacetyl) in the ET region have moderate to low liquid/tissue:air P values and water solubility. Gases with low uptake (<25% - hydrogen sulfide, ethyl acrylate and propylene oxide) have among the lowest liquid/tissue:air P values in this group of gases. However, these gases also exhibit a range of water solubilities and reactivities. In general, high ET uptake gases tend to be more reactive and scrubbed more efficiently in nasal tissues with little penetration to the lower respiratory tract and less potential for systemic distribution. Likewise, low ET uptake gases have the potential to reach the lower respiratory tract and produce an effect and/or be more readily distributed systemically via the gas exchange area of the lung. An important consideration in examining the relationship among these properties and uptake is that they are substantiated by experimental observations of uptake in the rat. In addition, these generalities are to some extent illustrated when comparing the CFD-predicted flux values for formaldehyde, acrolein, and hydrogen sulfide. As shown in Tables 3-5 and 3-7, formaldehyde, the gas with the highest uptake, water solubility and reactivity, has the highest modeled flux values compared to acrolein and hydrogen sulfide. Taken together, such information may help one predict in which region of the respiratory tract a given chemical may preferentially produce an effect or if the chemical might instead or also produce systemic effects.

Table 3-5. Primary toxicological endpoint(s), uptake, properties, and physicochemical descriptor for representative gases

	Endpoint/ Effect	[A]Uptake in Rat	Liquid/tissue: air P values	Water Solubility	[B]Physico-chemical Descriptor	References
Formaldehyde	RE[C]Tumors and squamous metaplasia	> 90%	72,000 (calculated)	400 g/L	soluble-reactive	Kimbell et al. (2001b)
Acrylic Acid	OE degeneration	> 90%	6,100	1000 g/L	soluble-reactive	Frederick et al. (1998); Andersen et al. (2000)
Acrolein	OE degeneration and atrophy	80– 60%	88 (or 200)	212 g/L	soluble-reactive	Schroeter et al. (2008); Morris (1998)
Acetaldehyde	RE and OE degeneration	80– 40%	140	1000 g/L	soluble-reactive	Teegaurden et al. (2008); Dorman et al. (2008); Morris et al. (1997)
Diacetyl	Nasal, tracheal, bronchial toxicity	76– 36%	550	200 g/L	soluble-reactive	Morris et al. (2009)
Vinyl Acetate	OE degeneration	93– 40%	29	20 g/L	nonsoluble-nonreactive	Bogdanffy et al. (1999)
Hydrogen Sulfide	OE degeneration and necrosis	26– 18%	2.8	4-5 g/L	nonsoluble-nonreactive	Schroeter et al. (2006)
Ethyl Acrylate	OE toxicity	18– 25%	86	15 g/L	nonsoluble-nonreactive	Sweeney et al. (2004); Frederick et al. (2002)
Dimethyl Sulfate	Nasal tissue tumors	NA[D]	100	28 g/L	moderately soluble-reactive	Sarangapani et al. (2004)
Propylene Oxide	RE hyperplasia and OE degeneration	11– 23%	68	590 g/L	moderately soluble-reactive	Csanady et al. (2007); Morris (2004)

[A]Uptake – measured percent of inspired vapor that is retained or deposited in the URT of the rat
[B]Physicochemical Descriptor from Medinsky and Bond (2001) (see text for details)
[C]RE = respiratory epithelium; OE = olfactory epithelium
[D]NA = not available

However, these generalizations do not always hold. For example, propylene oxide has less nasal uptake than might be predicted based solely on its water solubility and/or reactivity and comparable liquid/tissue:air P to that of acrolein, thus highlighting its hazard categorization. Conversely, the nasal uptake of vinyl acetate is greater than might be predicted based on those same two properties as well as its relatively low liquid/tissue:air P. In the case of vinyl acetate, nasal metabolism via carboxylesterase greatly enhances its uptake into nasal tissues and also

plays a role in its toxicity. Yet, the primary toxicity induced by both of these gases is damage to the nasal epithelium. In addition, it is critical to note that some high uptake gases can be systemically distributed via the circulation after absorption in nasal tissues just as low uptake gases absorbed primarily in the lungs can be delivered to the nose. These observations highlight the complexity of interspecies dose extrapolation for inhalation as well as the limitations in the application of a strict categorization or descriptor scheme. Therefore, it is important that dosimetry extrapolations/calculations should be based on the effect and the target tissue, and not based solely on physicochemical properties.

Using the physicochemical descriptors scheme proposed by Medinsky and Bond (2001), an attempt was made to characterize or classify the selected gases based on their criteria as discussed in Section 3.2. For the majority of the chemicals shown in Table 3-5, application of these descriptors appears straightforward. For example, formaldehyde and acrylic acid are highly soluble and/or reactive with tissue components with little potential for systemic distribution, have high liquid/tissue:air P values, and high uptake in the nasal cavity. Acrolein, acetaldehyde, and diacetyl are also best described as soluble and/or reactive with some potential for systemic distribution because of their water solubility, moderate to high liquid/tissue:air P values, and moderate to high uptake in the nasal cavity. Hydrogen sulfide is best described as non-soluble based on its low water solubility, low liquid/tissue:air P and low uptake, and nonreactive based on its hypothesized mode of action – inhibition of cyotchrome oxidase due to competitive binding. On the other hand, ethyl acrylate is best described as non-soluble based on its low water solubility, moderate liquid/tissue:air P, and low uptake, and non-reactive as its toxicity is mediated via metabolism to acrylic acid. However, similar to the 1994 *RfC Methods*, a set of qualitative descriptors cannot capture the impact of multiple, interacting quantitative properties, thus highlighting the limitations in applying a strict categorization or descriptor scheme. For example, in Table 3-5, propylene oxide and dimethyl sulfate could best be characterized as moderately-soluble and reactive based on their moderate to high water solubility, moderate liquid/tissue:air P values and ability to react directly with tissue macromolecules such as glutathione and form DNA adducts, although their nasal uptake is either unknown or low. In the case of propylene oxide, nasal uptake is lower than might be expected for a water soluble and reactive chemical because it is not particularly reactive compared to a chemical such as acrolein which has a similar solubility and liquid/tissue:air P. As discussed above, vinyl acetate also stands out for a number of reasons. It is relatively non-soluble as a result of its low solubility and partition coefficient and is non-reactive. Both its toxicity mediated by being a reactive aldehyde and its acid metabolites and higher than expected uptake is due to the presence of carboxylesterase in nasal tissues. Further adding to the complexity and limitations of applying such a scheme in a strict manner is the consideration of metabolism. As noted in Section 3.2,

metabolism is also considered a component of reactivity in characterizing gas transport in the tissue and predicting site of gas uptake and effect, but based on the examples provided by Medinsky and Bond (2001), metabolism appears to be excluded in designating the parent gas as "reactive".

As discussed in the previous section, two parameters integral to these models shown are K_g and one of its components k_g. K_g, the overall mass transfer coefficient, describes the movement of gas from the air phase into the liquid or tissue phase by combining k_g, the gas phase mass transfer coefficient, with a liquid or mucus phase transfer coefficient, k_ℓ or k_{mc}. The CFD-PBPK model developed by Bush et al. (1998) and expanded upon by Frederick et al. (1998) describes and highlights the importance of these parameters in the basic model structure for estimating target tissue dose for a wide range of inhaled gases in regions of the nasal cavity for different exposure scenarios. The model was initially used to evaluate the rodent nasal deposition of several poorly metabolized gases, but was further validated using the physicochemical and toxicity properties information for acrylic acid. Because this model provides the basis for the approach used for several of the gases presented here, the hybrid modeling results for acrylic acid (Frederick et al., 1998) are presented below for illustrative purposes.

The modeling results for acrylic acid demonstrated several findings regarding interspecies inhalation target tissue dosimetry. First, the CFD simulations provided estimates of the volume of the airflow through the various regions of the rat and human nasal cavities at various flow rates. These data confirmed the results observed in other studies (and discussed above) showing that a relatively small fraction of inspired air ventilates the human olfactory region compared to the rat. Second, the CFD simulations also showed that where the data can be compared, the regional k_g values for the rat are higher (up to one to two orders of magnitude in the respiratory epithelium) than those for the human (Table 3-6) for all of the gases listed. Other data from these studies indicate that this difference is maintained over a range of ventilation rates. This difference in k_g values indicates that rat nasal cavity is much more efficient in scrubbing gas from inspired air than the human. Since the k_g values for the rat are so much greater, the rat nasal uptake of gases may be described as limited by tissue phase resistance (i.e. the rate of liquid phase diffusion dominates the extent of uptake in this species as shown in Bush et al. 1998). Also as a result, these higher k_g values for the rat lead to higher K_g values compared to the human. The remarkably high animal to human overall K_g ratios for the highly water soluble and reactive (and therefore highly scrubbed) gases formaldehyde and acrylic acid also reflects this difference in scrubbing efficiency. Third, the available data demonstrate that the anterior half of the rat nasal cavity is also more efficient in scrubbing organic gases than the entire human nasal cavity. On a regional basis in the nasal cavity, this interspecies difference in

the delivery of inspired gases in the overall nasal cavity is significant due to differences in air flow patterns and distribution of target epithelium. Fourth, unlike the rat model that was found to be sensitive to variation in the liquid/tissue:air P and liquid phase diffusivity, the human model was sensitive to variation in air phase parameters. Therefore, air phase resistance to uptake of inhaled vapors is a significant factor that limits uptake in the human nasal cavity. Overall, the output from these CFD-PBPK hybrid simulations indicates that the target tissue (olfactory epithelium) in the rat nasal cavity is exposed to two- to threefold greater concentrations of acrylic acid than human under similar exposure conditions (i.e., equal external exposure concentration and equivalent species specific ventilatory flow rates). Further model refinement for acrylic acid by Andersen et al. (2000) indicate that a DAF of approximately 1.3 be applied to determine the HEC based on target tissue dose at the NOAEL for rats of 25 ppm (see Table 3-7).

The data in Table 3-6 is complementary to Tables 3-5 and 3-7. Table 3-6 compiles the k_g and a calculated K_g as described below for each of the gases listed. The manner in which the individual k_g values were generated is also documented in this table. For formaldehyde, the k_g for mucus-coated epithelium was calculated based on an empirically derived k_g for nonmucus-coated epithelium using human epidermal tissue; these values were used in all subsequent model simulations for the rat and human (Kimbell et al., 2001b). For acrolein, however, an approximation of a simplified mass transfer rate was derived by scaling the k_g derived for nonmucus-coated epithelium for formaldehyde based on differences in diffusivity and partition coefficient; this value was used for both the rat and human nasal CFD model (Schroeter et al., 2008). For acrylic acid, k_g values for both respiratory epithelial (RE) and olfactory epithelial (OE) region surface were derived directly from rat and human CFD simulations (Section 3.5.2). Several other examples in this table also used this same approach, employing the CFD derived k_g values from Frederick et al. (1998).

For illustrative and comparative purposes, a K_g value for each gas for both the RE and OE was calculated by applying the k_g values derived from Frederick et al. (1998) and the chemical specific parameters outlined in Equations 11 and 12. The animal (rat):human K_g for each gas and for each nasal tissue region resulting from these calculations are presented in Table 3-6. For example, the rat and human OE K_g values for acetaldehyde were calculated using the data from Frederick et al. (1998) where: $1/k_g$ in the rat = 0.00012 cm/min, and $1/k_g$ in the human = 0.00014 cm/min. For the OE, a ℓ_{muc} value of 0.001 cm for the rat, and a value of 0.002 cm for the human were used. A partition coefficient (P) of 224 and a liquid diffusivity (D) value of 0.000846 cm^2/min for acetaldehyde were also used. Use of these values resulted in an animal (rat):human K_g for the OE of 362:185 and thus, an approximately twofold higher rat K_g. It should be noted that comparisons based on calculated K_g values alone only provide an indication of

qualitative differences in dose estimates and not actual quantitative estimates of target tissue dose.

Several aspects of Table 3-7 warrant further comment. One basic observation is that the default DAF for the ET region is approximately 0.2 for each of the gases whereas DAF values based on modeling are different for nearly every gas, over a range of sevenfold in this group. These differences are indications of the models' capacity to employ and integrate numerous critical gas- and species-specific parameters and variables in characterizing gas transport through the air and tissue phases for the ET region. For example, the models for ethyl acrylate and dimethyl sulfate indicate that a DAF of 3 or 7, respectively, be applied to the rat POD to determine the HEC. The model predicted DAF for each gas is based on more detailed dose metrics: for ethyl acrylate, internal metabolite concentration; and for dimethyl sulfate, specific DNA adduct concentration. The fact that quantitative differences exist in the DAF values estimated for the ET region is an indication that the comparative dosimetry is sensitive to some combination of these parameters and variables. On the other hand, the default method is *de facto* restricted in its use of the relationship between just two general parameters, $\dot{V}_E$ and SA_{ET}, to characterize gas transport through the air and tissues phases. Another observation from Table 3-7 is that the DAF values from modeling are all one or greater despite the wide range of gas descriptions and characteristics shown in Table 3-5, including uptake (11 - >90%), water solubility (5 – 1,000 g/L), and tissue:air partition coefficient values (<3 to >6000). Additionally, these modeled outputs of DAF $\geq$ 1 were achieved through a similarly wide range of dose metrics including those based on maximum target tissue flux and/or maximum target tissue flux at the rat NOAEL, target tissue concentration, target tissue metabolite concentration, adduct concentration, and even changes in intracellular pH. Despite these wide ranges of sensitive parameters and variables, and gas descriptors ranging from "soluble- reactive", to "nonsoluble-reactive" to "nonsoluble-nonreactive", the gases in Table 3-7 all achieved the same internal target tissue dose in both rats and humans at either similar (DAF $\approx$ 1) or greater for humans (DAF > 1) external concentration.

As is the case with all "state-of-the-science" techniques and approaches, limitations and restrictions need be considered, including those of the CFD-PBPK hybrid models presented and described here. These hybrid models may be considered somewhat limited in their refinement of typical PBPK models relative to the linked CFD model. The surface area characterized by the PBPK tissue "stack" (e.g., see Figure 3-11) is much less refined and defined than the flux values to that same area characterized by the linked CFD model. The gas flux portion of the hybrid model for this area is represented by a localized k_g into which some of the flux has been collapsed and incorporated. Therefore, small localized areas of very high flux may be diluted or not sufficiently characterized especially for gases exhibiting high flux, i.e., gases that are highly

reactive and that have high uptake. Conversely, this refinement limitation would be less applicable to gases that are not highly reactive and that have lower uptake. In addition, due to the common practice of having and utilizing a single constant value for partition coefficients, these models are most appropriately used under exposure conditions that do not approach the limits of solubility and the concomitant establishment of biphasic conditions. In general, these conditions would be those within the linear range of solubility that also allow for maximization of all clearance processes, i.e. low level, long term exposures. Thus, although the currently available CFD-PBPK models are considered to provide better estimates of target tissue dose compared to conventional default methods, they may also be characterized as providing more certainty for relatively nonreactive gases versus highly reactive gases and for lower rather than higher concentrations of reactive gases. Improvements and advances in refinement of CFD-PBPK hybrid models remain in the future.

Table 3-6. Animal (rat) to human ratios of modeled or calculated gas K_g and k_g values for each representative gas

	[A]Gas phase MTC - k_g	[B]Calculated Overall MTC - K_g A/H	References
Formaldehyde	Same values for Animal and Human used: k – nonmucous = 0.41 cm/s; k – mucous = 4.7 cm/s determined by uptake simulations	RE: 46 OE: 1.2	Kimbell et al. (2001b)
Acrylic Acid	Regional k_g values estimated using CFD: Rat – RE 333 cm/s, OE 134 cm/s; Human – RE 6.4 cm/s, OE 117 cm/s	RE: 16 OE: 1-1.6	Frederick et al. (1998); Andersen et al. (2000)
Acrolein	Same values used for Rat and Human: mass transfer rate[C] for nonmucus-coated epithelium scaled from Kimbell et al. 2001b by a factor of 362	RE: 1.3-2.3 OE: 1-2	Schroeter et al. (2008); Morris et al. (1998)
Acetaldehyde	Based on Frederick 1998 values: Rat – RE 333 cm/s, OE 134 cm/s; Human – RE 6.4 cm/s, OE 117 cm/s	RE: 2-3 OE: 1-2	Teegaurden et al. (2008); Dorman et al. (2008); Morris et al. (1997)
Diacetyl	Used Frederick 1998 values: Rat – RE 333 cm/s, OE 134 cm/s; Human – RE 6.4 cm/s, OE 117 cm/s	RE: 1.7-2.7 OE: 1-2	Morris et al. (2009)
Vinyl Acetate	Based on Frederick 1998 values: Rat – RE 333 cm/s, OE 134 cm/s; Human – RE 6.4 cm/s, OE 117 cm/s	RE: 1.1-2 OE: 1-2	Bogdanffy et al. (1999)
Hydrogen Sulfide	Calculated only for the rat and combined for the entire nasal cavity: 2.13 cm/s at a flow rate of 150 ml/min	RE: 1-2 OE: 1 - 2	Schroeter et al. (2006)
Ethyl Acrylate	Used Frederick 1998 values: Rat – RE 333 cm/s, OE 134 cm/s; Human – RE 6.4 cm/s, OE 117 cm/s	RE: 1.2-2.2 OE: 1-2	Sweeney et al. (2004); Frederick et al. (2002)
Propylene Oxide	Not reported	RE: 1.2-2.2 OE: 1-2	Csanady et al. (2007); Morris (2004)
Dimethyl Sulfate	Based on Frederick 1998 values: Rat – RE 4.3 cm/h, OE 4.8 cm/h; Human – RE 1.8 cm/h, OE 1.2 cm/h	RE: 1.2-2.2 OE: 1-2	Sarangapani et al. (2004)

[A]Gas phase mass transport coefficient - MTC (k_g) as reported or the method referenced for model input
[B]Calculated Overall MTC (K_g) animal (rat)/human ratio (A/H) comparisons for respiratory epithelium (RE) and olfactory epithelium (OE) shown – based on Frederick et al. (1998) (Equations 11 and 12; see text for details)
[C]Simplified scaled mass transfer rate used; not a true k_g.

Table 3-7. Comparison of approaches for calculating the DAF for representative gases in determining the HEC - portal of entry ET or nasal effects

	[A]V/SA_{ET}	[B]CFD	[C]CFD-PBPK hybrid	[C]PBPK	References
Formaldehyde	HEC = 0.2 * AEL	DAF = 1.26 (based on the target tissue max flux of 2620 in Rat and 2082 in Human at 1 ppm)			Kimbell et al. (2001b)
Acrylic Acid	HEC = 0.2 * AEL		DAF = 1.36 (based on target tissue dose at the Rat NOAEL of 25 ppm)		Frederick et al. (1998); Andersen et al. (2000)
Acrolein	HEC = 0.2 * AEL	DAF = 1.4 (based on Rat OE NOAEL = 0.6 ppm: highest flux of 682 in Rat and 476 in Human)			Schroeter et al. (2008); Morris et al. (1998)
Acetaldehyde	HEC = 0.2 * AEL		DAF = 1.4 (based on steady-state tissue concentrations at the Rat NOAEL = 50 ppm		Teegaurden et al. (2008); Dorman et al. (2008); Morris et al. (1997)
Diacetyl	HEC = 0.2 * AEL		DAF = 1 (based on nasal and tracheal target tissue concentration)		Morris et al. (2009)
Vinyl Acetate	HEC = 0.2 * AEL		DAF = 1.14 (based on equivalent change in OE intracellular pH at the Rat NOAEL)		Bogdanffy et al. (1999)
Hydrogen Sulfide	HEC = 0.2 * AEL	DAF = 2.6 (based on Rat OE NOAEL = 10 ppm: highest flux of 34 in Rat and 13 In Human)			Schroeter et al. (2006)
EthylAcrylate	HEC = 0.2 * AEL		DAF = 3 (based on target internal metabolite concentration		Sweeney et al. (2004); Frederick et al. (2002)

	[A]V/SA_{ET}	[B]CFD	[C]CFD-PBPK hybrid	[C]PBPK	References
Propylene Oxide	HEC = 0.2 * AEL			DAF = 1 (based on equivalent concentrations in RE and venous blood at < 50ppm)	Csanady et al. (2007); Morris (2004)
Dimethyl Sulfate	HEC = 0.2 * AEL		RE: DAF = 7; OE: DAF = 2 (based on tissue N7mG adduct concentration)		Sarangapanni et al. (2004)

[A] Calculated based on procedures in U.S. EPA (1994) RfC Methodology where:

- HEC = DAF (RGDR) x Adjusted Exposure Level (AEL - based on NOAEL, LOAEL, or BMCLx)
- DAF or RGDR = V_E /$SA_{ET\text{-}animal}$/V_E /$SA_{ET\text{-}human}$
- DAF_{ET} = (0.18 L/min/15 cm^2)/(13.8 L/min/200 cm^2) = 0.18 or 0.2 ($SA_{ET\text{-}animal}$ = 15 cm^2; V_E = 0.18 L/min for a 250 g rat; $SA_{ET\text{-}human}$ = 200 cm^2; V_E = 13.8 L/min for a 70 kg human)

[B] Results from CFD simulation modeling – DAF based on comparative animal (rat): human flux values as indicated

[C] Results from CFD-PBPK hybrid or PBPK modeling – DAF based on modeled target tissue dose or dose metric as indicated

The relationship of the air phase and tissue resistance terms in determining K_g (see Equations 11 and 12) is further evaluated in Figures 3-12 and 3-13. Presented in these two figures are plots of the calculated K_g, for both the respiratory epithelium (RE) and olfactory epithelium (OE) in animals and humans, versus the partition coefficients for the gases presented in Tables 3-5 and 3-6. These plots demonstrate the influence of the partition coefficient on K_g; the differences in K_g in each tissue and between animals and humans; and thus, the differences in k_g in each tissue and between animals and humans. In both nasal tissues, gases with higher partition coefficients had higher calculated K_g values. For each gas, the calculated K_g in the rat is greater than in the human mainly because the regional k_g values determined from the CFD simulations are greater in the rat. The greatest differences between the rat and human were seen in the RE and for gases with the highest liquid/tissue:air P values (i.e. formaldehyde and acrylic acid). For gases such as these, uptake in the nasal cavity tends to be higher because the gas phase mass transfer coefficient (k_g) predominates the determination of K_g. Gases with lower partition coefficients which tend to have lower nasal uptake, such as hydrogen sulfide, since the tissue phase resistance predominates the determination of K_g. The output from the dosimetry models for the gases presented in Table 3-7 support the relationship of these parameters and of K_g in that the calculated rat/human target tissue dose (i.e. DAF) is $>$ or ≈ 1.

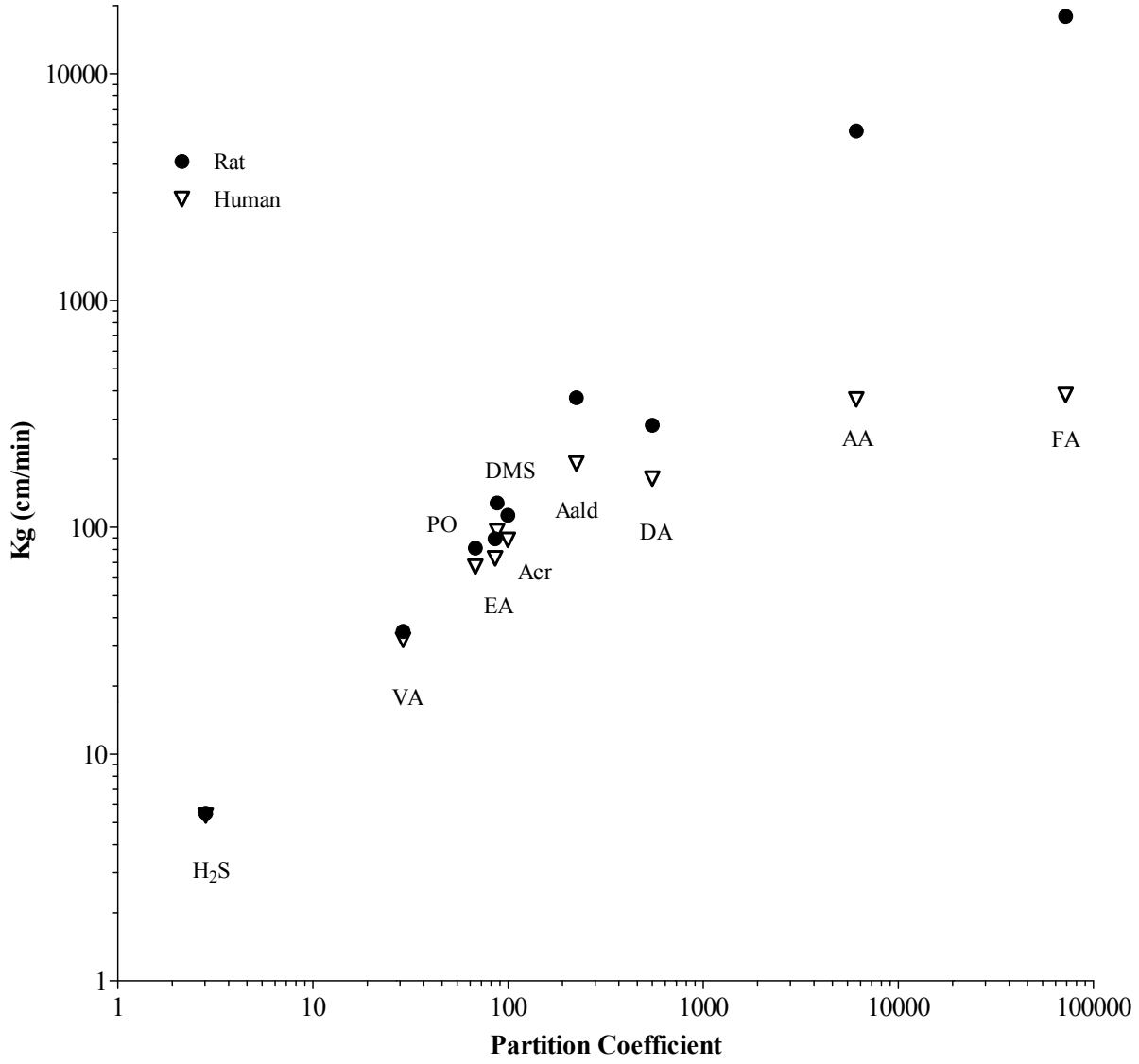

Figure 3-12. Plot of Kg (overall MTC) for respiratory epithelium (RE) in rats and humans versus partition coefficient for the gases shown in Tables 3-5, 3-6, and 3-7. MTC calculated as described by Frederick et al. (1998) (Equations 11 and 12; see text for details). (H_2S – Hydrogen Sulfide, VA – Vinyl Acetate, PO – Propylene Oxide, EA – Ethyl Acrylate, DMS – Dimethyl Sulfate, Acr – Acrolein, Aald – Acetaldehyde, DA – Diacetyl, AA – Acrylic Acid, FA – Formaldehyde).

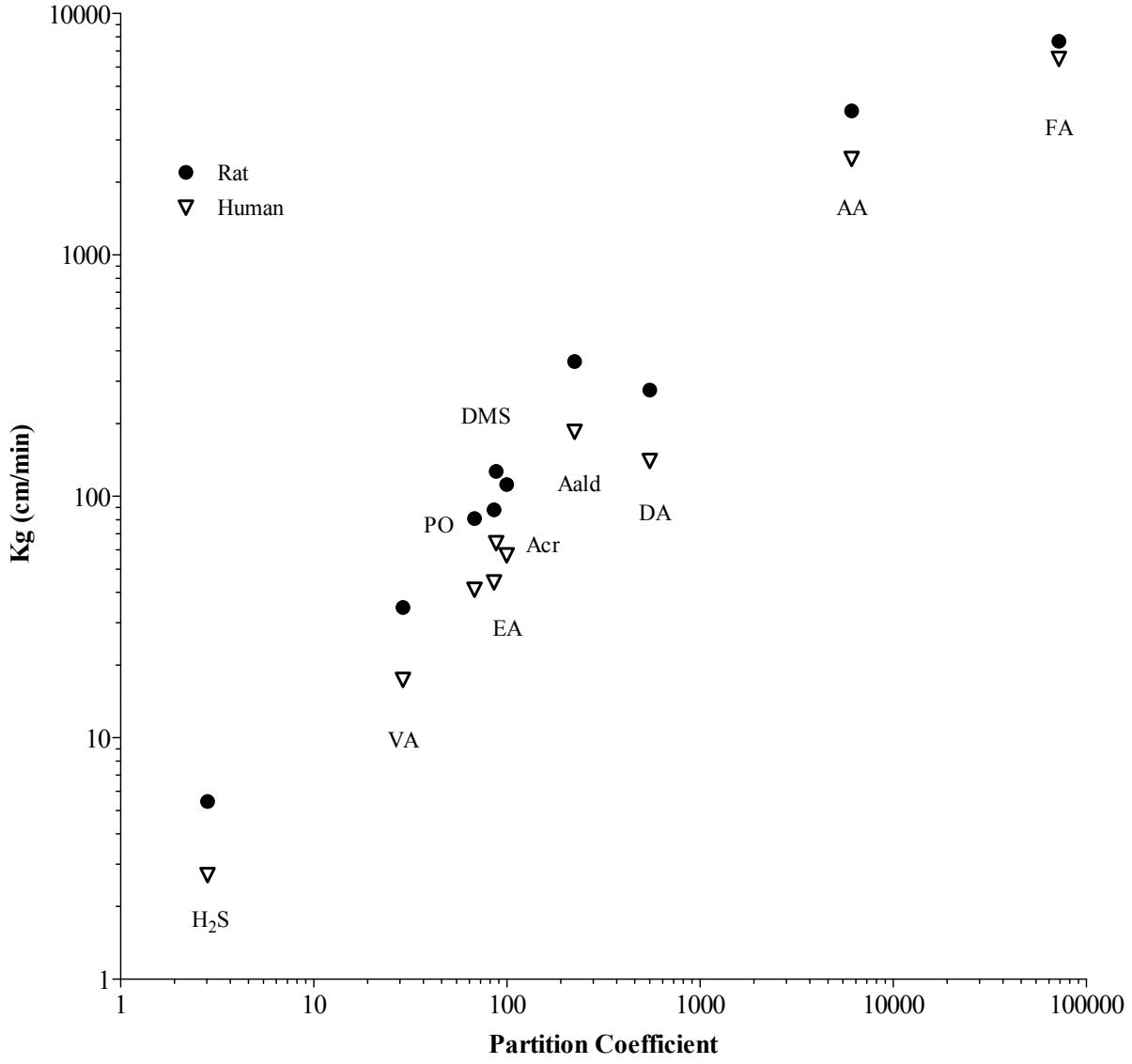

Figure 3-13. Plot of Kg (overall MTC) for olfactory epithelium (OE) in rats and humans versus partition coefficient for the gases shown in Tables 3-5, 3-6, and 3-7. MTC calculated as described by Frederick et al. (1998) (Equations 11 and 12; see text for details). (H_2S – Hydrogen Sulfide, VA – Vinyl Acetate, PO – Propylene Oxide, EA – Ethyl Acrylate, DMS – Dimethyl Sulfate, Acr – Acrolein, Aald – Acetaldehyde, DA – Diacetyl, AA – Acrylic Acid, FA – Formaldehyde).

The interspecies dosimetry modeling results for the selected gases presented in Table 3-7 indicate that for the ET region, the dose (i.e., HEC) to animals is either greater (up to sevenfold) compared to humans or close to unity. Comparison of these approaches demonstrates this point whether the dosimeter is quantitative (e.g., based on target tissue flux, target tissue concentration

of parent or metabolite) or qualitative (e.g. based on overall or regional mass transfer coefficients – K_g and k_g) over a range of gases having differing solubility, reactivity, uptake, and partition coefficients.

3.5.4. Summary and Conclusions - Modeling Developments and Results

The overall goal of this section is to summarize and put into context critical modeling developments that have occurred in the fundamental areas of target tissue dosimetry of gases. These developments should inform users of the utility and inherent limitations in the existing default *RfC Methods* which employ dose estimates from $\dot{V}_E$ and SA. The general aspects to consider are air phase transport (related to $\dot{V}_E$ in the default approach) and disposition of gases into the liquid/tissue phase (related to SA).

The capacity of CFD techniques to solve and describe air phase behavior in complex geometries represented by different species has been clearly demonstrated. Further, this technique has been repeatedly shown to be capable of indicating potential exposure (through flux) of target tissues of the ET region at a highly refined level with considerable accuracy, much more so than the use of $\dot{V}_E$ and SA ratios as a basic default procedure.

The development of PBPK models to describe the toxicokinetic behavior of gas flow and disposition into the tissue phase relating to SA_{ET} has been illustrated and demonstrated to be realistic. Model construction of tissue stacks with underlying blood flow for simulating gas flow into and through the tissues subtending the areas exposed to CFD-estimated flux has been shown to correspond with observations.

The capabilities of CFD and PBPK models to describe these individual phases have been integrated in a quantitative manner with CFD- PBPK hybrid modeling approaches. The development of this approach through use of a "permeability" coefficient (i.e. overall mass transport coefficient, K_g) to combine elements of flux from CFD modeling and of permeability from PBPK modeling in defining the diffusion of the gas through the air and tissue phases has been demonstrated. For target tissue dose, CFD- PBPK hybrid models represent a best available model for air and tissue phase elements of target tissue dosimetry that the $\dot{V}_E/SA_{ET}$ surrogate attempts to approximate. Finally, this section demonstrates the application of the best available model of tissue dosimetry, the CFD-PBPK hybrid models. These published applications consistently indicate that interspecies target tissue doses (human:animal) relative to external exposure are close to or greater than 1:1.

This outcome of the analysis for the ET region is graphically summarized in Figure 3-14. This figure may be viewed as a follow-on and complementary representation of Figures 3-1 and

3-10 which provided a backdrop for the information presented in this Chapter. The assumptions of uniformity for the ET region listed in Figures 3-1 and 3-10 have been altered in Figure 3-15 to better represent the information presented in this section – namely, that air flow and gas deposition to surface areas in the ET region are nonuniform. Also, CFD-PBPK hybrid models have been entered in that area concerned with outcomes to the assumptions of uniformity of the ET region shown in Figures 3-1 and 3-10. This entry reflects the capability of these modeling approaches to integrate and apply conditions of nonuniform gas behavior. The far right of Figure 3-14 now indicates the outcome predicted by these models as shown by the examples presented in this section. The examples presented here generally indicate that the ET regions of animals and humans receive nearly equivalent doses at equivalent external exposure concentrations. For some gases, however, the dose to the ET regions of animals is estimated to be three- to sevenfold greater than of humans.

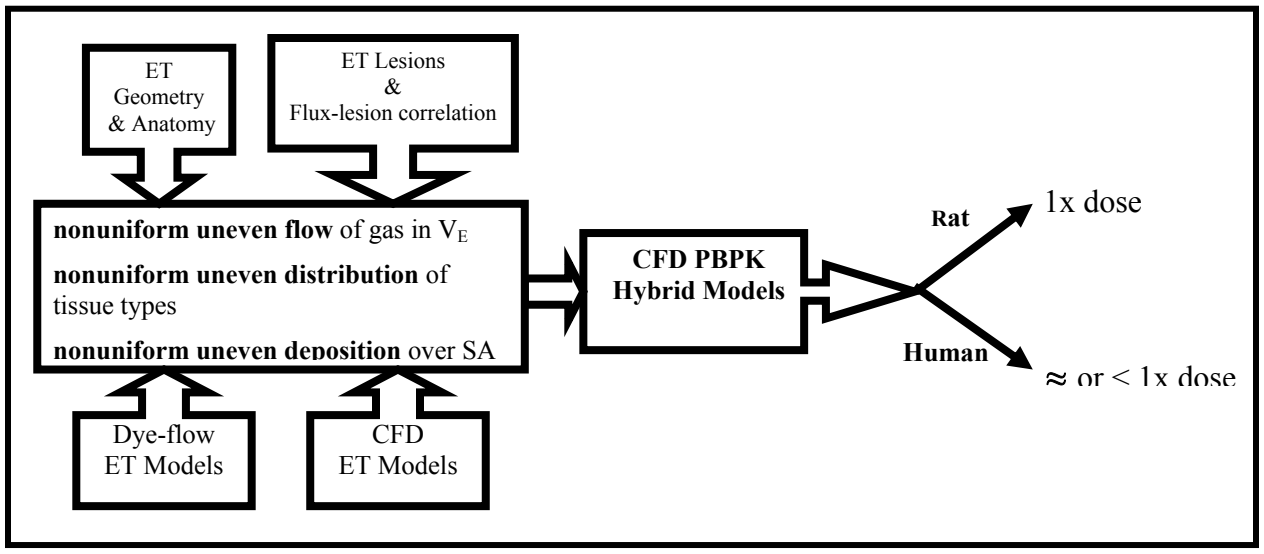

Figure 3-14. A revised schematic representation of the outcomes for interspecies inhalation dosimetry of gases for the ET region following from the advances presented.

The analysis, summary, and conclusions presented in this report on the state-of-the-science advances in inhalation dosimetry are intended to serve as a foundation for potential revisions to gas dosimetry procedures in the *RfC Methods.* Future reports will review advances in gas dosimetry for other regions of the respiratory tract. This report relates to methods for interspecies extrapolation and not to differences in dosimetry among individuals in the human population (intraspecies variability). This report is intended neither to displace the current

procedures for gas dosimetry in *RfC Methods* nor to reflect on use of these procedures in assessments currently in IRIS.

4. REFERENCES

List of specific references cited in the text:

Aharonson EF; Menkes H; Gurtner G; Swift DL; and Proctor DF. (1974). Effect of respiratory airflow rate on removal of soluble vapors by the nose. J Appl Physiol, 37(5), 654-657.

Andersen M; Sarangapani R; Gentry R; Clewell H; Covington T; and Frederick CB. (2000). Application of a hybrid CFD-PBPK nasal dosimetry model in an inhalation risk assessment: an example with acrylic acid. Toxicol Sci, 57(2), 312-325.

Bailie N; Hanna B; Watterson J; and Gallagher G. (2006). An overview of numerical modelling of nasal airflow. Rhinology, 44(1), 53-57.

Bogdanffy MS; Sarangapani R; Plowchalk DR; Jarabek A; and Andersen ME. (1999). A biologically based risk assessment for vinyl acetate-induced cancer and noncancer inhalation toxicity. Toxicol Sci, 51(1), 19-35.

Bush ML; Frederick CB; Kimbell JS; and Ultman JS. (1998). A CFD-PBPK hybrid model for simulating gas and vapor uptake in the rat nose. Toxicol Appl Pharmacol, 150(1), 133-145.

Bush ML; Zhang W; Ben-Jebria A; and Ultman JS. (2001). Longitudinal distribution of ozone and chlorine in the human respiratory tract: simulation of nasal and oral breathing with the single-path diffusion model. Toxicol Appl Pharmacol, 173(3), 137-145.

Casanova M; Morgan KT; Steinhagen WH; Everitt JI; Popp JA; and Heck HD. (1991). Covalent binding of inhaled formaldehyde to DNA in the respiratory tract of rhesus monkeys: pharmacokinetics, rat-to-monkey interspecies scaling, and extrapolation to man. Fundam Appl Toxicol, 17(2), 409-428.

Chang JC; Gross EA; Swenberg JA; and Barrow CS. (1983). Nasal cavity deposition, histopathology, and cell proliferation after single or repeated formaldehyde exposures in B6C3F1 mice and F-344 rats. Toxicol Appl Pharmacol, 68(2), 161-176.

Chometon F; Gillieron P; Laurent J; Ebbo D; Kos-man F; Lecomte F; and Sorrel-Dejerine N. (2000). Aerodynamics of nasal airways with application to obstruction. Ann Otolaryngol Chir Cervicofac 117:98-104

Corley RA. (2009). Magnetic Resonance Imaging and Computational Fluid Dynamics (CFD) Simulations of Rabbit Nasal Airflows for the Development of Hybrid CFD/PBPK Models Inhalation Toxicol, 1-7.

Csanady GA; and Filser JG. (2007). A physiological toxicokinetic model for inhaled propylene oxide in rat and human with special emphasis on the nose. Toxicol Sci, 95(1), 37-62.

Dahl AR. (1990). Dose concepts for inhaled vapors and gases. Toxicol Appl Pharmacol, 103(2), 185-197.

de Rochefort L; Vial L; Fodil R; Maitre X; Louis B; Isabey D; Caillibotte G;Thiriet M; Bittoun J; Durand E; and Sbirlea-Apiou G. (2007). In vitro validation of computational fluid dynamic simulation in human proximal airways with hyperpolarized 3He magnetic resonance phase-contrast velocimetry. J Appl Physiol, 102(5), 2012-2023.

Dorman DC; Struve MF; Wong BA; Gross EA; Parkinson C; Willson GA; Tan, YM; Campbell, JL;Teeguarden, JG;Clewell, H J; and Andersen, ME. (2008). Derivation of an inhalation reference concentration based upon olfactory neuronal loss in male rats following subchronic acetaldehyde inhalation. Inhal Toxicol, 20(3), 245-256.

Elad DL R; Wenig BL; Einav S. (1993). Analysis of Air Flow Patterns in the Human Nose. Medical and Biological engineering and Computing, 31, 585-592.

Frederick CB; Bush ML; Lomax LG; Black KA; Finch L; Kimbell JS; Morgan, KT; Subramaniam, RP; Morris, JB; Ultman, JS. (1998). Application of a hybrid computational fluid dynamics and physiologically based inhalation model for interspecies dosimetry extrapolation of acidic vapors in the upper airways. Toxicol Appl Pharmacol, 152(1), 211-231.

Frederick CB; Lomax LG; Black KA; Finch L; Scribner HE; Kimbell JS; Morgan, KT; Subramaniam, RP; and Morris, JB.(2002). Use of a hybrid computational fluid dynamics and physiologically based inhalation model for interspecies dosimetry comparisons of ester vapors. Toxicol Appl Pharmacol, 183(1), 23-40.

Geelhaar A; and Weibel ER. (1971). Morphometric estimation of pulmonary diffusion capacity. 3. The effect of increased oxygen consumption in Japanese Waltzing mice. Respir Physiol, 11(3), 354-366.

Gehr P; Mwangi DK; Ammann A; Maloiy GM; Taylor CR; and Weibel ER. (1981). Design of the mammalian respiratory system. V. Scaling morphometric pulmonary diffusing capacity to body mass: wild and domestic mammals. Respir Physiol, 44(1), 61-86.

Gross EA; Swenberg JA; Fields S; and Popp JA. (1982). Comparative morphometry of the nasal cavity in rats and mice. J Anat, 135(Pt 1), 83-88.

Guilmette RA; W JD; Wolff RK. (1989). Morphometry of human nasal airways in vivo using magnetic resonance imaging. J Aerosol Med, 2, 365-377.

Hanna LM; Frank R; and Scherer PW. (1989). Absorption of soluble gases and vapors in the respiratory system. In H. K. a. P. Chang, M. (Ed.), Respiratory physiology: an analytical approach. (pp. 277-316). New York, NY: Marcel Dekker, Inc.

ICRP. (1993). Gases and vapours. In I. C. o. R. Protection (Ed.), Human respiratory tract model for radiological protection: a report of Committee 2 of the International Commission on Radiological Protection. (pp. 57-66). Sutton, Surrey, United Kingdom: International Commission on Radiological Protection.

Kepler GM; Joyner DR; Fleishman A; Richardson RB; Gross EA; Morgan KT; Godo MN; and Kimbell JS. (1995). Method for obtaining accurate geometrical coordinates of nasal airways for computer dosimetry modeling and lesion mapping. Inhal. Toxicol. 7:1207-1224.

Kepler GM; Richardson RB; Morgan KT; and Kimbell JS. (1998). Computer simulation of inspiratory nasal airflow and inhaled gas uptake in a rhesus monkey. Toxicol Appl Pharmacol, 150(1), 1-11.

Keyhani KS; and Mozell MM. (1995). Numerical Simulation of Airflow in the Human Nasal Cavity. J Biomemechanical Engineering, 117, 429-441.

Kimbell JS; Godo MN; Gross EA; Joyner DR; Richardson RB; and Morgan KT. (1997a). Computer simulation of inspiratory airflow in all regions of the F344 rat nasal passages. Toxicol Appl Pharmacol, 145(2), 388-398.

Kimbell JS; Gross EA; Joyner DR; Godo MN; and Morgan KT. (1993). Application of computational fluid dynamics to regional dosimetry of inhaled chemicals in the upper respiratory tract of the rat. Toxicol Appl Pharmacol, 121(2), 253-263.

Kimbell JS; Gross EA; Richardson RB; Conolly RB; and Morgan KT. (1997b). Correlation of regional formaldehyde flux predictions with the distribution of formaldehyde-induced squamous metaplasia in F344 rat nasal passages. Mutat Res, 380(1-2), 143-154.

Kimbell JS; Overton JH; Subramaniam RP; Schlosser PM; Morgan KT; Conolly RB; and Miller FJ. (2001a). Dosimetry modeling of inhaled formaldehyde: binning nasal flux predictions for quantitative risk assessment. Toxicol Sci, 64(1), 111-121.

Kimbell JS; and Subramaniam RP. (2001). Use of computational fluid dynamics models for dosimetry of inhaled gases in the nasal passages. Inhal Toxicol, 13(5), 325-334.

Kimbell JS; Subramaniam RP; Gross EA; Schlosser PM; and Morgan KT. (2001b). Dosimetry modeling of inhaled formaldehyde: comparisons of local flux predictions in the rat, monkey, and human nasal passages. Toxicol Sci, 64(1), 100-110.

Kliment V. (1973). Similarity and dimensional analysis, evaluation of aerosol deposition in the lungs of laboratory animals and man. Folia Morphol. (Prague) 21, 59-64.

Kurtz DB; Zhao K; Hornung D. E; and Scherer P. (2004). Experimental and numerical determination of odorant solubility in nasal and olfactory mucosa. Chem Senses, 29(9), 763-773.

Lechner AJ. (1978). The scaling of maximal oxygen consumption and pulmonary dimensions in small mammals. Respir Physiol, 34(1), 29-44.

Martonen TB; Zhang Z; Yu G; and Musante CJ. (2001). Three-dimensional computer modeling of the human upper respiratory tract. Cell Biochem Biophys, 35(3), 255-261.

Medinsky MA; and Bond JA. (2001). Sites and mechanisms for uptake of gases and vapors in the respiratory tract. Toxicology, 160(1-3), 165-172.

Mercer RR; Russell ML; and Crapo JD. (1994a). Alveolar septal structure in different species. J Appl Physiol, 77(3), 1060-1066.

Mercer RR; Russell ML; Roggli VL; and Crapo JD. (1994b). Cell number and distribution in human and rat airways. Am J Respir Cell Mol Biol, 10(6), 613-624.

Miller FJ; Overton JH, J; Jaskot RH; and Menzel DB. (1985). A model of the regional uptake of gaseous pollutants in the lung. I. The sensitivity of the uptake of ozone in the human lung to lower respiratory tract secretions and exercise. Toxicol Appl Pharmacol, 79(1), 11-27.

Minard KR; Einstein DR; Jacob RE; Kabilan S; Kuprat AP; Timchalk CA; Trease LL; and Corley RA. (2006). Application of magnetic resonance (MR) imaging for the development and validation of computational fluid dynamic (CFD) models of the rat respiratory system. Inhal Toxicol, 18(10), 787-794.

Morgan KT; Kimbell JS; Monticello TM; Patra AL; and Fleishman A. (1991). Studies of inspiratory airflow patterns in the nasal passages of the F344 rat and rhesus monkey using nasal molds: relevance to formaldehyde toxicity. Toxicol Appl Pharmacol, 110(2), 223-240.

Morgan MS; Frank R. (1977). Uptake of pollutant gases by the respiratory system. In J. D. P. Brain, D. F.; Reid, L. M; (Ed.), Respiratory defense mechanisms: part I. (pp. 157-189). New York, NY: Marcel Dekker, Inc.

Morris JB. (1997). Uptake of acetaldehyde vapor and aldehyde dehydrogenase levels in the upper respiratory tracts of the mouse, rat, hamster, and guinea pig. Fundam Appl Toxicol, 35(1), 91-100.

Morris JB. (1998). Effect of acrolein vapor on upper respiratory tract uptake of acetaldehyde. Inhal Toxicol, 10, 843-856.

Morris JB; Banton MI; and Pottenger LH. (2004). Uptake of inspired propylene oxide in the upper respiratory tract of the f344 rat. Toxicol Sci, 81(1), 216-224.

Morris JB; Hassett DN; and Blanchard KT. (1993). A physiologically based pharmacokinetic model for nasal uptake and metabolism of nonreactive vapors. Toxicol Appl Pharmacol, 123(1), 120-129.

Morris JB; and Hubbs AF. (2009). Inhalation dosimetry of diacetyl and butyric acid, two components of butter flavoring vapors. Toxicol Sci, 108(1), 173-183.

Morris JB; and Smith FA. (1982). Regional deposition and absorption of inhaled hydrogen fluoride in the rat. Toxicol Appl Pharmacol, 62(1), 81-89.

Moulin FJ; Brenneman KA; Kimbell JS; and Dorman DC. (2002). Predicted regional flux of hydrogen sulfide correlates with distribution of nasal olfactory lesions in rats. Toxicol Sci, 66(1), 7-15.

NRC (1994). Science and Judgment in Risk Assessment. Committee on Risk Assessment of Hazardous Air Pollutants Board on Environmental Studies and Toxicology Commission on Life Sciences National Research Council, Washington, D.C; National Academy Press,

NRC (2009). Science and Decisions: Advancing Risk Assessment. Committee on Improving Risk Analysis Approaches Used by the U.S. EPA, National Research Council; Washington, D.C; National Academy Press,

Overton JH; Graham RC; and Miller FJ. (1987). A model of the regional uptake of gaseous pollutants in the lung. II. The sensitivity of ozone uptake in laboratory animal lungs to anatomical and ventilatory parameters. Toxicol Appl Pharmacol, 88(3), 418-432.

Phalen, RF; Stuart, BO; and Lioy, PJ. (1988) Rationale for and implications of particle size-selective sampling. In: Advances in air sampling: [papers from the ACGIH symposium]; February 1987; Pacific Grove, CA. Chelsea, MI: Lewis Publishers, Inc.; p. 6. (Industrial hygiene science series).

Ramsey JC; and Andersen ME. (1984) a physiologically based description of the inhalation pharmacokinetics of styrene in rats and humans. Toxicol. Appl. Pharmacol 73:159-1 75

Sarangapani R; and Wexler AS. (2000). The Role of Dispersion in Particle Deposition in Human Airways. Tox Sci 54, 229-236

Sarangapani R; Teeguarden JG; Gentry PR; Clewell HJ, 3rd Barton HA; and Bogdanffy MS. (2004) Interspecies dose extrapolation for inhaled dimethyl sulfate: a PBPK model-based analysis using nasal cavity N7-methylguanine adducts. Inhal Toxicol 16: 593-605.

Schreck S; Sullivan KJ; Ho CM; and Chang HK. (1993). Correlations between flow resistance and geometry in a model of the human nose, J. Appl. Physiol. **75** (4) (1993), pp. 1767–1775.

Schreider JP; and Hutchens JO. (1980). Morphology of the guinea pig respiratory tract. The Anatomical Record 196(3):313-321

Schroeter JD; Kimbell JS; Andersen ME; and Dorman DC. (2006). Use of pharmacokinetic-driven computational fluid dynamics model to predict nasal extraction of hydrogen sulfide in rats and humans. Toxicol. Sci. 94:359–367

Schroeter JD; Kimbell JS; Gross EA; Willson GA; Dorman DC; Tan Y-M; and Clewell HJ. (2008). Application of physiological computational fluid dynamics models to precit interspecies nasal dosimetry of inhaled acrolein. Inhal Toxicol 20:227–243

Shome B; Wang LP; Santare MN; Prasad AK; Szeri AZ; and Roberts D (1998) Modeling of the Airflow in the Pharynx with Application to Sleep Apnea. Amer. Soc. Mechanical Engineers 120: 416-422.

Subramanian RP; Richardson RB; Morgan KT; Kimbell JS; and Guilmette RA. (1998). Computational fluid dynamics simulations of inspiratory airflow in the human nose and nasopharynx. Inhalation Toxicology, 10, 91-120.

Sweeney LM; Andersen ME; and Gargas ML. (2004). Ethyl acrylate risk assessment with a hybrid computational fluid dynamics and physiologically based nasal dosimetry model. Toxicol Sci, 79(2), 394-403.

Tarabichi M; and Fanous N. (1993). Finite element analysis of airflow in the nasal valve. Arch Otolaryngol Head Neck Surg, 119(6), 638-642.

Teeguarden JG; Bogdanffy MS; Covington TR; Tan C; and Jarabek AM. (2008). A PBPK model for evaluating the impact of aldehyde dehydrogenase polymorphisms on comparative rat and human nasal tissue acetaldehyde dosimetry. Inhal Toxicol, 20(4), 375-390.

Tenney SM; and Remmers JE. (1963). Comparative quantitative morphology of the mammalian lung: diffusing area. Nature, 197, 54-56.

U.S. EPA (1988a). Reference physiological parameters in pharmacokinetic modeling. Arms AD; Travis CC. U.S. Environmental Protection Agency, Office of Research and Development, Office of Health and Environmental Assessment, Washington, DC; EPA/600/S6-88/004

U.S. EPA. (1988b). Recommendations for and documentation of biological values for use in risk assessment. U.S. Environmental Protection Agency, Washington, DC; EPA/600/6-87/008.

U.S. EPA (1994). Methods for derivation of inhalation reference concentrations (RfCs) and application of inhalation dosimetry. U.S. Environmental Protection Agency, Office of Research and Development, Office of Health and Environmental Assessment, Washington, DC; EPA/600/8-90/066F.

U.S. EPA. (2006) Science policy council handbook. 3rd edition. Office of Science Policy Council, Office of Research and Development, Washington, DC; EPA/100/B-06/002.

Wen JI; Tu J; and Wang S. (2008). Numerical Simulations for Detailed Airflow Dynamics in a Human Nasal cavity. Resp Physiol neurobiology, 161(2), 125-135.

Yang GC; Scherer PW; and Mozell MM. (2007). Modeling inspiratory and expiratory steady-state velocity fields in the Sprague-Dawley rat nasal cavity. Chem Senses, 32(3), 215-223.

Yu CP; and Xu GB. (1987). Predictive models for deposition of inhaled diesel exhaust particles in humans and laboratory species. Res Rep Health Eff Inst(10), 3-22.

Zhao K; Dalton P; Yang GC; and Scherer PW. (2006). Numerical modeling of turbulent and laminar airflow and odorant transport during sniffing in the human and rat nose. Chem Senses, 31(2), 107-118.

Zhao K; and Dalton P. (2007). The Way the Wind Blows: Implications of Modeling Nasal Airflow. Current Allergy and Asthma reports, 7, 117-125.

Zhao K; Scherer PW; Hajiloo S; and Dalton P. (2004). Effect of Anatomy on Human Nasal Air Flow and Odorant Transport patterns: Implications for Olfaction. Chem Senses, 29(5), 365-379.

Other source references related to inhalation gas dosimetry:

Aitken, M. L., Franklin, J. L., Pierson, D. J., and Schoene, R. (1986). Influence of body size and gender on control of ventilation. J. Appl. Physiol. 60:1894-1899.

Andersen ME; Clewell HJ, III; and Frederick CB. (1995). Applying simulation modeling to problems in toxicology and risk assessment--a short perspective. Toxicol Appl Pharmacol, 133(2), 181-187.

Andersen ME; Green T; Frederick CB; and Bogdanffy MS. (2002). Physiologically based pharmacokinetic (PBPK) models for nasal tissue dosimetry of organic esters: assessing the state-of-knowledge and risk assessment applications with methyl methacrylate and vinyl acetate. Regul Toxicol Pharmacol, 36(3), 234-245.

Andersen, ME; and Sarangapani, R. (1999). Clearance concepts applied to the metabolism of inhaled vapors in tissues lining the nasal cavity. Inhal Toxicol, 11(10), 873-897.

Andersen ME; Sarangapani R; Frederick CB; and Kimbell JS. (1999). Dosimetric adjustment factors for methyl methacrylate derived from a steady-state analysis of a physiologically based clearance-extraction model. Inhal Toxicol, 11(10), 899-926.

Arens R; McDonough JM; Corbin AM; Hernandez ME; Maislin G; Schwab RJ; and Pack AI. (2002). Linear dimensions of the upper airway structure during development: assessment by magnetic resonance imaging. Am J Respir Crit Care Med, 165(1), 117-122.

Arens R; McDonough JM; Corbin AM; Rubin NK; Carroll ME; Pack AI; Liu J; and Udupa JK. (2003). Upper airway size analysis by magnetic resonance imaging of children with obstructive sleep apnea syndrome. Am J Respir Crit Care Med, 167(1), 65-70.

Basak SC; Mills D; Hawkins DM; and El-Masri HA. (2003). Prediction of human blood: air partition coefficient: a comparison of structure-based and property-based methods. Risk Anal, 23(6), 1173-1184.

Beals, J. A., Funk, L. M., Fountain, R., and Sedman, R. (1996). Quantifying the distribution of inhalation exposure in human populations: distribution of minute volumes in adults and children. Environ. Health Perspect. 104:974-979.

Bennett WD; Zeman KL; and Jarabek AM. (2003). Nasal contribution to breathing with exercise: effect of race and gender. J Appl Physiol, 95(2), 497-503.

Bogdanffy MS. (2002). Vinyl acetate-induced intracellular acidification: implications for risk assessment. Toxicol Sci, 66(2), 320-326.

Bogdanffy MS; and Jarabek AM. (1995). Understanding mechanisms of inhaled toxicants: implications for replacing default factors with chemical-specific data. Toxicol Lett, 82-83, 919-932.

Bogdanffy MS; and Sarangapani R. (2003). Physiologically-based kinetic modeling of vapours toxic to the respiratory tract. Toxicol Lett, 138(1-2), 103-117.

Bogdanffy MS; Sarangapani R; Kimbell JS; Frame SR; and Plowchalk DR. (1998). Analysis of vinyl acetate metabolism in rat and human nasal tissues by an in vitro gas uptake technique. Toxicol Sci, 46(2), 235-246.

Bogdanffy MS; and Valentine R. (2003). Differentiating between local cytotoxicity, mitogenesis, and genotoxicity in carcinogen risk assessments: the case of vinyl acetate. Toxicol Lett, 140-141, 83-98.

Burton RT; Isaacs KK; Fleming JS; and Martonen TB. (2004). Computer reconstruction of a human lung boundary model from magnetic resonance images. Respir Care, 49(2), 180-185.

Clewell HJ; Andersen ME; and Barton HA. (2002). A consistent approach for the application of pharmacokinetic modeling in cancer and noncancer risk assessment. Environ Health Perspect, 110(1), 85-93.

Clewell HJ; Teeguarden J; McDonald T; Sarangapani R; Lawrence G; Covington T; Genry R; and Shipp A. (2002). Review and evaluation of the potential impact of age- and gender-specific pharmacokinetic differences on tissue dosimetry. Crit Rev Toxicol, 32(5), 329-389.

Condorelli P; and George SC. (1999). Theoretical Gas Phase Mass Transfer Coefficients for Endogenous Gases in the lungs. Annals of Biomedical Engineering, 27, 326-339.

Conolly RB; Kimbell JS; Janszen, D; Schlosser PM; Kalisak D; Preston J; and Miller FJ. (2003). Biologically motivated computational modeling of formaldehyde carcinogenicity in the F344 rat. Toxicol Sci, 75(2), 432-447.

Conolly RB; Kimbell JS; Janszen D; Schlosser PM; Kalisak D; Preston J; and Miller FJ. (2004). Human respiratory tract cancer risks of inhaled formaldehyde: dose-response predictions derived from biologically-motivated computational modeling of a combined rodent and human dataset. Toxicol Sci, 82(1), 279-296.

da Costa GC; Churchwell MI; Hamilton LP; von Tungeln LS; Beland FA; Marques MM; and Doerge DR. (2003). DNA Adduct Formation from Acrylamide via Conversion To Glycidamide in Adult and Neonatal Mice. Chem Res Toxicol, 16, 1328-1337.

Dahl AR; and Gerde P. (1994). Uptake and metabolism of toxicants in the respiratory tract. Environ Health Perspect, 102 Suppl 11, 67-70.

Daigle CC; Chalupa DC; Gibb FR; Morrow PE; Oberdorster G; Utell MJ; and Frampton MW. (2003). Ultrafine particle deposition in humans during rest and exercise. Inhal Toxicol, 15(6), 539-552.

de Zwart LL; Haenen HE; Versantvoort CH; Wolterink G; van Engelen JG; and Sips AJ. (2004). Role of biokinetics in risk assessment of drugs and chemicals in children. Regul Toxicol Pharmacol, 39(3), 282-309.

Deloar HM; Watabe H; Nakamura T; Narita Y; Yamadera A; Fujiwara T; and Itoh M. (1997). Internal dose estimation including the nasal cavity and major airway for continuous inhalation of C15O2, 15O2 and C15O using the thermoluminescent dosimeter method. J Nucl Med, 38(10), 1603-1613.

Dorman DC; Brenneman KA; McElveen AM; Lynch SE; Roberts KC; and Wong BA. (2002). Olfactory transport: a direct route of delivery of inhaled manganese phosphate to the rat brain. J Toxicol Environ Health A, 65(20), 1493-1511.

Faller TH; Csanady GA; Kreuzer PE; Baur CM; and Filser JG. (2001). Kinetics of propylene oxide metabolism in microsomes and cytosol of different organs from mouse, rat, and humans. Toxicol Appl Pharmacol, 172(1), 62-74.

Gargas ML; Tyler TR; Sweeney LM; Corley RA; Weitz KK; Mast TJ; Paustenbach DJ; and Hays SM. (2000). A toxicokinetic study of inhaled ethylene glycol monomethyl ether (2-ME) and validation of a physiologically based pharmacokinetic model for the pregnant rat and human. Toxicol Appl Pharmacol, 165(1), 53-62.

Gentry PR; Covington TR; Andersen ME; and Clewell HJ, 3rd. (2002). Application of a physiologically based pharmacokinetic model for isopropanol in the derivation of a reference dose and reference concentration. Regul Toxicol Pharmacol, 36(1), 51-68.

Gentry PR; Covington TR; and Clewell HJ, 3rd. (2003). Evaluation of the potential impact of pharmacokinetic differences on tissue dosimetry in offspring during pregnancy and lactation. Regul Toxicol Pharmacol, 38(1), 1-16.

Gentry PR; Covington TR; Clewell HJ, 3rd; and Anderson ME. (2003). Application of a physiologically based pharmacokinetic model for reference dose and reference concentration estimation for acetone. J Toxicol Environ Health A, 66(23), 2209-2225.

Georgieva AV; Kimbell JS; and Schlosser PM. (2003). A distributed-parameter model for formaldehyde uptake and disposition in the rat nasal lining. Inhal Toxicol, 15(14), 1435-1463.

Gerde P; and Dahl AR. (1991). A model for the uptake of inhaled vapors in the nose of the dog during cyclic breathing. Toxicol Appl Pharmacol, 109(2), 276-288.

Gerde P; Muggenburg BA; Lundborg M; and Dahl AR. (2001). The rapid alveolar absorption of diesel soot-adsorbed benzo[a]pyrene: bioavailability, metabolism and dosimetry of an inhaled particle-borne carcinogen. Carcinogenesis, 22(5), 741-749.

Gerde P; and Scott BR. (2001). A model for absorption of low-volatile toxicants by the airway mucosa. Inhal Toxicol, 13(10), 903-929.

Gerrity TR. (1995). Regional deposition of gases and particles in the lung: implications for mixtures. Toxicology, 105(2-3), 327-334.

Ginsberg GL; Asgharian B; Kimbell JS; Ultman JS; and Jarabek AM. (2008). Modeling approaches for estimating the dosimetry of inhaled toxicants in children. Journal of Toxicology and Environmental Health, Part A, 71: 166–195.

Ginsberg G; Hattis D; Miller R; and Sonawane B. (2004). Pediatric pharmacokinetic data: implications for environmental risk assessment for children. Pediatrics, 113(4 Suppl), 973-983.

Ginsberg G; Hattis D; Russ A; and Sonawane B. (2004). Physiologically based pharmacokinetic (PBPK) modeling of caffeine and theophylline in neonates and adults: implications for assessing children's risks from environmental agents. J Toxicol Environ Health A, 67(4), 297-329.

Ginsberg G; Hattis D; and Sonawane B. (2004). Incorporating pharmacokinetic differences between children and adults in assessing children's risks to environmental toxicants. Toxicol Appl Pharmacol, 198(2), 164-183.

Green T; Toghill A; and Foster JR. (2001). The role of cytochromes P-450 in styrene induced pulmonary toxicity and carcinogenicity. Toxicology, 169(2), 107-117.

Guilmette RA; C YS; and Griffith WC. (1997). Characterising the Variability in Adult Human airway Dimensions. Ann Occup Hyg, 41(Supplement 1), 491-496

Haddad S; Beliveau M; Tardif R; and Krishnan K. (2001). A PBPK modeling-based approach to account for interactions in the health risk assessment of chemical mixtures. Toxicol Sci, 63(1), 125-131.

Hanna LM; Lou SR; Su S; and Jarabek AM. (2001). Mass transport analysis: inhalation rfc methods framework for interspecies dosimetric adjustment. Inhal Toxicol, 13(5), 437-463.

Harkema JR; Carey SA; and Wagner JG. (2006). The nose revisited: a brief review of the comparative structure, function, and toxicologic pathology of the nasal epithelium. Toxicol Pathol, 34(3), 252-269.

Hinderliter PM; Thrall KD; Corley RA; Bloemen LJ; and Bogdanffy MS. (2005). Validation of human physiologically based pharmacokinetic model for vinyl acetate against human nasal dosimetry data. Toxicol Sci, 85(1), 460-467.

Hofmann W; Asgharian B; Bergmann R; Anjilvel S; and Miller FJ. (2000). The effect of heterogeneity of lung structure on particle deposition in the rat lung. Toxicol Sci, 53(2), 430-437.

Hubal EA; Fedkiw PS; and Kimbell JS. (1996). Mass-transport models to predict toxicity of inhaled gases in the upper respiratory tract. J Appl Physiol, 80(4), 1415-1427.

Hubal EA; Schlosser PM; Conolly RB; and Kimbell JS. (1997). Comparison of inhaled formaldehyde dosimetry predictions with DNA-protein cross-link measurements in the rat nasal passages. Toxicol Appl Pharmacol, 143(1), 47-55.

International Commission on Radiological Protection (ICRP). 1994. Publication 66. Human Respiratory Tract Model for Radiological Protection. Ann. ICRP 24. Oxford: Pergamon Press

Jarabek AM. (1995). Interspecies Extrapolations Based on Mechanistic determinants of Chemical Disposition. Human and Ecological Risk Assessment, 1(5), 641-662.

Kelly JT; Prasad AK; and Wexler AS. (2000). Detailed flow patterns in the nasal cavity. J Appl Physiol, 89(1), 323-337.

Kimbell JS; Segal RA; Asgharian B; Wong BA; Schroeter JD; Southall JP; Dickens CJ; Brace G; and Miller FJ. (2007). Characterization of deposition from nasal spray devices using a computational fluid dynamics model of the human nasal passages. J Aerosol Med. 20(1):59-74.

Kohn MC. (1997). The importance of anatomical realism for validation of physiological models of disposition of inhaled toxicants. Toxicol Appl Pharmacol, 147(2), 448-458.

Layton, D. W. (1993). Metabolically consistent breathing rates for use in dose assessments. Health Phys. 64:23-36.

Lippmann M; and Schlesinger RB. (1984). Interspecies comparisons of particle deposition and mucociliary clearance in tracheobronchial airways. J Toxicol Environ Health, 13(2-3), 441-469.

Litman RS; Weissend EE; Shrier DA; and Ward DS. (2002). Morphologic changes in the upper airway of children during awakening from propofol administration. Anesthesiology, 96(3), 607-611.

Martonen TB; Schroeter JD; and Fleming JS. (2007). 3D in silico modeling of the human respiratory system for inhaled drug delivery and imaging analysis. J Pharm Sci. 96(3):603-17.

Morris JB. (1999). A method for measuring upper respiratory tract vapor uptake and its applicability to quantitative inhalation risk assessment. Inhal Toxicol, 11(10), 943-965.

Morris JB. (2000). Uptake of styrene in the upper respiratory tract of the CD mouse and Sprague-Dawley rat. Toxicol Sci, 54(1), 222-228.

Morris JB. (2001). Overview of upper respiratory tract vapor uptake studies. Inhal Toxicol, 13(5), 335-345.

Morris JB. (2002). Sensory nerve-mediated nasal vasodilatory response to inspired ethyl acrylate. Inhal Toxicol, 14(6), 585-597.

Nodelman V; and Ultman JS. (1999). Longitudinal distribution of chlorine absorption in human airways: a comparison to ozone absorption. J Appl Physiol, 87(6), 2073-2080.

Oberdorster G. (1992). Lung Dosimetry: Extrapolation Modeling from Animals to man. Nickel and Human health: Current perspectives, 32, 421-436.

Overton JH; Kimbell JS; and Miller FJ. (2001). Dosimetry modeling of inhaled formaldehyde: the human respiratory tract. Toxicol Sci, 64(1), 122-134.

Pelekis M; Gephart LA; and Lerma, SE. (2001). Physiological-model-based derivation of the adult and child pharmacokinetic intraspecies uncertainty factors for volatile organic compounds. Regul Toxicol Pharmacol, 33(1), 12-20.

Plowchalk DR; Andersen ME; and Bogdanffy MS. (1997). Physiologically based modeling of vinyl acetate uptake, metabolism, and intracellular pH changes in the rat nasal cavity. Toxicol Appl Pharmacol, 142(2), 386-400.

Rigas ML; Catlin SN; Ben-Jebria A; and Ultman JS. (2000) Ozone uptake in the intact human respiratory tract: relationship between inhaled dose and actual dose. J Appl Physiol 88: 2015-2022.

Santiago LY; Hann MC; Ben-Jebria A; and Ultman JS. (2001) Ozone absorption in the human nose during unidirectional airflow. J Appl Physiol 91: 725-732.

Sarangapani R; Teeguarden JG; Cruzan G; Clewell HJ; Andersen ME. (2002) Physiologically based pharmacokinetic modeling of styrene and styrene oxide respiratory-tract dosimetry in rodents and humans. Inhal Toxicol 14: 789-834.

Sarangapani R; Clewell HJ; Cruzan G; and Andersen ME. (2002) Comparing respiratory-tract and hepatic exposure-dose relationships for metabolized inhaled vapors: a pharmacokinetic analysis. Inhal Toxicol 14: 835-854.

Sarangapani R; Gentry PR; Covington TR; Teeguarden JG; and Clewell HJ. (2003) Evaluation of the potential impact of age- and gender-specific lung morphology and ventilation rate on the dosimetry of vapors. Inhal Toxicol 15: 987-1016.

Schlesinger RB. (1995) Interaction of gaseous and particulate pollutants in the respiratory tract: mechanisms and modulators. Toxicology 105: 315-325.

Schroeter JD. (2009). The use of nasal dosimetry models in the risk assessment of inhaled gases. Toxicol Sci. 108(1):1-3.

Tardif R; Charest-Tardif, G; Brodeur J; and Krishnan K. (1997). Physiologically based pharmacokinetic modeling of a ternary mixture of alkyl benzenes in rats and humans. Toxicol Appl Pharmacol, 144(1), 120-134.

Teeguarden JG; Deisinger PJ; Poet TS; English C; Faber WD; Barton HA; Corley RA; and Clewell HJ. (2005). Derivation of a human equivalent concentration for n-butanol using a physiologically based pharmacokinetic model for n-butyl acetate and metabolites n-butanol and n-butyric acid. Toxicol Sci, 85(1), 429-446.

APPENDIX A. INDEPENDENT EXTERNAL PEER REVIEW – SUMMARY AND DISPOSITION OF COMMENTS

The "Status Report: Advances in Inhalation Dosimetry of Gases with Portal of Entry Effects in the Upper Respiratory Tract" has undergone a formal external peer letter review performed by scientists in accordance with EPA guidance on peer review (EPA, 2006b). The reviewers were tasked with providing written answers to charge questions on both general and specific scientific aspects of the report. A summary of significant comments made by the external reviewers to these charge questions and EPA's responses to these comments arranged by charge question follow. Editorial comments were considered and incorporated directly into the document as appropriate.

EXTERNAL PEER REVIEWER COMMENTS

Comments and Response to Charge:

Charge Question 1: The primary focus of this report relates to the pharmacokinetic component of interspecies gas dosimetry for portal of entry effects in the upper respiratory tract. Issues related to pharmacodynamics, including variability in response, are specifically excluded from this report. Is the scope and primary focus of this report clear?

Comments:

All three reviewers agreed that the scope and focus of the report are clear. Two of the reviewers elaborated that the report was well organized and maintains a clear focus on the issue of interspecies dosimetry for gases and vapors in the upper respiratory tract.

Response:

No response necessary.

Charge Question 2: Have the principal studies examining interspecies gas dosimetry for portal of entry effects in the upper respiratory tract that have appeared since the issuance of the 1994 *RfC Methods* been identified in this report? Please identify and provide a rationale for any other key studies that should be considered for inclusion.

Comments:

Two of the three reviewers thought the report includes and provides a detailed description of all of the key studies examining interspecies gas dosimetry for portal of entry effects in the upper respiratory tract. One of these reviewers further elaborated that the Medinsky and Bond (2001) paper put the topic of describing gases on terms of their physicochemical properties into perspective. This reviewer also commented that the majority of the important works describing airflow were included and described sufficiently to support the conclusions reached. However, this reviewer listed two more recent references that could be included in Section 3.4.6 to support

the correlation of flux and lesions incidence. These two reviewers provided additional source references specifically addressing dosimetry in children and ventilation rates among human populations that could be added to the reference list, but did not specifically state that they needed to be described as they would not change the conclusions of the report.

The third reviewer noted that not all the source references were cited in the text.

Response:

The reference list is divided into those publications that are cited in the report, and other source references related to inhalation dosimetry. The suggested references which address dosimetry in children and ventilation rates among human populations have been added to the reference sections as other sources (Ginsberg GL et al., 2008; Schroeter, 2009; ICRP, 1994; Aitken et al., 1986; Layton, 1993; and Beals et al., 1996). Some text describing two other suggested references (Schroeter et al., 2008; and Morris et al., 2009) for inclusion into Section 3.4.6 has also been added. This structure delineates the nature of reference materials and addresses the reviewer comments.

Charge Question 3: The state-of-the-science pertaining to the focus of this report is primarily presented in Chapter 3. Is the description of those studies in this report concerned with gas dosimetry appropriate and accurate? Are the analyses and evaluations of the scientific evidence supported by the studies cited?

Comments:

One of the three reviewers stated he was impressed by the consistency of the cited and described studies. This reviewer further stated that the analysis in Chapter 3 of the report is accurate and the conclusions are appropriate.

Another of the three reviewers commented that the major conclusions from the CFD models with respect to nasal airflow patterns are well-described. The major conclusions related to gas dosimetry from these studies were also described appropriately and in-depth in this report. In particular, this reviewer stated that Table 3-7 provides compelling evidence that the evaluations in this report are supported by the literature cited, noting that the DAF is equal or greater than 1 for each compound listed in this table.

One of the three reviewers thought that the focus of the report was too narrow with respect to discussion and analyses of dosimetry experiments specifically in areas related to the development and application of mass transport principles to all airways. This reviewer also cited the lack of inclusion of information the criteria gases ozone, sulfur dioxide, and nitrogen dioxide, and that Table 3-5 should be expanded to include these gases. This reviewer did state, however, that the information presented does support the use of Equation 11 of the report.

Response:

The intent of this report was to focus on presenting the advances in inhalation interspecies dosimetry for the URT noting that similar evaluations and analyses will be conducted for other regions of the respiratory tract as well as for extrarespiratory/systemic regions. The intent of this report was not to provide an exhaustive comparative list of all the chemicals/compounds that could potentially be included in a report such as this. Specifically, the criteria gases - while providing large databases to examine for potential comparisons across species - do not rely on the 1994 *RfC Methods* to estimate dose. These pollutants rely on actual human dosimetry and concentration-response relationships in assessing risk and health, not on extrapolations from animal studies. The animal and human dosimetry information for the criteria pollutants primarily deal with regions other than the URT. Thus, a chemical such as ozone should provide information for evaluating interspecies extrapolation for other regions of the respiratory tract.

Charge Question 4: The primary focus of this report relates to the pharmacokinetic component of interspecies gas dosimetry for portal of entry effects in the upper respiratory tract. Is this report successful in presenting and evaluating the state-of-the-science relating to this focus?

Comments:

Two of the three reviewers commented that the report was successful in presenting and evaluating the state-of-the-science related to interspecies upper respiratory tract inhalation dosimetry, specifically the pharmacokinetic component. The presentation and evaluation of the key studies and findings was considered accurate and objective, and the quality of the synthesis of the new information and the analysis of its implications for cross-species dosimetry of the upper respiratory tract was stated as impressive. One of these reviewers further commented that this report presents an excellent summary of the numerous models that have been developed since the mid-1990s, including CFD and CFD-PBPK models, and their application in interspecies inhalation dosimetry.

One of the three reviewers commented that the theoretical basis of the RfC Methodology presented in Chapter 2 does not provide an adequate perspective for the material in Chapter 3. The reason being that the ET default presented in the 1994 RfC document was preceded in the RfC document by a one-dimensional model in which Kg appeared as a parameter - equivalent to the Aharonson model. This reviewer thought it would be helpful to present the Aharonson equation and its theoretical limitations in Chapter 2.

Response:

The purpose of Chapter 2 was to provide a brief review and summary of the major applications of the 1994 *RfC Methods*. In practice, the RfC derivation is made from applying the default dosimeter of V_E/SA without use of the k_g term as it often not known as discussed in the methodology. Although the work of Aharonson is cited in the *RfC Methods*, it is not described in detail. Thus, for the purposes of this report, addition of the Aharonson approach would be historically interesting but such inclusion is not necessary as a foundation for Chapter 3. However, much of the theory supporting the development of the hybrid modeling that was initially presented in Appendix I of the 1994 *RfC Methods* is outlined in Chapter 3.

Charge Question 5: The latter part of the report deals extensively with advanced state-of-the-science dosimetry models including CFD and the CFD-PBPK hybrid models. The strengths and limitations of these models to estimate target-tissue are highlighted in Chapter 3. However, as with any state-of-the-science approach, limitations exist with respect to application and outcome of these models - and some of which have been recognized and discussed (see in particular Section 3.5.3). Have the strengths and limitations of these advanced models been sufficiently characterized? Is there any information that would further support as well as limit the overall conclusions drawn from the results of these models and, more broadly, the new science published since creation of RfC Methods?

Comments:

One of the three reviewers stated that the report sufficiently characterizes the strengths and limitations of the CFD and CFD-PBPK models relied upon for the analysis. In addition, this reviewer commented that the power and general acceptance of these modeling approaches is exemplified by their use in the development of inhalation pharmaceuticals and provided references to be added to the source reference list.

Another of the three reviewers commented that the report clearly states the strengths of these models and their usefulness in estimating DAFs for inhaled gases in the URT. Additionally, as related to k_g values in Table 3-6, is that different methods were used to compute k_g values. For example, the k_g for formaldehyde was calculated using empirical results while the k_g values used in CFD-PBPK models (typically from Frederick et al., 1998) were derived from CFD models.

This reviewer also provided specific commentary in regards to the dosimetry models in two sections of the report as well as the overall conclusion. In Section 3.4.6: It is stated that a limitation of the CFD models used in flux versus lesion correlations is that they only include the URT – this reviewer commented that this isn't really a limitation of the models per se, but is a convenient use of URT models when pathology is observed in the URT. In Section 3.5, a comprehensive summary of interspecies nasal dosimetry results using CFD or CFD-PBPK models for a multitude of gases is presented with the primary conclusion that, in all cases, a DAF equal to or greater than 1 is achieved. This reviewer commented that this is in sharp contrast to results from the current RfC Methods, which using default approaches, arrives at a DAF of 0.2 with the implication that since the chemicals considered here cover a wide range of gas descriptions that these results can be extrapolated to all gases. Thus, one limitation is that since these models are chemical-specific, one can only infer that similar results would be expected for other compounds.

One of the three reviewers commented that the impact of different physical-chemical properties of a gas on mathematically modeling and understanding its dosimetry needs further clarification and that the classification scheme in Figure 3-2 helps in this regard. This reviewer further elaborated that it is not clear how the two different solubility parameters given in table 3-5, namely, liquid/air partition coefficients and water solubility or some combination of the two should be specifically used in the classification scheme in Figure 3-2. In addition, this review does not understand why the definition of reactive gas in the report appears to exclude metabolic reaction.

Response:

The suggested references (Kimbell et al., 2007; and Martonen et al., 2007) regarding the modeling approaches as applied in pharmaceuticals were added to the source reference list.

The statement made in Section 3.4.6 on the limitation of CFD models, flux, and lesion correlation was removed.

The intent of discussing the Medinsky and Bond (2001) physicochemical descriptor scheme was not to imply that it directly impacts dosimetry modeling. The intent was to show how this particular descriptor scheme may provide an improvement in examining the relationship between these physicochemical parameters and sites of toxicity versus a strict "numerical categorization" that may potentially influence default dosimetry application. Thus, the aspect of Figure 3-2 that improves the understanding of dosimetry is the de-emphasis of the overly simplified and proscriptive categorization scheme described in the 1994 *RfC Methods*. Figure 3-2 instead allows for the realization of the continuous nature of the named variables (reactivity and solubility) and the uncertainty and shortcomings inherent in this scheme. These points are made in the text of the Report.

The point regarding the two different solubility parameters given in Table 3-5 is valid, especially regarding implementation of such models as it is likely that partition coefficients would either change or become increasingly unstable under exposure conditions approaching the limits of solubility. Text concerning this point has been added to Section 3.5.3.

The definition of reactivity does not exclude metabolism as discussed in Section 3.2. However, in the examples provided in Medinsky and Bond (2001), a gas that is metabolized to a toxic moiety is described as "nonreactive" highlighting a limitation of this scheme. Text discussing this issue of metabolism and reactivity has been added to Section 3.2 and 3.5.3.

Other Reviewer Comments:

One reviewer was uncomfortable with the attempt to use the categorization suggested by Medinsky and Bond (2001) as a modified gas/vapor dosimetry scheme (p. 3-2 to 3-4 and 3-28 to 3-31). The reviewer commented that the Medinsky and Bond (2001) categorization suffers from the same limitation as the 1994 RfC Methods: water solubility and chemical reactivity alone are simply not adequate to classify gas/vapor uptake/toxicity. Further, the descriptors should at least include: water solubility, tissue/air partition coefficient, chemical reactivity, pK, and susceptibility to metabolism in the URT.

Another of the three reviewers commented on the statement (p 3-28) that "K_g may also be scaled from one gas to other gases by scaling to the water diffusivity and partition coefficient" is not entirely correct. This was done in Schroeter et al. (2008) to scale a simplified mass transfer rate on squamous epithelium from formaldehyde to acrolein. The mass transfer term was not a "K_g" as described earlier in this section and was also not stated correctly on page 3-33. Also, this was a specific case for comparing two gases that share similar molecular structures.

Response:

The intent of presenting and discussing the Medinsky and Bond (2001) scheme was to show how this descriptor scheme may provide an improvement in examining the relationship between these physicochemical parameters and sites of toxicity compared to a strict "numerical categorization" that may potentially influence default dosimetry application. Thus, the aspect of this descriptor scheme that improves the understanding of dosimetry is the de-emphasis of the overly simplified categorization scheme described in the 1994 *RfC Methods*. Figure 3-2 allows for the realization of the continuous nature of the named variables (reactivity and solubility) and the uncertainty and shortcomings inherent in this scheme. Text highlighting the limitations of this scheme has been added to section 3.5.3.

In considering the reviewer's comment concerning the statement made on p 3-28, the text was removed. Similarly, corrections to the text and Tables regarding the "mass transfer term" relating to acrolein not being a true k_g were made.

Other specific text suggestions and corrections were considered and incorporated as appropriate in revising the draft report.